Characterizing the impact of glucose deprivation on the lysine acetyltransferase complex NuA4

By

David Czosniak

A thesis submitted to the Faculty of Graduate and Postdoctoral Studies

in partial fulfillment of the requirements for the degree of MSc of Biochemistry

Department of Biochemistry, Microbiology, and Immunology

Faculty of Medicine

University of Ottawa

© David Czosniak, Ottawa, Canada, 2017

ABSTRACT

Upon the loss of glucose as the main carbon source cells have developed different mechanisms in order to adapt to this stress and promote survival. In *Saccharomyces cerevisiae* one such mechanism is acetylation, a post-translational modification performed by a lysine acetyltransferase (KAT) complex, such as NuA4, which has been previously shown to regulate different glucose metabolic pathways. Despite its known role upon glucose starvation, it is not currently understood how NuA4 itself is regulated in response to acute glucose deprivation (GD). I determine here that NuA4 complex protein levels (including catalytic protein Esa1), structure, activity, and localization are not impacted by acute GD. Despite GD showing no impact to NuA4 itself, it does result in the remodelling of both the interactome and acetylome of the complex where 160 proteins were identified to change interaction with Esa1-TAP and 93 acetylation sites were identified. As well GD results in a shift in localization of interacting proteins from nuclear upon standard growth to cytoplasmic. As well the changing interactome shows enrichment for proteins related to regulation of transcription and translation, metabolic pathways like glycolysis and gluconeogenesis, and others related to the cellular stress response. From the interactome three sets of proteins, Pab1, Eaf5/7/3, and Fas1 and Fas2, were studied further to greater characterize their interaction with NuA4 as they change interaction upon GD. Eaf7 protein levels were shown to decrease upon GD and both Fas1 and Fas2 levels were shown to increase in response to NuA4 deletion mutants. Together this work provides a greater understanding of the cellular response to acute GD stress, and how NuA4 plays a role in response to that stress in order to promote cell survival.

ACKNOWLEDGEMENTS:

I would like to thank my supervisor Kristin Baetz for providing me with the opportunity to pursue a master's degree in her lab and for her guidance throughout.

I would like to thank the current and past members of the Baetz lab, Dr. Sylvain Huard, Dr. Mike Kennedy, Dr. Bo Liao, Dr. Trang Pham, Jingwen Du, Mike Cotrut, Jennifer Takuski, Meaghen Rollins, Louis Dacquay, Amanda Defela, Madelyn Abraham, Roger Fong, and Kavita Srivastava for their guidance, friendship, and support during my studies.

I would also like to thank Dr. JP Lambert, and the Gingras lab for their mass spectrometry help and analysis. As well I would like to thank Hilary Phenix for her help in microscopy and quantification.

I would especially like to thank Barb Sibiga for all she has done for me and other members of the Baetz lab to help us with our theses.

Finally I would like to thank my family and friends for their continued help, guidance, and support during my studies.

TABLE OF CONTENTS

LIST OF ABBREVIATIONS AND DEFINITIONS

Acetylome	Protein acetylation network
ANOVA	Analysis of variance
aNSQ	Average normalized spectral quantity
Co-IP	Co-immunoprecipitation
EDTA	Ethylenediaminetetraacetic acid
EGTA	Ethylene Glycol Tetraacetic acid
G6PDH	Glucose-6-phosphate dehydrogenase
GD	Glucose deprivation
GFP	Green fluorescent protein
H3	Histone protein 3
H4	Histone protein 4
HPR	Horseradish peroxidase
IgG	Immunoglobulin G
Interactome	Protein interaction network
IP	Immunoprecipitation
KAT	Lysine acetyltransferase
KDAC	Lysine deacetylase
LC-MS/MS	Liquid Chromatography–Tandem Mass Spectrometry
MS	Mass Spectrometry
mChIP	Modified chromatin immunoprecipitation
MYST	MOZ, Ybf2/Sas3, Sas2, and Tip60
NP-40	Nonidet P-40
NSQ	Normalized spectral quantity
NuA4	Nucleosome acetyltransferase of histone H4
OD_{600}	Optical density at 600 nm
PAGE	Polyacrylamide gel electrophoresis
PicNuA4	Piccolo NuA4 subcomplex
PTM	Posttranslational modification
RNase	Ribonuclease
SC	Synthetic complete
SD	Standard deviation
SDS	Sodium dodecyl sulfate
TAP	Tandem affinity purification
TCA	Trichloroacetic acid
TINTIN	Trimer Independent of NuA4 involved in Transcription Interactions with Nucleosomes
TRIS	Tris(hydroxymethyl)aminomethane
T-test	Students T-test
WCE	Whole cell extract
WT	Wild type
YP	Yeast extract peptone
YPD	Yeast extract peptone dextrose

LIST OF FIGURES:

LIST OF TABLES:

1. INTRODUCTION

Upon encountering environmental stress, cells must adapt and remodel different processes in order to promote survival (reviewed in Carmona-Gutierrez et al., 2010). One stress that is commonly encountered by cells is nutrient limitation, such as glucose deprivation, where they respond to loss of glucose by remodelling pathways to use alternative carbon sources for energy. Within the cell there are different regulatory mechanisms and pathways that tightly monitor glucose metabolism to ensure correct levels of glucose availability at a given time. One such mechanism is the post-translational modification of glucose metabolic enzymes by lysine acetylation.

Lysine acetylation is performed by a group of enzymes known as lysine acetyltransferases (KATs) and is a conserved process from prokaryotes to eukaryotes. Acetylations importance is heightened due to specific acetylated lysines themselves showing significant cross-species conservation (Choudhary et al., 2009; Downey et al., 2015; Henriksen et al., 2012; Lin et al., 2009; Weinert et al., 2011; Zhang et al., 2009). NuA4, a KAT complex in *Saccharomyces cerevisiae,* has a previously established role in the regulation of glucose through its acetylation of Sip2 and Pck1, two proteins that directly influence glucose metabolism (Lin et al., 2009; Lu et al., 2011). While NuA4 has these known roles in glucose regulation, numerous questions still remain in order to determine NuA4's regulatory roles in response to stress. My thesis will explore these questions, specifically how GD impacts the NuA4 complex itself, and how GD impacts NuA4's role in regulation of other proteins within the cell.

This introduction will provide a review of the NuA4 complex, subcomplexes, and individual members of the complex, potential mechanisms of regulation of NuA4, the ways in which NuA4 can regulate other proteins, NuA4's currently acknowledged role in regulation upon GD, and the clinical impact of studying NuA4.

1.1 The NuA4 complex and sub-complexes

Lysine acetylation is a posttranslational modification (PTM) where there is the transfer of an acetyl group (CH_3CO-) onto the ε-amino group of a lysine residue. This transfer is accomplished by a lysine acetyltransferase (KAT) and its removal is accomplished by a lysine deacetylase (KDAC) (Figure 1). NuA4 is one of the 8 confirmed KAT complexes found in yeast (reviewed in Downey and Baetz, 2015). NuA4 is a member of the MYST (MOZ, Ybf2/Sas3, Sas2, and Tip60) family of KATs, a family characterized by its conserved zinc finger domain, and acetyl-CoA binding site. In addition to being found in yeast the NuA4 complex has homologs throughout different levels of the taxonomic hierarchy including a human homolog, the Tip60 complex (Sapountzi and Côté, 2011).

The NuA4 complex consists of thirteen different proteins: Esa1 (the essential acetyl-catalytic complex) (Clarke et al., 1999), Eaf6, Epl1, Yng2, Act1, Arp4, Swc4, Tra1, Yaf9, Eaf1, Eaf5, Eaf7, and Eaf3 (Chittuluru et al., 2011; reviewed in Doyon and Côté, 2004) (Figure 2). Within the NuA4 complex there are three distinct submodules: Piccolo NuA4, the recruitment module, and TINTIN. Piccolo NuA4 (PicNuA4), consists of the proteins Esa1, Eaf6, Epl1, and Yng2 and is speculated to be a non-targeted lysine acetyltransferase of histone proteins H4 and H2A independent of the larger role of NuA4 (Boudreault et al., 2003; Friis et al., 2009). The recruitment module, which consists of the other members of the NuA4 complex, is thought to recruit the entirety of the NuA4 complex to specific substrates, including non-histone targets (reviewed in Doyon and Côté, 2004). For example the targeted interaction of the NuA4 complex with transcription factor protein Hap4 is mediated its through direct interaction with Tra1 (Brown et al., 2001).

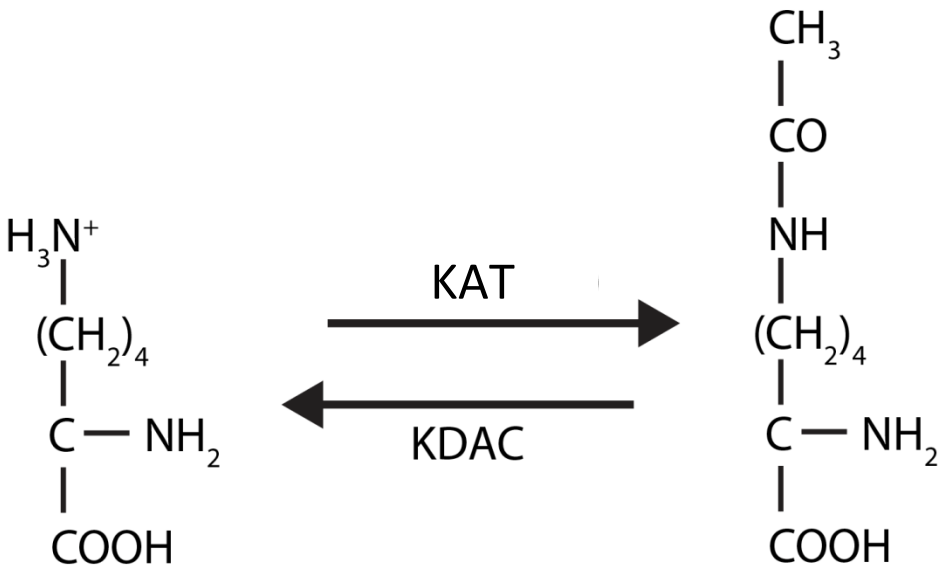
H3N+
(CH2)4
C — NH2
COOH
KAT
KDAC
CH3
CO
NH
(CH2)4
C — NH2
COOH

Figure 1: Acetylation and de-acetylation of a lysine residue. Schematic showing acetylation and deacetylation of a lysine residue by a lysine acetyltransferase (KAT) and a lysine deacetylase (KDAC).

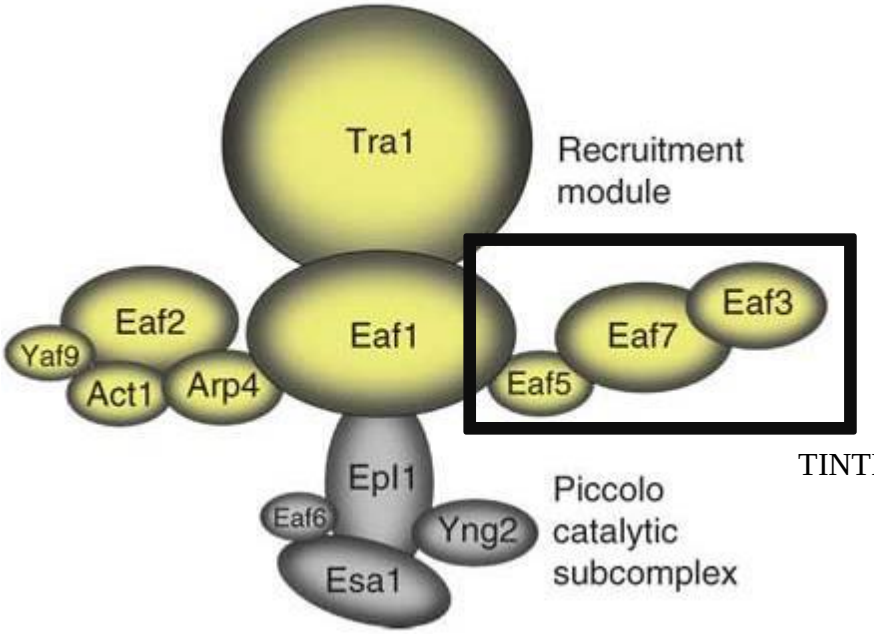
Tra1
Recruitment module
Eaf2
Yaf9
Act1
Arp4
Eaf1
Eaf7
Eaf3
Eaf5
Epl1
Eaf6
Yng2
Esa1
Piccolo catalytic subcomplex

TINTIN

Figure 2: Schematic of the NuA4 complex and subcomplexes. Adapted from (Chittuluru et al., 2011).

Within the recruitment module there is also the recently discovered subcomplex called "Trimer Independent of NuA4 involved in Transcription Interactions with Nucleosomes" (TINTIN), which consists of the proteins Eaf5, Eaf7, and Eaf3 (reviewed in Bhat et al., 2015; Cheng and Côté, 2014). Under standard cellular growth conditions, the TINTIN sub-complex is found to be both a part of the whole NuA4 complex as well as its own individual complex which functions independently of the greater whole. Like NuA4, TINTIN has been shown to localize to DNA, however the two complexes show different patterns of DNA interaction. NuA4 binding shows greater affinity for promoter regions of the DNA, while TINTIN has greater affinity across the gene coding region of the DNA. It has also been shown that TINTIN positively affects transcription through its interaction with RNA polymerase II by helping in the elongation of mRNA (Rossetto et al., 2014).

Given the working model that distinct subunits of NuA4 may play unique roles in substrate targeting, it is not unexpected that mutants of NuA4 subunits display varying phenotypes. Temperature sensitive alleles of the essential protein Esa1 have been generated, such as *esa1-L254P*, which renders the protein inactive upon culturing temperatures of 37 °C. Upon heat shift the *esa1-L254P* mutant cells displays defects in cell cycle control, where it arrests in G_2/M and also exhibits a decrease in H4 lysine acetylation (Clarke et al., 1999). Deletion of *EAF1* results in a drastic change to the complex integrity causing the separation of PicNuA4 from the recruitment module resulting in a variety of defects, including slow growth, impact on purine biosynthesis, transcription regulation, vesicle mediated transport, and septin dynamics (Auger et al., 2008; Cheng et al., 2015; Mitchell et al., 2008, 2011). In contrast, deletion of genes encoding the components of the TINTIN complex results in more subtle phenotypes. For example, *eaf7Δ* cells do not display significant growth defects under standard culture conditions, however this is not the case for certain stresses such as acute glucose deprivation (GD), where

stress granule formation is impeded (unpublished data of M. Rollins) as well as DMSO where the cells show sensitivity (Gaytán et al., 2013). While *eaf5Δ* cells have not been as extensively studied as *eaf7Δ* cells, both display similar genetic interactions profiles including with deletion of the protein Htz1, as well as deletions of genes that are a part of the Swr-C complex implying a similar role to Eaf7 (Krogan et al., 2004; Mitchell et al., 2008). In contrast, while *eaf3Δ* cells show some of these same interactors as Eaf5 and Eaf7(Mitchell et al., 2008), it also has more extensive and varied phenotypes and genetic interactions where the deletion mutant results in changes to specific sites of histone H4 acetylation (Reid et al., 2004), and inability to deacetylate histone H3 (Carrozza et al., 2005). These different phenotypes can potentially be explained by Eaf3 being a member of not just NuA4 and TINTIN, but also the KDAC complex Rpd3 providing it with contrasting roles within the cell (Gavin et al., 2002; Ho et al., 2002).

1.2 Regulation of NuA4 and human homolog Tip60 upon stress

Though the mechanisms are poorly defined it appears that the activity, localization and substrate specificity of NuA4, as well as its human homolog, the Tip60 complex, can be modulated by a variety of stresses. For example the protein levels of Tip60 complex protein Tip60 (homolog of Esa1) are stabilized in response to genotoxic stress or DNA damage (Dar et al., 2013; Peng et al., 2012). In contrast, Tip60 protein levels and cellular KAT activity decrease in response to stresses such as HPV E6 treatment, adenovirus, and HCMV (Gupta et al., 2013; Jha et al., 2010; Reitsma et al., 2011). Similar regulation of NuA4 subunit protein levels have been documented in yeast. NuA4-dependent acetylation of Yng2 at K170 masks an ubiquitin binding site preventing the degradation of Yng2. The protein levels of Yng2 are important under double stranded break conditions, where it, along with other members of the NuA4 complex, is recruited to the break. However after the initial recruitment to the site of the DNA damage, Yng2

is targeted for degradation by ubiquitination which allows for H4 deacetylation which may be required for efficient break repair (Lin et al., 2008).

In addition stress has been shown to impact the localization of NuA4 complex proteins. Under standard growth conditions NuA4 subunits have been found to be primarily localized to the nucleus (Huh et al., 2003). However upon nitrogen starvation a small subset of cellular pools of Esa1 and Epl1 have been shown to localize to pre-autophagosomal structures in the cytoplasm where NuA4 acetylates Atg3, a regulator of autophagy (Yi et al., 2012). This suggests that one mechanism by which NuA4 regulates substrate specificity is through localization to substructures within the cell. Further as many of NuA4's putative non-histone targets under standard growth conditions have localizations outside the nucleus it is likely that a fraction of NuA4 may localize to different cellular compartments (Downey et al., 2015; Lin et al., 2009; Mitchell et al., 2011, 2013).

1.3 Histone and non-histone targets of NuA4

The role of lysine acetylation has traditionally been limited to its effects on histone proteins and the weakening of DNA-histone interactions allowing for greater chromatin accessibility, thereby increasing transcription from the DNA at the opened loci. However it has recently been determined that lysine acetylation plays a global role in cellular signaling events beyond its regulation of transcription. Large scale acetylome studies have identified thousands of non-histone acetylation sites on a wide variety of proteins indicating that it may have a ubiquitous role within the cell as a regulatory tool (Choudhary et al., 2009; Downey et al., 2015; Henriksen et al., 2012; Mitchell et al., 2013).

The most well characterized substrates of NuA4 acetylation are the histone proteins H4 and histone H2A variant, Htz1. NuA4 has been shown to be the primary KAT for acetylation of lysines 5, 8, and 12 of histone protein H4, as well as lysine 14 of Htz1 (Allard et al., 1999;

Keogh et al., 2006). While Htz1 has an effect in promoting transcription (Guillemette and Gaudreau, 2006), and therefore NuA4 has a potential role in regulation of transcription through its acetylation of Htz1, this is likely not NuA4's sole regulatory role. mRNA microarray analysis has shown that NuA4's effect on the transcriptome is relatively minor in comparison to the phenotypes of *esa1ts* mutants (Choy et al., 2001; Krogan et al., 2004; Lindstrom et al., 2006; Zhang et al., 2004). Though the impact of NuA4 on cellular function through histone acetylation cannot be ruled out, protein microarrays and proteomic studies have identified over 200 *in vivo* and *in vitro* putative targets of NuA4 acetylation indicating a potential wide spread regulatory role on other proteins (Downey et al., 2015; Lin et al., 2009; Mitchell et al., 2013). In addition to these targets of NuA4, deletion mutants of the complex have shown defects in a variety of cellular processes including: transcription (Doyon et al., 2004), DNA damage repair (Bird et al., 2002), cell cycle (Choy et al., 2001; Clarke et al., 1999), stress response (Lindstrom et al., 2006; Mitchell et al., 2008), vesicle mediated transport (Mitchell et al., 2008), autophagy (Yi et al., 2012), septin dynamics (Mitchell et al., 2011), spindle dynamics (Mitchell et al., 2013), chromosome segregation (Baetz et al., 2004), and glucose metabolism (Lin et al., 2009; Lu et al., 2011).

1.4 NuA4's known role in glucose regulation

Glucose is the preferred carbon energy source of *S. cerevisiae* and as such it will be used whenever it is available over other carbon sources (Ullmann, 1996). In the presence of glucose the cell will go through fermentation to produce ATP, and not continue through to aerobic respiration as long as glucose is still available. As a result the ability to sense changing levels of glucose is essential to the cell as this allows for differential regulation of proteins directly related

to glucose metabolism, such as cytochrome proteins, which are transcriptionally downregulated in high glucose conditions as they are not utilized (reviewed in Johnston, 1999; Towle, 2005).

NuA4 has been shown to have a direct impact on regulation of glucose metabolic pathways through its differential acetylation of two proteins, Sip2 and Pck1 (Figure 3). Sip2 is a member of the Snf1 (yeast AMPK) kinase complex. The Snf1 kinase complex acts to regulate both transcription and protein localization through its phosphorylation of proteins in response to changes in glucose availability. For example the Snf1 complex regulates Mig1, a transcriptional repressor of over 90 genes under standard glucose conditions (reviewed in Santangelo, 2006). Under low glucose levels Snf1 prevents the transcriptional repression of Mig1 by phosphorylating it which results in Mig1 detachment from the repressed genes and changing its localization from the nucleus to the cytoplasm (García-Salcedo et al., 2014; Treitel et al., 1998). The Snf1 complex itself consists of three different subunits, the catalytic Snf1 protein, the γ protein Snf4 (an activator of the complex), and one of three β subunits, which includes the protein Sip2 a repressor of Snf1 kinase function (reviewed in Ghillebert et al., 2011). Under standard growth conditions Sip2 is acetylated by NuA4. This acetylation leads to a high affinity interaction between Sip2 and Snf1 leading to an inactivation of Snf1 kinase activity. However upon low glucose conditions Sip2 acetylation is decreased, resulting in a less favourable interaction between Sip2 and Snf1. This decrease in interaction allows the Snf1 complex to become active and phosphorylate its target proteins, leading to downstream expression of glucose repressed genes (Lu et al., 2011).

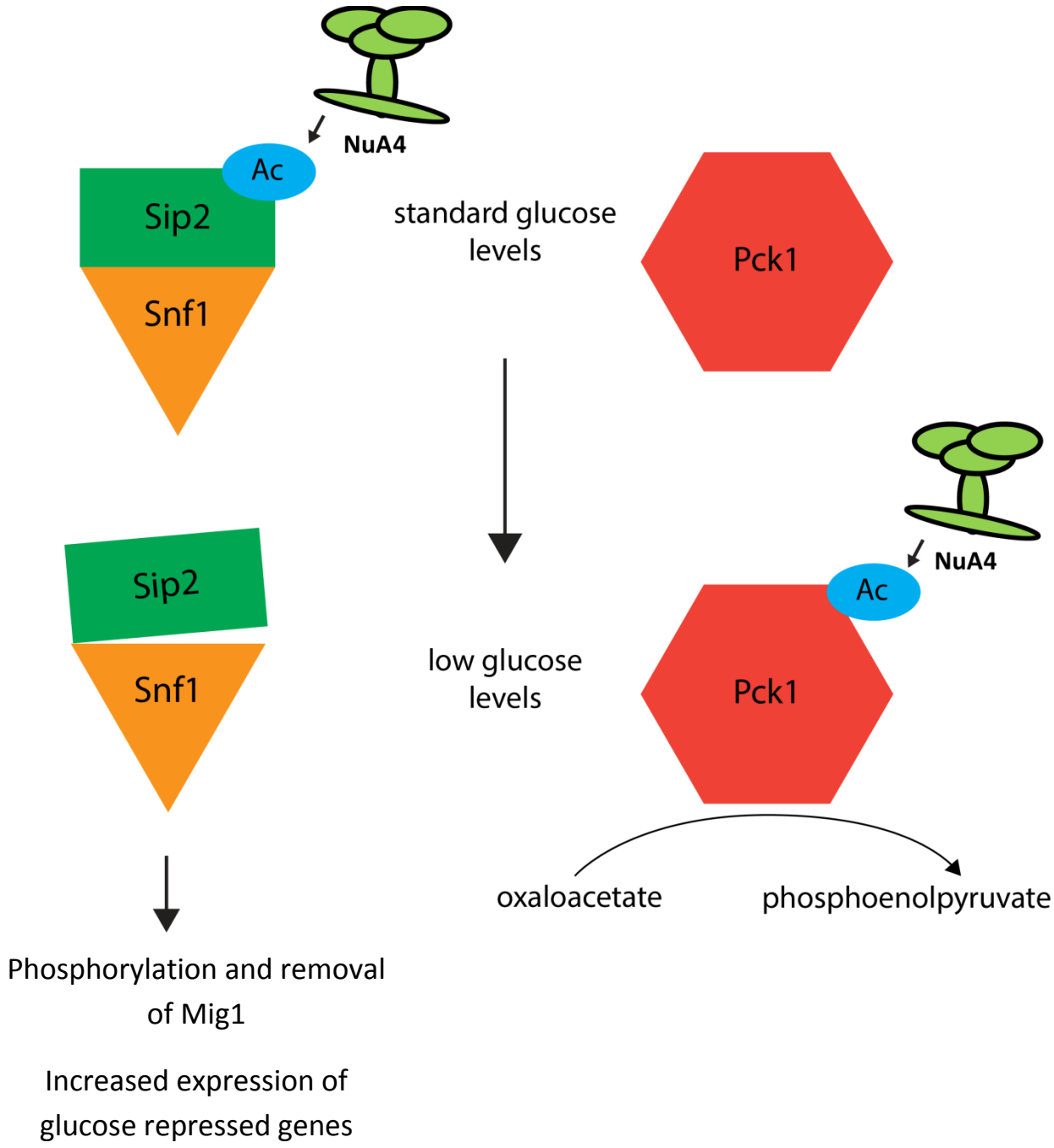
NuA4
Ac
Sip2
Snf1
standard glucose levels
Pck1
Sip2
Snf1
low glucose levels
NuA4
Ac
Pck1
oxaloacetate
phosphoenolpyruvate
Phosphorylation and removal of Mig1
Increased expression of glucose repressed genes

Figure 3: Model of NuA4-dependent regulation of Sip2 and Pck1 by acetylation. Under normal glucose conditions Sip2 is acetylated by NuA4 resulting in a stronger interaction between Sip2 and Snf1 which inhibits Snf1's kinase activity. This repression of Snf1 prevents it from phosphorylating proteins like Mig1 allowing for its removal and expression of glucose repressed genes. Under low glucose conditions Pck1 is acetylated by NuA4, which allows for activation of Pck1 enzymatic activity, resulting in the progression of the gluconeogenesis pathway in order to produce greater amounts of glucose so that the cell may extract energy from them.

Pck1 is a rate limiting enzyme in the gluconeogenesis pathway, which converts oxaloacetate and ATP to phosphoenolpyruvate, ADP, and carbon dioxide. This pathway is needed to generate glucose from non-fermentable carbon sources under low glucose conditions to allow for process that require glucose to maintain function in response to the stressed condition. Under low glucose conditions Pck1 is acetylated by NuA4 which leads to an increase in enzymatic activity, allowing for an increase in cellular glucose levels (Lin et al., 2009).

While these two proteins show regulatory roles of NuA4 with response to glucose deprivation, they also hint to a potential greater role of NuA4 in response to stress. These two proteins are acetylated under opposing glucose availability conditions, with Sip2 being acetylated under standard glucose conditions, and Pck1 being acetylated upon low glucose availability. NuA4 is thereby shown to be active under both glucose replete and glucose depleted conditions (Figure 3). This indicates that NuA4 changes substrate specificity during different cellular conditions, and that there is differential protein acetylation in response to these changes in conditions.

In addition, glucose levels have an effect on histone acetylation. Known NuA4 acetylation targets histone H4 lysines 5, 8, and 12 are differentially acetylated in response to cellular glucose levels (Allard et al., 1999). During stationary phase, or prolonged glucose deprivation, these lysine sites as well as total H4 lysine acetylation decrease globally within the cell as determined by a hyperacetylated H4 antibody (Friis et al., 2009; Sandmeier, 2002). It has also been determined that upon reintroduction of glucose to quiescent cells, an increase in acetylation at these same acetylation sites, as well as total H4 lysine acetylation by NuA4, is seen within one hour (Friis et al., 2009). It is not however known what happens to these H4 acetylation sites upon acute GD.

1.5: Expanding on the regulation and regulatory role of NuA4 upon glucose deprivation

NuA4 has a wide spread impact within the cell, across numerous processes including known regulatory roles of glucose metabolic proteins (Lin et al., 2009; Lu et al., 2011). While the known roles provide context to NuA4's regulatory function, they do not provide the entire scope of NuA4's activity, nor do they provide an in depth characterization as to what happens to NuA4 in response to acute glucose-deprivation stress. Given the conservation of KATs, discerning how NuA4 substrate specificities and/or activity are modulated upon stresses such as acute GD may provide novel insight into KAT biology and regulation. This is especially important given that Tip60 has been implicated in numerous diseases, including cancer, and neurodegeneration (Sapountzi et al., 2006; Su et al., 2016; Sun et al., 2010; Xu and Elefant, 2015). Misregulation of Tip60 appears to have multiple effects in cancer. It has been shown to be both down and upregulated in a variety of cancers such as colorectal cancer, gastric cancer and acute myeloid leukemia, which all show decreased expression, while prostate cancer shows an increased expression (reviewed in Halkidou et al., 2003; Sakuraba et al., 2009, 2011; Zhao et al., 2012). Further Tip60 function has direct effects on different diseases, such as cancer, through its acetylation of transcription factor and known cancer suppressor p53 (Soussi et al., 1994; Tang et al., 2006). Tip60 has also been shown to play a role in the response to double strand DNA breaks, where its acetylation of different histones allows for opening up of the DNA which is required in the response (reviewed in Xu and Price, 2011).

Given the breadth of potential targets and cellular roles of NuA4 in both the healthy and disease state, it is imperative to being to understand the mechanisms through which NuA4 activity and substrate selectivity are regulated. In order to accomplish this objective our lab has previously characterized the protein-protein interactors, as well as acetylation targets of NuA4

under standard growth conditions. The research presented here was conducted to expand on these findings by attempting to discern the effect of GD on the cell and the role that NuA4 plays in response to it. It is imperative to understand the role of GD within the cell to gain a greater understanding of the regulatory mechanisms in the cell and how the cell adapts to this stress.

HYPOTHESIS:

I hypothesize that upon glucose deprivation the NuA4 complex will change in abundance, remodel its structure, change in activity, or change in localization. Using a combined approach of cell biology, biochemistry, and proteomics I propose:

Aim 1: To determine the impact of glucose deprivation on Esa1-TAP protein levels, NuA4 complex composition, *in vivo* H4 acetylation levels, and Esa1-GFP localization.

Aim 2: To determine the impact of glucose deprivation on Esa1-TAP interactome and acetylome.

Aim 3: To characterize the interactions of Esa1with protein interactors Pab1, TINTIN and Fatty acid synthetase complex proteins Fas1 and Fas2.

Together these aims seek to address if acute glucose deprivation impacts the complex integrity, activity or substrate specificity of the NuA4 complex.

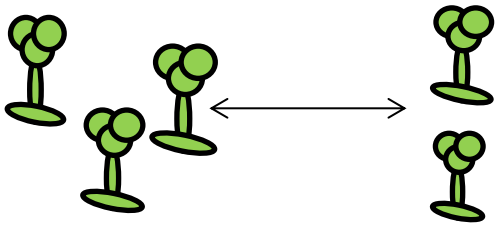

Change in complex abundance

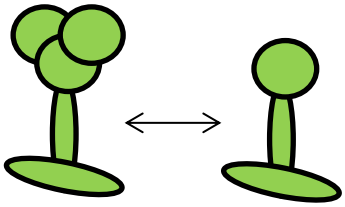

Change in complex structure

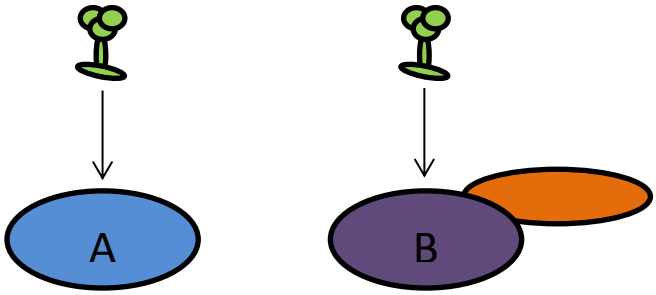

Change in interactions, and acetylation

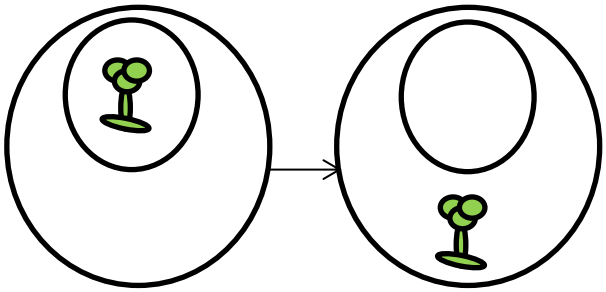

Change in localization

Figure 4: Schematic representing potential modes of regulation of NuA4 and its interactors upon glucose deprivation stress.

2. MATERIALS AND METHODS

2.1: Yeast strains

Yeast strains used to generate the results in this thesis are listed in Table S2.

Strains constructed for this study were generated by using standard PCR-mediated technique as previously described (Longtine et al., 1998) and were confirmed by PCR, western blot, and microscopy.

2.2 Yeast cell culture growth, and glucose deprivation

Yeast strains were grown in YPD media (1% yeast extract, 2% peptone, and 2% dextrose) for standard growth conditions and YP media (1% yeast extract, 2 % peptone) for glucose deprived (GD) conditions unless otherwise indicated. The yeast cell culture growth was conducted at 30 °C unless otherwise indicated. For GD experiments strains were grown overnight in YPD at 30 °C, re-suspended at an OD_{600} (optical density at 600 nm) of 0.1 in YPD, and grown at 30 °C to mid-log phase (OD_{600} of 0.5-0.8) prior to being harvested by centrifugation (3 min, 3000 rpm, 4 °C), washed in YP or YPD media, re-harvested by centrifugation, and re-suspended in either YP or YPD media for the allotted time points of GD. The samples were then harvested, frozen in liquid nitrogen and stored at -80 °C.

Cell cultures for microscopy were first grown in YPD overnight at 30 °C, and then resuspended in 50 mL of YPD at an OD_{600} (optical density at 600 nm) of 0.1 and grown at 30 °C to mid-log phase (OD_{600} of 0.5-0.8). From these cultures 1 mL of the sample was harvested and resuspended in 20 µL of synthetic complete (SC) media (0.67% yeast nitrogen base without amino acids, 2% glucose, 0.2% amino acid mixture) for imaging. After imaging the cell culture was then harvested by centrifugation (3 min, 3000 rpm, 22 °C) and resuspended in warmed (30

°C) YP media for GD. 1 mL from this culture was then harvested in and resuspended in 20 µL of SC media without glucose for imaging.

2.3 Immunoprecipitation of Tandem Affinity Purification (TAP) tagged proteins

2.3.1 Lysis of whole cell extracts and co-IPs by modified chromatin immunoprecipitation

Cell lyses performed to obtain either whole cell extracts (WCE) or lysates for co-IP were obtained through the use of the previously established modified chromatin immunoprecipitation (mChIP) protocol (Lambert et al., 2009). Briefly, mid-log phase cells (OD_{600} of 0.5-0.8) from YPD cultures of 25 to 250 mL were collected by centrifugation (3 min, 3000 rpm, 4 °C), washed in 25 mL of ice-cold water, transferred to 1.5mL Eppendorf tubes, pelleted, and frozen in liquid nitrogen and stored at -80 °C. For lysis the cell pellets were re-suspended in an equal volume of cold mChIP lysis buffer (100mM HEPES (pH 8.0), 20mM magnesium acetate, 300mM sodium acetate, 10% glycerol (v/v), 10mM EGTA, 0.1mM EDTA) supplemented with protease inhibitors (cOmplete Tablets, mini EDTA-free Sigma; cat. no. P8215; 1 tablet/10mL of buffer) and KDAC inhibitors (Nicotinamide: Sigma; cat. no.72340; 500ul of 1M solution /10mL of buffer and Sodium Butyrate: Sigma; cat. no. B5887; 500ul of 1M solution/10mL of buffer). Acid washed glass beads (Fisher Scientific, USA; cat. no. 35-535) were added to this solution to completely cover the sample in beads. The cells were lysed by vortexing for 1 minute intervals 6 to 8 times to achieve approximately 75 % cell lysis with 1 minute incubation on ice in between each vortex. Whole cell lysates were then isolated from the beads by poking a hole in 1.5 mL Eppendorf tubes and placing these tubes into new 1.5 mL tubes. The lysates were subsequently centrifuged (2 min, 1000 rpm, 4 °C) to isolate them from the beads. All same lysates were then combined and put into new 1.5 mL Eppendorf tubes. The lysates were then sonicated 3 times for 20 second intervals using a Misonix Sonicator 3000 at setting 4 with 1 minute incubations on ice

between sonications. Nonidet P-40 (NP-40) was then added to each lysate to a concentration of 1% (v/v). The samples then underwent end to end rotation (10 min, 4 °C) and clarification by centrifugation (10 min, 3000 rpm, 4 °C) was then performed. Protein concentrations were then measured using Bradford reagent (Bio-Rad, USA; cat. no. 500-0006) and the lysate was normalized to get 20 mg/mL of protein WCE.

For purification of TAP tagged proteins, 20 mg of WCE was incubated with magnetic beads (Dynabeads Invitrogen; cat. no. 143-01) cross-linked to rabbit immunoglobulin G (IgG) (Chemicon; catalog no. PP64). 25 µL of magnetic beads were used per 10 mg of protein purified. WCEs were incubated with beads for 2 hours under end to end rotation at 4 °C. After incubation the beads were collected with a magnet and washed three times using 1 mL of cold mChIP wash buffer (100mM HEPES (pH 8.0), 20mM magnesium acetate, 300mM sodium acetate, 10% glycerol (v/v), 10mM EGTA, 0.1mM EDTA), 0.5% NP-40 (v/v)). After each wash the sample was transferred to a new 1.5 mL Eppendorf tube. After the third wash 40µl of 1x loading buffer [50mM Tris pH 6.8, 2% SDS, 0.1% bromophenol blue, 10% glycerol] was added to the beads and proteins were eluted from the beads (10 min, 65 °C). The sample was then briefly spun, and placed on a magnet and removed from the magnetic beads. The loading buffer was then transferred to a new 1.5 mL Eppendorf tube, and 2-β-mercaptoethanol was added to a concentration of 200mM.

2.3.2 Trichloroacetic Acid Lysis

Trichloroacetic acid (TCA) lysis was performed as previously described (Kao and Osley, 2003). Briefly cells from 50 mL mid-log phase cultures (OD_{600} of 0.5-0.8) were collected by centrifugation (3 min, 3000 rpm 4 °C), and then washed in 25 mL of ice-cold water, transferred to 1.5mL Eppendorf tubes, pelleted, frozen in liquid nitrogen, and stored at -80 °C. For experiments requiring glucose deprivation, cultures were resuspended in media lacking glucose

as previously described in section 2.2. Pellets were lysed by first thawing them on ice and then resuspending them in 200 µL of cold 20% TCA lysis buffer. Acid washed glass beads (Fisher Scientific, USA; cat. no. 35-535) were then added to this solution to completely cover the sample in beads. The cells were lysed by vortexing for 1 minute intervals 6 to 8 times to achieve approximately 75 % cell lysis with incubation on ice for 1 minute in between vortexing. Whole cell lysates were then isolated from the glass beads by poking a hole in 1.5 mL Eppendorf tubes and placing these tubes into new 1.5 mL tubes. The lysates were subsequently centrifuged (1 min, 4000 rpm 4 °C) to collect the lysate. The glass beads were then washed with 500 µL of 5% TCA lysis buffer and centrifuged under the same conditions. The pellet was then resuspended in the buffer and incubated on ice for 15 minutes. The extracts were then centrifuged (15 minutes, 132000 rpm, 4 °C) and the supernatant was discarded. Pellets were then resuspended in 350 µL of 1x loading buffer [50mM Tris pH 6.8, 2% SDS, 0.1% bromophenol blue, 10% glycerol, 200mM β-2-mercaptoethanol]. 1M Tris buffer (50 µL pH 8.8) was then added to the solution.

2.3.3 Stringent purification of the NuA4 complex

For stringent purification of the NuA4 complex, a one-step purification of NuA4 was performed following a previously established protocol (Mitchell et al., 2008). Briefly, cells from 250 mL mid-log phase cultures (OD_{600} of 0.5-0.8) were collected by centrifugation (3 min, 3000 rpm, 4 °C), washed in 25 mL of ice-cold water, transferred to 1.5mL Eppendorf tubes, pelleted and frozen in liquid nitrogen and stored at -80 °C. The cells were then re-suspended in an equal volume of Tackett extraction lysis buffer (20 mM HEPES, pH 7.4, 0.1% Tween 20, 2 mM $MgCl_2$, 300 mM NaCl, protease inhibitor cocktail [Sigma; cat. no. P-8215]). Acid washed glass beads (Fisher Scientific; cat. no. 35-535) were then added to the sample to completely cover the sample itself. The samples were then vortexed for 1 minute intervals 6 to 8 times to achieve approximately 75% cell lysis with incubation on ice for 1 minute intervals in between vortexing.

The soluble whole cell extract was then isolated by centrifugation (15 minutes, 13200 rpm, 4 °C). Protein amounts in the lysate were subsequently ascertained by using Bradford reagent (Bio-Rad, USA; cat. no. 500-0006) and the lysate was then normalized to 20 mg/mL of protein.

20 mg of WCE was then incubated with 50 µL of magnetic beads (Dynal, Invitrogen; cat. no. 143-01) crossed-linked to rabbit immunoglobulin G (IgG) (Chemicon; cat. no. PP64) for a two-hour incubation at 4 °C under end to end rotation. After incubation the beads were collected with a magnet and washed 5 times using 1 mL of wash buffer (20 mM HEPES, pH 7.4, 0.1% Tween 20, 2 mM $MgCl_2$, 300 mM NaCl) changing the 1.5 mL Eppendorf tubes each wash. After the final wash, the beads were re-suspended in 40µl of 1x loading buffer [50mM Tris pH 6.8, 2% SDS, 0.1% bromophenol blue, 10% glycerol] and then incubated (10 min, 65 °C) to elute the tagged protein and its interactors. The sample was then briefly spun and placed on a magnet to separate it from the magnetic beads. The loading buffer was transferred to a new tube and 2-β-mercaptoethanol was added to a concentration of 200mM. The sample was then resolved on a NuPAGE Novex gradient SDS/PAGE 4–12% Bis-Tris Protein Gels (Invitrogen; cat. no. NP0321) and silver stained.

2.4 Esa1-TAP Glucose Deprivation Interactome

An Esa1-TAP mChIP interactome was constructed from 3 replicates of the mChIP-KAT-MS protocol generated as previously described (Mitchell et al., 2013), with the following modifications. Briefly, Esa1-TAP, as well as wild type strain yeast cultures were grown overnight in YPD at 30 °C prior to being diluted into 4 L of YPD media to an OD_{600} of 0.1 and grown to mid-log phase (OD_{600} 0.6-0.8) at 30 °C. The cells were then harvested (3 min, 3000 rpm, 4 °C) resuspended in either YPD or YP media prior to re-harvesting and re-suspended in 4 L total of the corresponding media for incubation periods of 30 minutes of YPD, and 10, 30, and

60 minutes in YP. After the designated incubation period, cells were harvested, washed in 25 mL of cold water, harvested and pelleted in Eppendorf tubes, and frozen in liquid nitrogen prior to being stored at -80 °C.

Cells were subsequently lysed following the mChIP protocol (section 2.3.1) and 100 mg of protein was immunoprecipitated per sample. Ten percent of the IP sample was then removed to be run by SDS PAGE. The rest of the samples were subsequently washed, and re-suspended in 1× KAT buffer (50 mM Tris pH 8.0, 50 mM NaCl, 5 mM MgCl2, 1 mM DTT), after which it was subjected to a KAT reaction with isotopically labelled acetyl-CoA for 1 hour with end over end rotation. Following this, the samples were sent for mass spectrometry analysis which was performed by the Gingras lab at the University of Toronto.

The mass spectrometry analysis was performed using previously established methods (Lambert et al., 2015). Briefly the samples were suspended in 7.5 μL of 20 mM Tris–HCl (pH 8.0) containing 750 ng of trypsin (Sigma, T7575) and the mixture was incubated at 37 °C with agitation overnight. Another 250 ng of trypsin was added to the mixture and further digested, without agitation, for 3–4 hours. The sample was acidified with formic acid to a final concentration of 2% and the tryptic digests were stored at − 40 °C until ready for mass spectrometry analysis. The sample was then separated by HPLC using 5 μL of sample loaded at 400 nL/min onto a 75 μm × 12 cm emitter packed with 3 μm ReproSil-Pur C_{18}-AQ (Dr.Maisch HPLC GmbH, Germany). The peptides were eluted from the column over a 90 min gradient generated by a NanoLC-Ultra 1D plus (Eksigent, Dublin CA) nano-pump and analyzed on a TripleTOF™ 5600 instrument (AB SCIEX, Concord, Ontario, Canada). The gradient was delivered at 200 nL/min starting from 2% acetonitrile with 0.1% formic acid to 35% acetonitrile with 0.1% formic acid over 90 min followed by a 15 min clean-up at 80% acetonitrile with 0.1%

formic acid, and a 15 min equilibration period back to 2% acetonitrile with 0.1% formic acid for a total of 120 min. To minimize carryover between each sample, the analytical column was washed for 3 h by running an alternating sawtooth gradient from 35% acetonitrile with 0.1% formic acid to 80% acetonitrile with 0.1% formic acid, holding each gradient concentration for 5 min. The instrument method was set to a discovery or IDA mode which consisted of one 250 ms MS1 TOF survey scan from 400 to 1300 Da followed by twenty 100 ms MS2 candidate ion scans from 100 to 2000 Da in high sensitivity mode. Only ions with a charge of 2 + to 4 + which exceeded a threshold of 200 cps were selected for MS2, and former precursors were excluded for 10 s after 1 occurrence.

The Esa1-TAP glucose deprivation interactome and acetylome was created using the mass spectrometry dataset which was produced (dataset found in Table S1). Protein interactors were included in the interactome if they were identified as being reproducible which was defined as two or more spectral counts being identified to interact with Esa1-TAP in at least two of three replicates in a single condition. All acetylations identified on interacting proteins were included in this analysis. In order to determine changes in interaction upon glucose deprivation, spectral counts of each protein were normalized to the spectral count of Esa1-TAP in that replicate and condition, at which time the three normalized values from each condition were averaged. A ratio was then determined between the YPD and the GD condition to identify changing interactions. Proteins that had a greater than two-fold increase or decrease in interaction with Esa1-TAP upon glucose deprivation were then included to determine the interactome.

2.5 GO term analysis

GO term enrichment analysis was performed using the DAVID database (Huang et al., 2009a, 2009b). The database of yeast proteins used to perform this analysis was the Saccharomyces

Genome Database which consists of 6604 open reading frames (Cherry et al., 2012). Enrichments were performed on the changing Esa1-TAP interactome for each of the YPD, 10, 30, and 60 minutes of GD tested. All GO terms with a p-value greater than 0.05 were included in the analysis.

2.6 Gel electrophoresis and Western blotting

Protein samples in loading dye of either WCE or IP were boiled (10 min, 95 °C) prior to loading. The samples were then resolved on either SDS-PAGE (sodium dodecyl sulphate-polyacrylamide gel electrophoresis) gels, TGX Stain-Free™ FastCast™ Acrylamide Kit, 7.5% (BioRad; cat. no. 161-0181), or NuPAGE Novex gradient SDS/PAGE 4–12%Bis-Tris Protein Gels (Invitrogen; cat. no. NP0321). Following separation, proteins were transferred for 5-12 minutes on to pure nitrocellulose blotting membranes (PALL, Pall Corporation; cat. no. 66485) or pure PVDF blotting membranes (Immobilon; cat. no. IPVH00010) using a Trans-Blot Turbo Transfer System (Bio Rad; cat. no. 1704155). Membranes were subsequently blocked in 5% milk in a sodium phosphate buffer with 1% Tween 20 (PBST) for 30 minutes at room temperature, followed by incubation in 5% milk PBST to which the primary antibody was added at 4 °C overnight. Primary antibody dilutions are as follows: α-GFP (Roche; cat. no. 11814460001; dilution 1/3000-1/2000); α-TAP (Thermo Scientific; cat. no. CAB1001; dilution 1/5000); α-HA (Covance; cat. no. MMS-101P; dilution 1/1000); α-Pab1 (EnCor Biotechnology; cat. no. MCA-1G1; 1/5000) α-G6PDH (Sigma; cat. no. A9521 1/10,000) α-hyperacetylated histone H4 (Penta) (Millipore; cat. no. 06-946; dilution 1/1000), α-acetyl histone H4 (Lys 5) (Millipore; cat. no. 07-327; dilution 1/5000), α-acetyl histone H4 (Lys 8) (Millipore; cat. no. 07-328; dilution 1/1000), and α-acetyl histone H4 (Lys 12) (Millipore; cat. no. 07-595; dilution 1/1000) α-histone protein H3, CR, pan, clone A3S (Millipore; cat. no. 05-928; dilution 1/1000). After primary antibody incubation, the blots were washed three times for 10 minutes each in PBST at room temperature,

and then incubated for 2 hours at room temperature in 5% milk to which the secondary HRP conjugated antibody was added as indicated: goat α-mouse IgG (Thermo Fisher; cat. no. A24518; dilution 1:5000-1:10000), goat α-rabbit IgG (Thermo Fisher; cat. no. A24537, 1:5000-1:10000), goat α-mouse IgG (BioRad; cat. no. 170-6516, 1:5000), and goat α-rabbit IgG (Chemicon; cat. no. AP307P, 1:5000). Membranes were developed using the Western Chemiluminescent HRP Substrate Detection System (Millipore; cat. no. WBKLS0500). Membranes were imaged using a Chemi-Doc™ MP system (BioRad; cat. no. 1708280) or LI-COR Odyssey FC imaging system (LICOR Biosystems).

2.7 Western blot quantification

Relative quantification of western blots was completed using LI-COR technology. Briefly, the western blots of interest, as well as the loading controls, were converted to grey scale. A box was then drawn to sufficiently cover the entirety of the band of interest. The same box was then copied to cover all other bands of interest in the different conditions. The same technique was also used for the loading controls. The signal produced by each band was then quantified relative to background intensity. A ratio was subsequently determined between the sample of interest and the loading control to give relative quantity of protein signal. The samples were then normalized relative to the quantity of the YPD condition. Finally, averages of three independent replicates were produced to display the relative amount of the protein of interest (A. Schutz-Geschwender, Y. Zhang, T. Holt, D. Mcdermitt, et al. 2004). Statistical significance was determined through the use of ANOVA were applicable with a p-value of 0.05 being the threshold for significance.

To further validate our protein detection levels the new TGX Stain-Free™ FastCast™ Acrylamide Kit, 7.5% was utilized (BioRad; cat. no. 161-0181) (Taylor et al., 2013). Briefly, gels were cast following the protocol outlined by the kit. Upon completion of SDS-PAGE, the gel is imaged on a Chemi-Doc™ MP system (BioRad; cat. no. 1708280) using Image Lab™ software (BioRad; cat. no. 1709690) under UV light to allow a halocompound in the acrylamide to crosslink to tryptophan residues of protein in the gel. The halocompound can then be visualized to determine the total protein loaded within each gel lane. The proteins were then transferred and western blot analysis was performed following the same procedure previously outlined until the final wash. Next the blots were exposed on the Chemi-Doc™ MP system (BioRad; cat. no. 1708280) and the total protein loaded in the lane, as determined using the halocompound was used for blot quantification. The quantification is performed by first drawing a box to sufficiently cover the entirety of the band of interest. Next the peaks of the bands of interest were outlined to obtain the quantity of band signal. A ratio is then obtained by comparing the band signal to the whole lane signal. The samples were then normalized relative to the quantity of the first condition. Finally, relative values of three independent replicates were averaged to display the relative amount of the protein of interest (Taylor et al., 2013, 2014). Statistical significance was measured by ANOVA or T-test where applicable with a p-value of 0.05 being the threshold for significance.

2.8 Microscopy

Microscopy of yeast cultures was completed using a Leica DMI 6000 florescent microscope (Leica Microsystems GmbH, Wetzler Germany) equipped with a Hamamatsu Orca AG camera (Hamamatsu Photonics, Herrsching am Ammersee, Germany). [Microscope features:

Sutter DG4 light source (Sutter Instruments, USA), Ludl emission filter wheel equipped with Chroma bandpass emission filters (Ludl Electronic Products Ltd., USA)].

Yeast cultures were prepared for imaging by growth in YPD media to mid-log phase (OD_{600} 0.6-0.8) prior to being harvested (3 minutes, 3000 rpm, 22 °C), washed in synthetic complete (SC) media, re-suspended in SC media and then imaged. For GD Cells were subsequently centrifuged (3 minutes, 3000 rpm, 22 °C), washed in YP media, re-suspended in pre-warmed (30 °C) YP media, and incubated for the specified times of glucose deprivation. Upon completion of the GD time course, the cells were harvested and re-suspended in SC media without glucose for imaging. For all time points of imaging, 7 µL of media was spotted onto a glass plate and imaged immediately. Z-stacked images were obtained using Volocity 4.3.2 (Perkin Elmer) using a 63x objective without binning.

2.9 Microscopy Image quantification

Microscopy image quantification was performed by Hilary Phenix of the Kaern lab. The quantification was done using a MATLAB program. Quantification was done by first identifying the image from the z-stack in bright field with the focus most amenable to cell identification. Once the image was identified, the optimal intensity threshold was chosen to optimize cell identification. The corresponding GFP images were subsequently corrected for background fluorescence by subtracting from each pixel the median fluorecsence from non-cell pixels in the image. Each identified cell then had its total corrected GFP pixel and cell area totalled. Finally, a ratio between the two was determined to identify changes in total GFP tagged protein expression on average per cell. Eighty cells or more were imaged for each condition.

2.10 RNase treatment

RNase treatment was performed prior to immunoprecipitation of Tandem Affinity Purification (TAP) tagged proteins as outlined in 2.3.1. Briefly cell pellets were lysed according to the mChIP lysis protocol (2.3.1) up until the addition of magnetic beads. At this point RNase A (Thermo Fisher; cat. no. 12091-021) was added at a dilution of 100 µg/mL to the lysate and incubated for 30 minutes at 4 °C . After incubation the sample was split with one half being used for mChIP (2.3.1) and the remainder being used for confirmation of RNA degradation from the sample. The RNA degradation was confirmed by purifying RNA using a PureLink RNA Mini Kit (Life Technologies; cat. no. 12183018A) and then resolving the RNA samples by gel electrophoresis on a 1% agarose gel. The RNA was then visualized using SYBR Safe gel stain (Invitrogen; cat. no. S33102) on a Chemi-Doc™ MP system (BioRad; cat. no. 1708280).

3. RESULTS

3.1 Aim 1: To determine the impact of glucose deprivation on Esa1-TAP protein levels, NuA4 complex composition, *in vivo* H4 acetylation levels, and Esa1-GFP localization.

3.1.1 Acute glucose deprivation does not impact Esa1-TAP protein levels.

As NuA4 has been previously established as a regulator of different glucose metabolic pathways (Lin et al., 2009; Lu et al., 2011), I first sought to determine if the complex itself is regulated in response to acute glucose deprivation stress. To begin this analysis I first chose to determine if acute glucose deprivation impacts the protein level of Esa1, the catalytic subunit of the NuA4 complex. The experiment was performed using a wildtype (WT) strain and one with endogenously integrated Esa1-TAP Gds1-HA. Briefly cell cultures of these strains were grown to mid-log phase under standard growth conditions, harvested and then resuspended in either YPD (glucose replete) for continued growth for 30 minutes (0 minutes GD), or transferred to glucose deprived (GD) media for 10, 30, and 60 minutes prior to being harvested and frozen in liquid nitrogen. The cell pellets were then lysed and the whole cell extracts (WCE) were then resolved by SDS PAGE using the TGX Stain-Free™ FastCast™ Acrylamide Kit to allow for quantitative western blot analysis (Taylor et al., 2013, 2014). To determine if the GD treatment was effective Gds1-HA protein levels were used as a positive control as Gds1 rapidly decreases in the WCE upon a variety of stresses including acute GD (unpublished data, M. Cotrut). The GD treatment was effective, as Gds1 is only detectable in the YPD condition and not under any GD stress time points (Figure 5). Despite the effectiveness of the treatment, the protein levels of Esa1-TAP show no significant difference between YPD and any time point of GD (p-value . These results indicate that acute GD has no direct regulatory impact on Esa1-TAP protein levels.

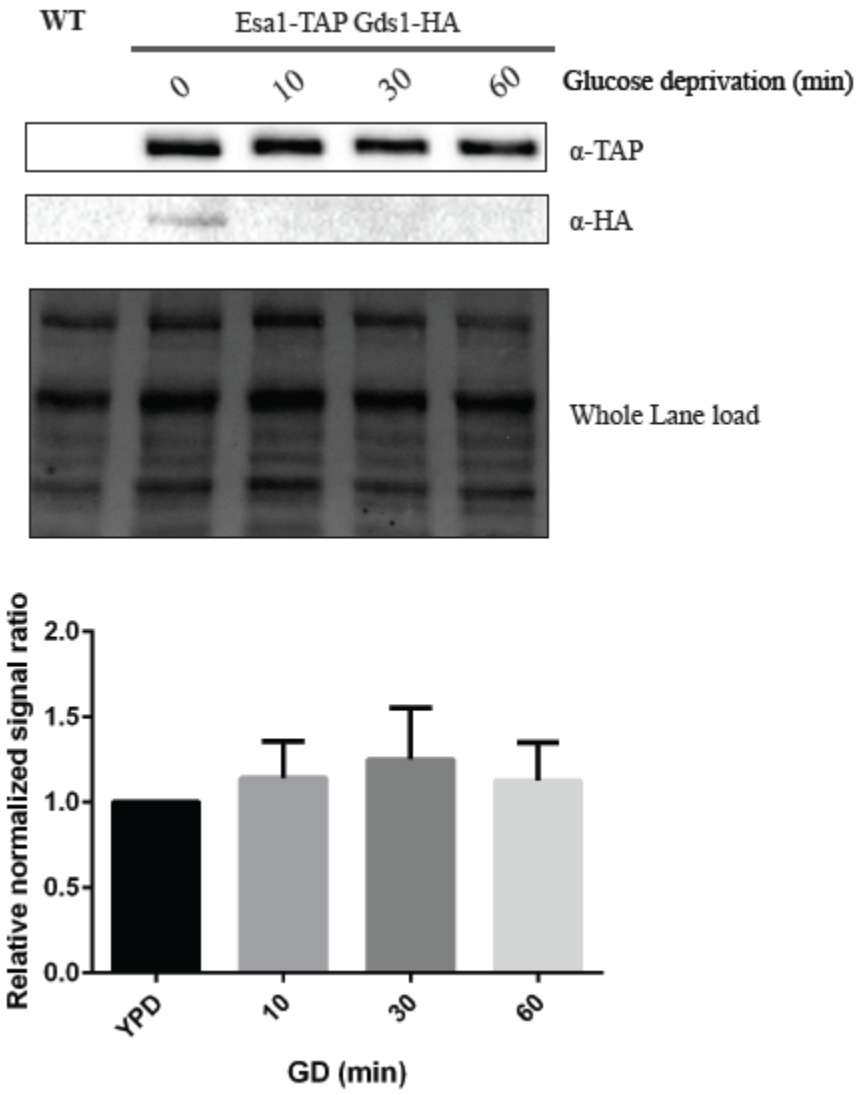
WT
Esa1-TAP Gds1-HA
0
10
30
60
Glucose deprivation (min)
α-TAP
α-HA
Whole Lane load
Relative normalized signal ratio
2.0
1.5
1.0
0.5
0.0
YPD
10
30
60
GD (min)

Figure 5: Glucose deprivation does not significantly impact the protein levels of Esa1-TAP. (A) Cell cultures of wildtype (WT, YKB1079) and *ESA1-TAP GDS1-HA* (YKB3941) were grown to mid-log phase at 30 °C, harvested, at which point the *ESA1-TAP GDS1-HA* cells were reinocculated into either glucose replete (YPD) or into glucose deprived (YP) media and harvested at the indicated time points. The cells were then lysed according to the mChIP protocol (Lambert et al., 2009 Methods 2.3.1) and extracts were resolved by SDS-PAGE using the Stain-Free™ FastCast™ acrylamide system. Western blot analysis was performed using α-TAP and α-HA antibodies and quantification of Esa1-TAP was performed (Methods 2.6). (B) Average Esa1-TAP protein level of each condition normalized glucose replete conditions (YPD) for three biological replicates; error bar indicate standard deviation. ANOVA was performed to identify significant differences in the means ($p<0.05$). Images are representative of 3 independent experimental replicates.

3.1.2 Acute glucose deprivation does not result in any observable changes in NuA4 complex composition.

As other subunits of the NuA4 complex have been shown to be differentially regulated in response to other stresses, such as the loss of Yng2 upon DNA damage (Lin et al., 2008), I next sought to determine if there are any gains or losses of proteins within the NuA4 complex in response to acute GD. Using a previously established method of stringent NuA4 purification (Mitchell et al., 2008), the NuA4 complex was purified through Esa1-TAP from mid-log phase cultures grown in YPD or after 10, 30, or 60 minutes of glucose deprivation. After IP the samples were resolved by SDS-PAGE they were silver stained to determine if there are any changes to the proteins that co-IP with Esa1-TAP. A western blot of the IPed sample was run in order to ensure equal loading of sample for the silver stain. This technique allowed for the detection of complex members Tra1, Eaf1, Epl1, Act1, and Yng2, along with the co-migrating proteins Arp4 and Swc4 (Mitchell 2008). Each of these proteins was detected without gross changes to protein levels from YPD to the different acute GD conditions (Figure 6). However this silver staining method does not allow for the robust detection of the TINTIN subunits due to co-migration of Eaf3 with IgG, the negative charge of Eaf7, and the small mass Eaf5. While I cannot exclude that subtler changes in complex composition occur, this work suggests that the NuA4 complex subunits Tra1, Eaf1, Epl1, Act1, and Yng2 are still present in the whole cell extract and can co-purify with Esa1-TAP after glucose deprivation.

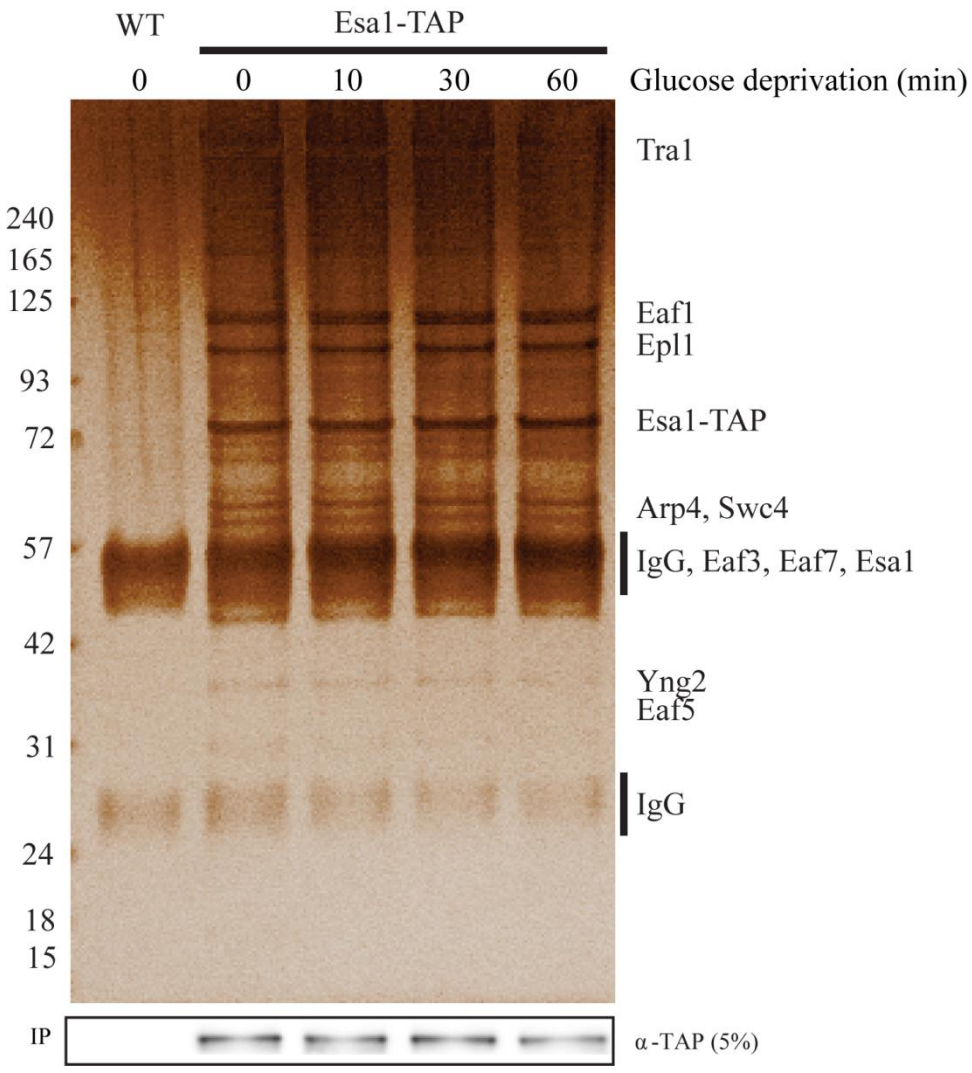
WT
Esa1-TAP
0
0
10
30
60
Glucose deprivation (min)
240
165
125
93
72
57
42
31
24
18
15
Tra1
Eaf1
Epl1
Esa1-TAP
Arp4, Swc4
IgG, Eaf3, Eaf7, Esa1
Yng2
Eaf5
IgG
IP
α-TAP (5%)

Figure 6: Glucose deprivation does not result in gross observable changes to the NuA4 complex. Cell cultures of WT (YKB1079) and *ESA1-TAP* (YKB3875) were grown to mid-log phase at 30 °C in glucose replete (YPD) media, prior to being harvested and resuspended in YP media for acute glucose deprivation stress. Cells were harvested at the indicated times and NuA4 complex was purified through Esa1-TAP as previously described (Mitchell et al., 2008 and methods section 2.3.3). 95% of the IPed samples were resolved on a NuPAGE Novex gradient SDS/PAGE 4-12% Bis-Tris protein gel and then silver stained. 5% of the IPed sample was resolved by SDS-PAGE and western blot analysis was then performed using an α-TAP antibody. Images are representative of 3 independent experimental replicates.

3.1.3 Acute glucose deprivation impacts histone H4 acetylation by NuA4 at ten minutes of GD.

As the integrity of the visible members of the NuA4 complex appears to be unaffected throughout the acute GD time course, I next sought to determine if the complex's acetylation activity was impacted by acute GD. I analyzed the acetylation state of NuA4's best-characterized targets, histone H4 lysines 5, 8, and 12, along with global H4 acetylation to provide good estimates of NuA4 function (Allard et al., 1999). WT cell cultures in mid-log phase were harvested and resuspended in either YPD (glucose replete, time point 0) or YP (glucose deprivation) for 10, 30, and 60 minutes prior to harvesting. As a control for NuA4-dependent H4 acetylation the temperature sensitive allele *esa1-L254P* (*esa1-ts*) strain was used as it shows decreased global histone H4 acetylation at non-permissive temperature (37 °C) (Clarke et al., 1999). Acetylation at lysines 5, 8, and 12, as well as total H4 acetylation were detected by western blot using antibodies targeted to those specific acetylation sites. Histone H3 protein levels were used as a measure of the total histone protein load. *esa1-ts* cells incubated at non-permissive temperature were shown to have a decrease in H4 acetylation for each lysine, as well as the total H4 lysine, however significance was only detected for Lys 5 (Figure 7). When compared to total histone protein load (H3) no significant difference in acetylation is detected for H4 Lys 5, Lys 8, or Lys 12 (Figure 7C-E). However a significant decrease is observed using the hyperacetylated H4 antibody at 10 minutes of GD, though there is recovery of the acetylation by 30 minutes of GD (Figure 7B). I detect a similar trend in a decrease for H4-K5 acetylation at 10 minutes GD, but it was not significant. It is possible that the change in acetylation is only significantly observed for total H4 acetylation as H4 is also acetylated on lysine 16, however this lysine is not a main target of NuA4 and therefore was not measured for this experiment. These results contrast what is seen for GD longer than 4 hours or stationary phase, where a dramatic

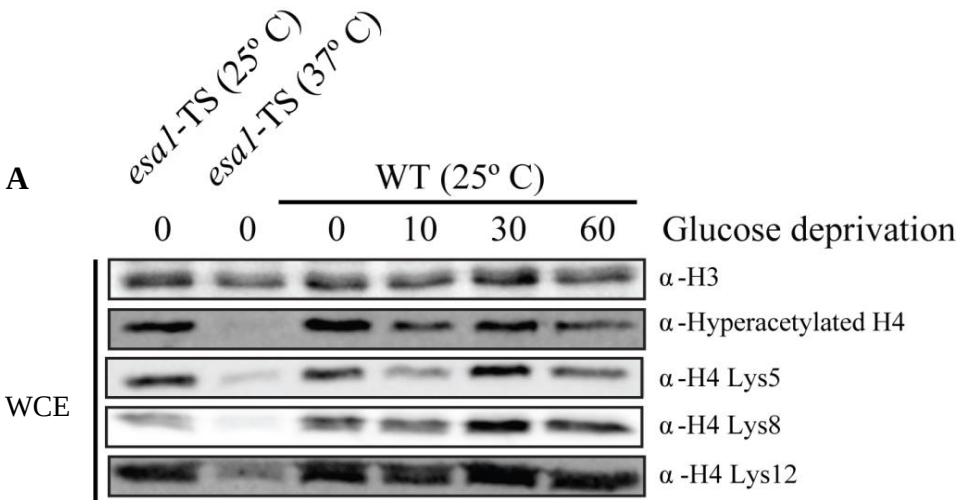
A
esa1-TS (25° C)
esa1-TS (37° C)
WT (25° C)
0 0 0 10 30 60
Glucose deprivation
WCE
α-H3
α-Hyperacetylated H4
α-H4 Lys5
α-H4 Lys8
α-H4 Lys12

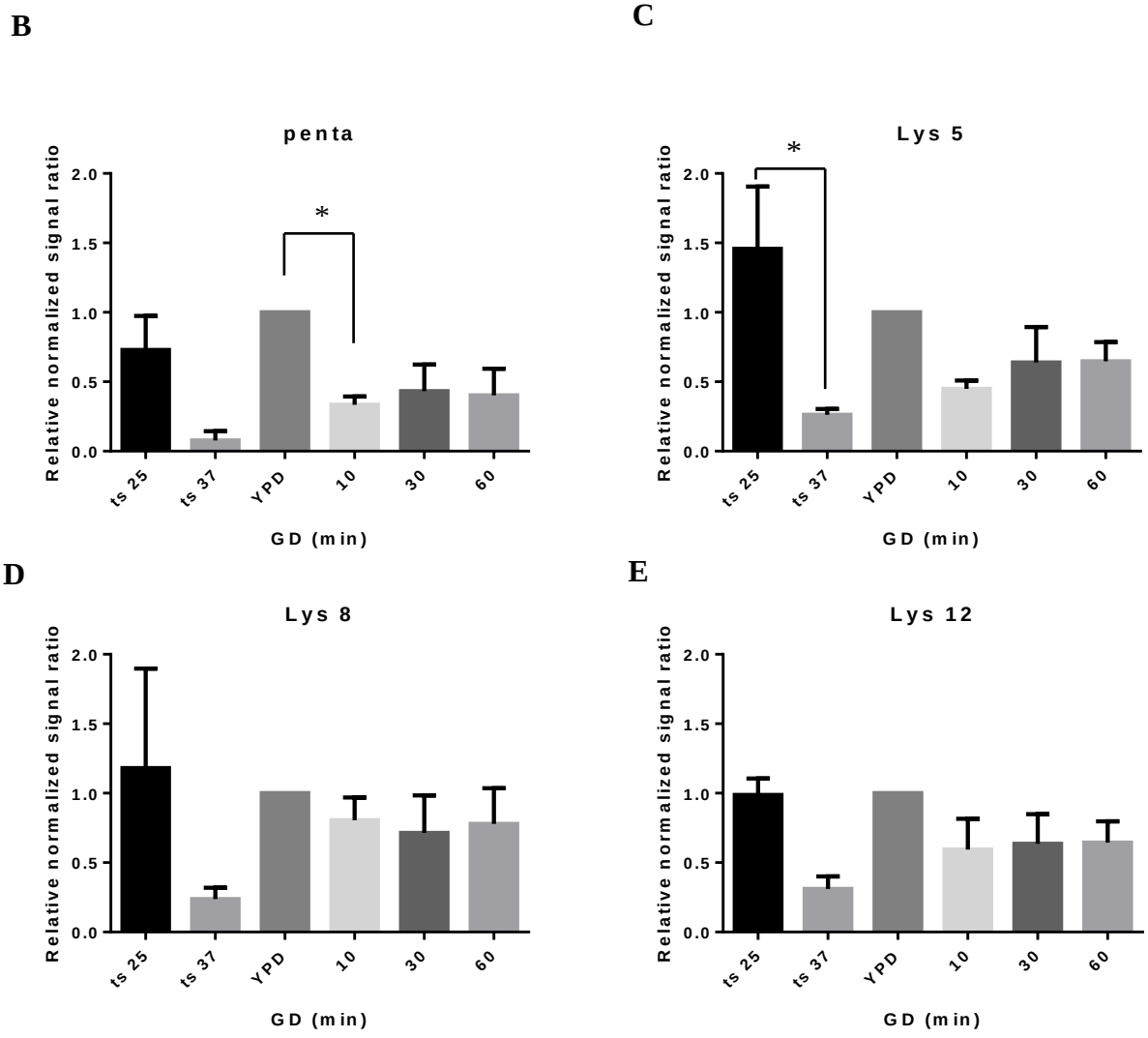
B
penta
Relative normalized signal ratio
2.0
1.5
1.0
0.5
0.0
*
ts 25
ts 37
YPD
10
30
60
GD (min)
C
Lys 5
Relative normalized signal ratio
2.0
1.5
1.0
0.5
0.0
*
ts 25
ts 37
YPD
10
30
60
GD (min)
D
Lys 8
Relative normalized signal ratio
2.0
1.5
1.0
0.5
0.0
ts 25
ts 37
YPD
10
30
60
GD (min)
E
Lys 12
Relative normalized signal ratio
2.0
1.5
1.0
0.5
0.0
ts 25
ts 37
YPD
10
30
60
GD (min)

Figure 7: Total Histone H4 acetylation decreases at 10 minutes of glucose deprivation. (A) Cell cultures of wild type yeast (WT, YKB1079) were grown to mid-log phase at 25º C, harvested, and resuspended in either YPD media (0 minutes of GD) or YP media (10, 30, and 60 minutes of GD) prior to being harvested. The temperature sensitive allele *esa1-L254P* (esa1-ts, YKB4236), was incubated in YPD for an additional 4 hours at 37 ºC. The cells were then lysed according to the mChIP protocol, extracts were resolved by SDS PAGE and then subjected to Western blot analysis against antibodies of α-H3, α-hyperacetylated H4, α-H4 Lys 5, α-H4 Lys 8, and α-H4 Lys 12. (B-E) Graph depicts average ratio of acetylation signal to histone H3 signal in WCE and normalized to the YPD for hyperacetylated H4, Lysine 5, Lysine 8, and Lysine 12 respectively. Error bars indicate the standard deviation. ANOVA was performed to identify significant differences in the means ($p<0.05$). Images are representative of 3 independent experimental replicates.

reduction in histone H4 acetylation is observed (Friis et al., 2009; Sandmeier, 2002). My results imply that while transient changes may occur to histone H4 lysine acetylation, especially upon immediate GD conditions, these effects are not lasting, as there are no significant changes to histone H4 acetylation during the latter stages of acute GD. As NuA4 is the primary H4 KAT, it suggests that NuA4 maintains its histone acetylation activity during acute GD.

3.1.4 Acute glucose deprivation does not identifiably impact Esa1-GFP localization.

As Esa1 and Epl1, two members of the NuA4 complex, have been shown to change localization from the nucleus to pre-autophagosomal bodies upon nitrogen starvation (Yi et al., 2012), I sought to determine if acute GD would also result in relocalization of Esa1. To identify whether Esa1-GFP changes location upon GD live fluorescent microscopy was conducted on yeast cells containing genomically tagged Esa1-GFP (green fluorescent protein) and Pab1-mCh (mCherry). Pab1-mCh was used as a marker for effective GD treatment as under standard growth conditions Pab1 has a diffuse cytoplasmic localization, but upon acute GD it forms cytoplasmic foci, termed stress granules (SGs) (Buchan et al., 2008; Hoyle et al., 2007; Swisher and Parker, 2010). Microscopy was performed on mid log phase yeast cell cultured in YPD and after 10 and 60 minutes of acute GD treatment (Figure 8). While Pab1-mCh SGs are formed by 10 minutes of GD treatment and largely resolved at 60 minutes, indicating that the GD treatment was effective, Esa1-GFP remained nuclear at both 10 and 60 minutes of GD. Though possible that our microscopy might not have the sensitivity required to detect small changes in localization or that changes occurred at times not tested, this work suggests that in contrast to nitrogen starvation stress, that acute glucose deprivation does not result in relocalization of a pool of NuA4 to distinct cytoplasmic sites.

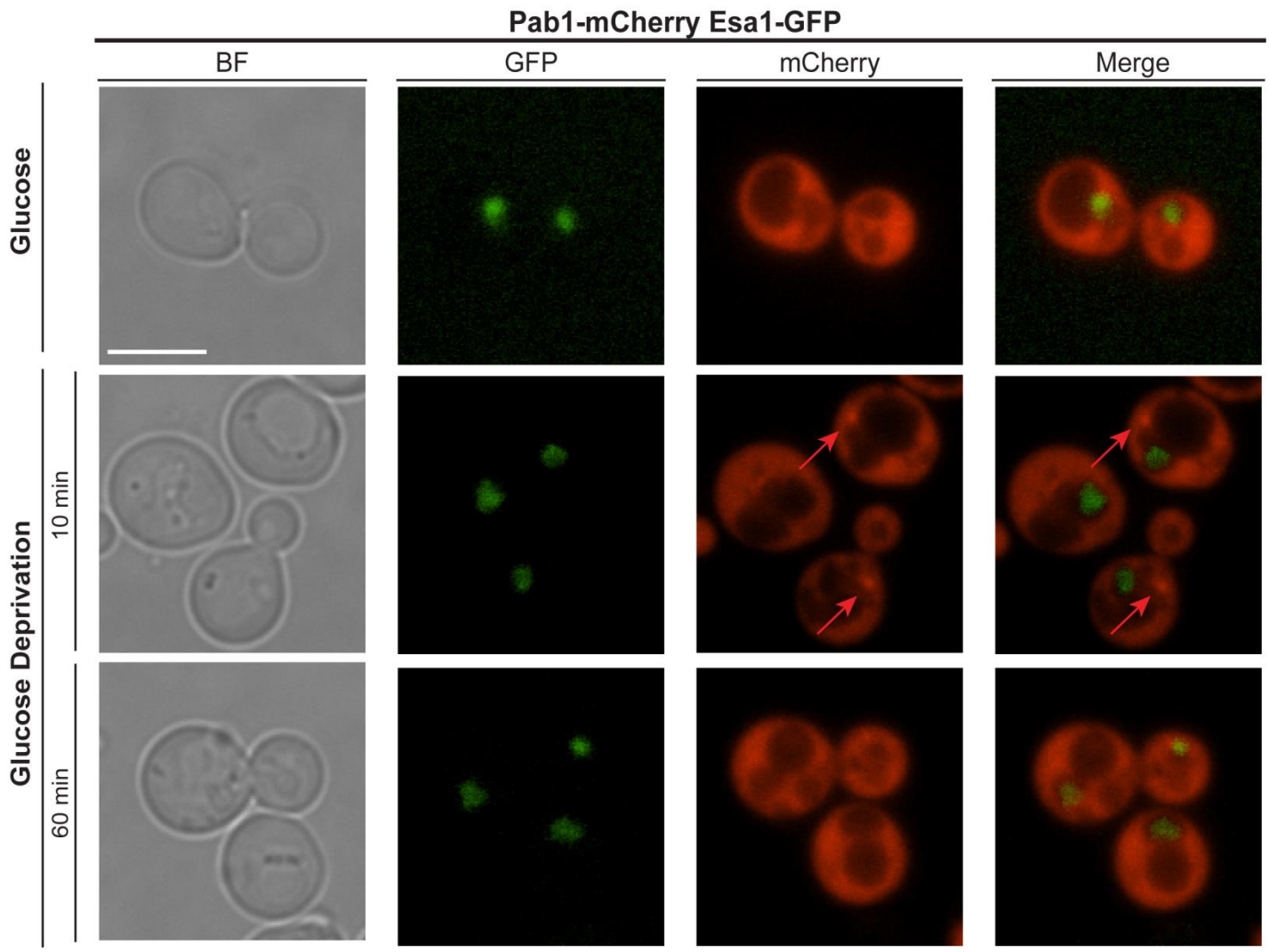
Pab1-mCherry Esa1-GFP
BF
GFP
mCherry
Merge
Glucose
Glucose Deprivation
10 min
60 min

Figure 8: Esa1-GFP localization is not impacted by acute glucose deprivation. *ESA1-GFP PAB1-mCh* (YKB4069) cells were grown to mid-logarithmic phase at 30°C in YPD media (glucose), prior to being harvested and resuspended in YP (glucose deprivation for 10 or 60 minutes. Cells were imaged on a confocal microscope. Three independent experimental replicates were performed and more than 100 cells were imaged per condition. Images shown are from a single plane. Arrows indicate punctate Pab1 formation upon 10 minutes of glucose deprivation. Size bar 5µM

Aim 2: Characterize the impact of acute glucose deprivation on the Esa1-TAP interactome and acetylome.

3.2.1 The Esa1-TAP interactome changes upon glucose deprivation.

Given that acute GD does not significantly change Esa1-TAP protein levels, grossly remodel the NuA4 complex, impact global Histone H4 acetylation or alter the localization of Esa1-GFP, I next sought to determine if either protein-protein interactions or potential acetylation targets of Esa1-TAP change upon acute GD. I addressed this by utilizing the mChIP-KAT-MS methodology previously used by the Baetz lab to generate the Esa1-TAP interactome and acetylome under standard growth conditions. Briefly, cell cultures of Esa1-TAP are grown to mid-log phase in YPD media, harvested, resuspended in either YPD (glucose) or YP media for 10, 30, or 60 minutes of GD prior to performing mChIP-KAT-MS. In the mChIP-KAT-MS protocol, Esa1-TAP along with interacting proteins are immunopreciptated using a modified ChIP protocol (Lambert et al., 2009), after which the samples undergo an in vitro KAT assay using C^{13} acetyl CoA to identify any NuA4 specific in vitro acetylation targets. Purifications were performed in triplicate and the samples are then sent for mass spectrometry analysis performed in collaboration with J.P. Lambert of the Gingras lab at The University of Toronto to identify interacting proteins, *in vivo* acetylations (light) and NuA4-dependent *in vitro* acetylations (heavy).

Interacting proteins included in this analysis are defined as being reproducible if two or more unique spectra of the protein were identified in a minimum of two out of three replicates of the experiment in a single media condition (YPD, 10, 30, or 60 minutes of GD). Ribosomal proteins were excluded from this analysis as due to their high abundance they could not be definitively identified as interactors with Esa1 as they are common contaminants of similar

purification protocols (Krogan et al., 2006). All other potential interactors were included in order to maximize the potential identification of changing protein interactors. In total 227 reproducible proteins were identified to interact with Esa1-TAP in at least one of the four conditions tested. All interacting proteins as well as the amount of unique spectra identified per interaction are found in the Appendix (Table S1). Of the total interactors, 174, 142, 161, and 163 proteins were identified to interact with Esa1 in the YPD, 10, 30, and 60 minutes of GD respectively. When compared to the previously published Esa1-TAP interactome data (Mitchell et al., 2013), there is 72% overlap of Esa1-TAP interacting proteins in YPD conditions, including 12/13 members of the NuA4 complex (Eaf7 was not reproducibly detected in any purification). The overlap between the Esa1-TAP interactomes indicates that the procedure is robust and reproducible.

All light and heavy acetylation sites detected on reproducibly interacting proteins were included in this analysis. A total of 93 acetylated residues, on 45 different proteins were detected in the interactome (Table 2). Of these acetylation sites, only 24 had been previously characterized (Downey et al., 2015; Henriksen et al., 2012; Mitchell et al., 2013).

To examine the changing protein interactors of Esa1-TAP upon GD stress conditions, a simple analysis was performed using spectral counts (Zhou et al., 2012). Briefly, the number of unique spectra of each reproducible protein was normalized to the number of unique spectra of Esa1-TAP in that trial to obtain a normalized spectral quantity (NSQ) to the bait. This step normalizes for any changes in Esa1-TAP spectra detected between replicates. The protein NSQ for each replicate was averaged within a condition (either two or three replicates) to provide an average NSQ (aNSQ) for each protein within a condition. To identify changes upon GD, the ratio of GD aNSQ/YPD aNSQ was generated for each protein and GD timepoint. If an interacting protein had either a two-fold greater or two-fold lower change in aNSQ they were

defined as having a change in interaction. Of the 227 reproducible interacting proteins, 67 "core" proteins co-purified in all conditions and did not significant change (Table S1). Included in these core interactors are the majority of NuA4 complex members: Tra1, Eaf1, Epl1, Esa1, Swc4, Arp4, Yng2, and Act1. In total 160 proteins, 70% of the total interactors, were found to change in interaction in at least one condition (Figure 9A). Hierarchical clustering analysis was performed on the changing interactome and it was determined that the YPD growth condition is the least similar of each of conditions tested (Figure 9B). Surprisingly, four NuA4 subunits, Yaf9, Eaf6, Eaf3 and Eaf5, were shown to have a decrease in co-purification with Esa1-TAP upon GD. Further many protein interactions detected were unique to only one condition (Figure 9B). These results indicate that Esa1-TAP interactome changes upon GD and suggests that one mechanism by which NuA4 response to stress is through changes in interaction and potentially substrates.

3.2.2: GO term analysis of the Esa1-TAP glucose deprivation interactome.

To identify common biological processes that may be regulated by NuA4 in response to GD, GO term analysis was performed on the 160 proteins that showed an increased or decreased interaction with Esa1-TAP upon GD (Table 1) using the DAVID database (Huang et al., 2009a, 2009b). Among lost protein interactions upon GD, regardless of the time point, were proteins implicated in nuclear localized processes, such as transcription and chromatin organization. In addition specific biological process GO terms that were lost at specific GD time points include nucleus organization (10 minutes), response to DNA damage (10 and 30 minutes), and nucleosome organization (30 and 60 minutes). Upon GD many of the GO terms gained are related to the regulation of protein production, including regulation of translation (10 and 30

A)

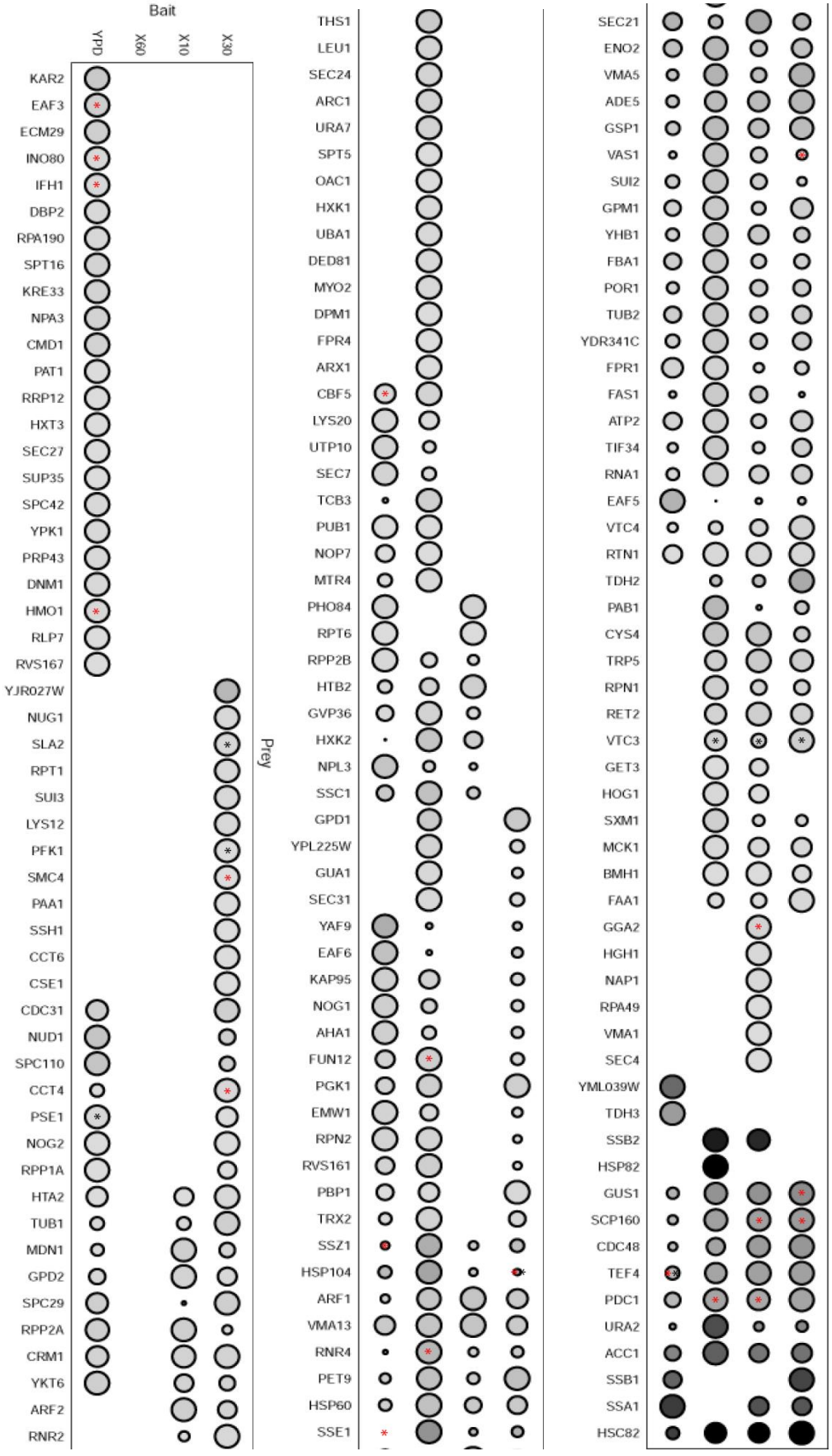
Bait
YPD
X60
X10
X30
Prey
KAR2
EAF3
ECM29
INO80
IFH1
DBP2
RPA190
SPT16
KRE33
NPA3
CMD1
PAT1
RRP12
HXT3
SEC27
SUP35
SPC42
YPK1
PRP43
DNM1
HMO1
RLP7
RVS167
YJR027W
NUG1
SLA2
RPT1
SUI3
LYS12
PFK1
SMC4
PAA1
SSH1
CCT6
CSE1
CDC31
NUD1
SPC110
CCT4
PSE1
NOG2
RPP1A
HTA2
TUB1
MDN1
GPD2
SPC29
RPP2A
CRM1
YKT6
ARF2
RNR2
THS1
LEU1
SEC24
ARC1
URA7
SPT5
OAC1
HXK1
UBA1
DED81
MYO2
DPM1
FPR4
ARX1
CBF5
LYS20
UTP10
SEC7
TCB3
PUB1
NOP7
MTR4
PHO84
RPT6
RPP2B
HTB2
GVP36
HXK2
NPL3
SSC1
GPD1
YPL225W
GUA1
SEC31
YAF9
EAF6
KAP95
NOG1
AHA1
FUN12
PGK1
EMW1
RPN2
RVS161
PBP1
TRX2
SSZ1
HSP104
ARF1
VMA13
RNR4
PET9
HSP60
SSE1
SEC21
ENO2
VMA5
ADE5
GSP1
VAS1
SUI2
GPM1
YHB1
FBA1
POR1
TUB2
YDR341C
FPR1
FAS1
ATP2
TIF34
RNA1
EAF5
VTC4
RTN1
TDH2
PAB1
CYS4
TRP5
RPN1
RET2
VTC3
GET3
HOG1
SXM1
MCK1
BMH1
FAA1
GGA2
HGH1
NAP1
RPA49
VMA1
SEC4
YML039W
TDH3
SSB2
HSP82
GUS1
SCP160
CDC48
TEF4
PDC1
URA2
ACC1
SSB1
SSA1
HSC82

B)

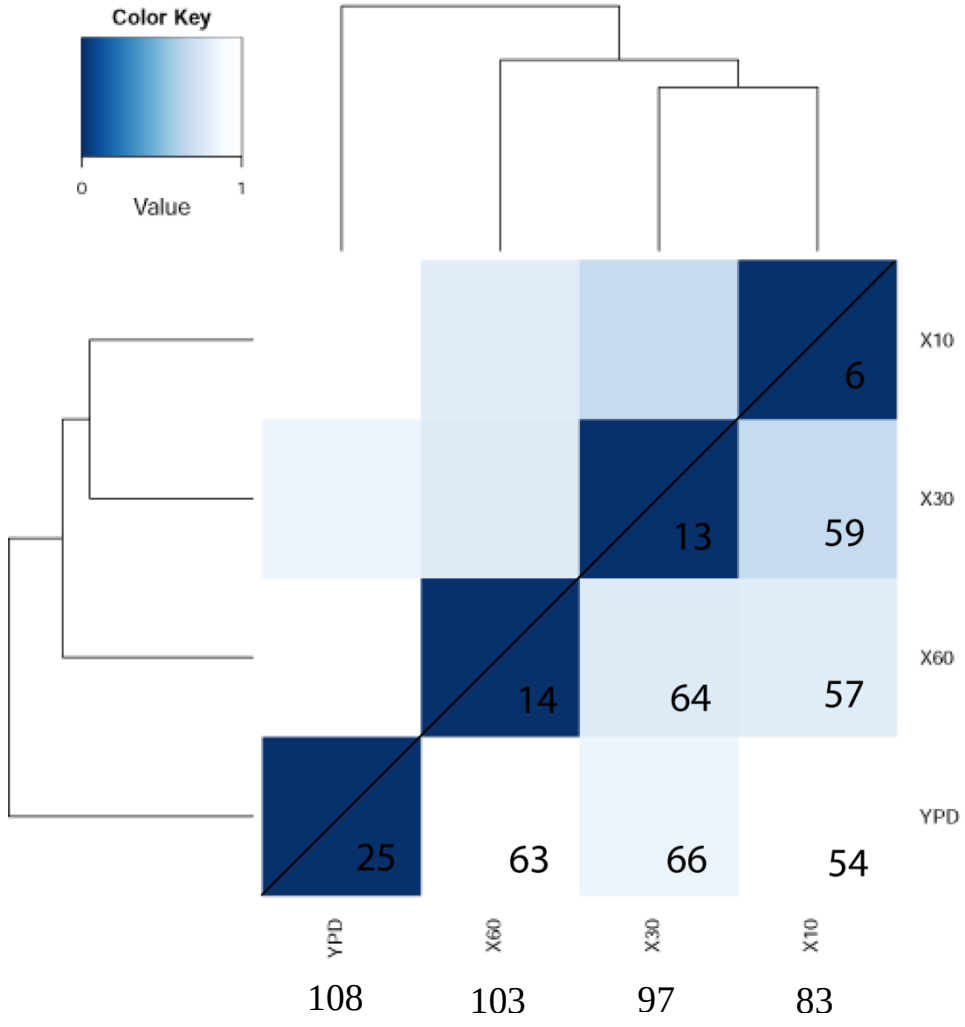
Color Key
0
1
Value
X10
X30
X60
YPD
6
13
59
14
64
57
25
63
66
54
YPD
X60
X30
X10
108
103
97
83

Figure 9: Esa1-TAP interactome and upon acute glucose deprivation. A) Hierarchical clustering of 160 Esa1-TAP protein interactors that change upon GD. The dotplot node size is proportional to the relative abundance of unique spectra of the protein in a specific condition to the total spectra identified for the protein of interest. The node colour intensity is defined by the total amount of unique spectra per condition relative to other proteins in the interactome. Red stars indicate in vivo acetylation, and black stars indicate in vitro acetylation by NuA4. B) The overlap of protein interactors per condition, and similarity between the conditions as well as the total amount of changing protein interactors in that condition.

Table 1: Biological process GO term analysis of proteins that change interaction upon acute GD

	GO term	Proteins	p value		GO term	Proteins	p value
10 minutes GD lost	Microtubule organization	Spc42, Spc29, Cdc31, Cmd1	3.0E-04	**10 minutes GD gained**	regulation of translation	Fas1, Ssb2, Tef4, Ssz1, Gus1, Vas1, Sxm1	1.1E-03
	rRNA processing	Mtr4, Rrp12, Rlp7, Dbp2, Nog1, Prp43, Utp10	4.8E-03		intracellular transport	Sec4, Get3, Arf1, Arf2, Nap1, Vtc4, Vtc3, Tub2, Gga2, Ret2, Sxm1	5.4E-03
	karyogamy	Kar2, Spc110, Cmd1	8.6E-03		Apoptosis	Por1, Tdh2, Cdc48	7.8E-03
	transcription	Ifh1, Spt16, Rpa190, Eaf5, Ino80, Yaf9, Eaf3, Utp10, Hmo1, Eaf6	9.9E-03		membrane fusion	Sec4, Cdc48, Vtc4, Vtc3	1.3E-02
	Nucleus organization	Kap95, Kar2, Spc110, Cmd1	1.2E-02		reproductive cellular process	Sec4, Mck1, Get3, Scp160, Nap1, Tub2	2.2E-02
	cytoskeleton organization	Spc42, Rvs161, Spc29, Cdc31, Spc110, Cmd1	1.5E-02		tRNA amino acylation	Ydr341c, Gus1, Vas1	3.2E-02
	Chromatin organization	Spt16, Eaf5, Ino80, Yaf9, Eaf3, Eaf6	1.5E-02		protein localization	Sec4, Get3, Arf1, Arf2, Cdc48, Nap1, Gga2, Ret2, Sxm1	4.2E-02
	response to DNA damage	Spt16, Eaf5, Ino80, Yaf9, Eaf3, Eaf6	4.4E-02				
30 minutes GD lost	ribonucleopotein complex biogenesis	Pat1, Mtr4, Rrp12, Rlp7, Dbp2, Cbf5, Nog1, Prp43, Utp10, Kre33	1.3E-04	**30 minutes GD gained**	posttranscriptional gene regulation	Vas1, Pdc1, Pfk1, Hsp60, Sxm1, Fas1, Pse1, Ssz1, Tef4, Gus1, Fba1, Ura2, Pab1	8.0E-07
	transcription	Ifh1, Spt16, Rpa190, Eaf5, Ino80, Yaf9, Eaf3, Utp10, Hmo1, Eaf6	1.7E-03		cellular carbohydrate catabolic process	Gpd2, Gpd1, Tdh2, Gpm1, Eno2, Fba1, Pfk1, Pdc1, Pgk1	1.4E-06
	chromatin organization	Spt16, Eaf5, Ino80, Yaf9, Eaf3, Eaf6	5.5E-03		regulation of translation	Fas1, Pse1, Tef4, Ssz1, Gus1, Fba1, Vas1, Pfk1, Pdc1, Ura2, Pab1, Sxm1	3.1E-06
	DNA repair	Spt16, Eaf5, Ino80, Yaf9, Eaf3, Eaf6	8.8E-03		glycolysis/gluconeogenesis	Tdh2, Gpm1, Eno2, Fba1, Pgk1	4.6E-05
	response to DNA damage	Spt16, Eaf5, Ino80, Yaf9, Eaf3, Eaf6	1.7E-02		protein transport	Sec31, Gsp1, Hsp60, Trx2, Ssa1, Nug1,	8.4E-04

						Rtn1, Ret2, Sxm1, Pse1, Arf1, Arf2, Cdc48, Sec21, Rna1	
	nucleosome organization	Spt16, Ino80, Yaf9	4.0E-02		Apoptosis	Por1, Tdh2, Cdc48, Pet9	1.3E-03
					protein import into nucleus	Pse1, Rna1, Ssa1, Rtn1, Sxm1	3.5E-03
					protein folding	Cct4, Ssz1, Hsc82, Sse1, Hsp60, Ssa1	6.3E-03
					vacuole fusion	Trx2, Vtc4, Vtc3	3.5E-02
60 minutes GD lost	chromatin organization/ DNA repair	Spt16, Eaf5, Hta2, Ino80, Eaf3, Eaf6	1.3E-03	**60 minutes GD gained**	posttranscriptional gene regulation	Ura7, Hsp60, Vas1, Sxm1, Sui2, Fas1, Ths1, Tef4, New1, Gus1, Fba1, Ura2	1.7E-09
	transcription	Ifh1, Spt16, Rpa190, Eaf5, Ino80, Eaf3, Hmo1, Eaf6	3.7E-03		Glycolysis	Tdh2, Gpm1, Eno2, Fba1, Hxk2, Hxk1	4.1E-06
	chromosome/ nucleosome organization	Spt16, Eaf5, Hta2, Ino80, Eaf3, Eaf6	2.2E-02		protein refolding	Hsc82, Sse1, Hsp60, Hsp82, Ssc1	9.5E-05
					tRNA aminoacylation for protein transaltion	Ths1, Ydr341c, Gus1, Ded81, Vas1, Arc1	2.3E-04
					gluconeogenesis	Tdh2, Gpm1, Eno2, Fba1	2.6E-03
					intracellular transport	Sec31, Acc1, Hsp60, Vtc3, Hsp82, Ret2, Sxm1, Get3, Arf1, Sec24, Ssc1, Myo2	1.6E-02
					Death	Por1, Tdh2, Atp2, Mir1	3.8E-02

GO analysis was performed using the DAVID database to identify which proteins are enriched for different biological processes. Proteins lost in a condition include the proteins that interacted with Esa1-TAP at YPD conditions, but either completely lost interaction with Esa1-TAP upon GD, or showed a two-fold or greater loss in interaction upon GD. Interactions gained are either proteins interacting in that GD condition that were not present in YPD, or had a two-fold or greater increase in interaction upon GD. Cut off of <0.05 was used for inclusion in this analysis.

minutes) and posttranscriptional gene regulation (30 and 60 minutes). These terms might be expected due to the cell changing the expression of certain genes in response to stress to promote the expression of ones needed during the stress response, and down regulating those that are not essential during a time of low energy availability. As anticipated, upon GD biological process GO terms related to glucose metabolism were also gained and include proteins enriched for roles in glycolysis and gluconeogenesis (30 and 60 minutes) such as Gpm1, Tdh2, and Eno2 each of which catalyze different reactions in both glycolysis and gluconeogenesis. Terms for both of the contrasting pathways of glycolysis and gluconeogenesis appear due to enzymes that can convert metabolites in both anabolism and catabolism of glucose. Finally GO terms related to the stress response appear to be gained upon GD including apoptosis (10 and 30 minutes) and cell death (60 minutes) suggesting NuA4 may have a role in these processes upon stress. The different roles that are seen from these GO terms suggest a varied and wide spread regulatory role for NuA4 within the cell upon GD.

3.2.3 Analysis of protein localization of Esa1-TAP interactors in response to glucose deprivation.

Though I could not detect changes in Esa1-GFP localization upon GD (Figure 8), it is possible that the changes in the interactome could reflect changes in NuA4 localization within the cell. Therefore, I sought to analyze the known cellular localizations of the Esa1-TAP interacting proteins and to determine if the distribution changed upon GD. Using previously annotated protein localizations of the yeast genome under standard growth conditions (Huh et al., 2003), I asked if the 160 interacting proteins that change were enriched to any subcellular

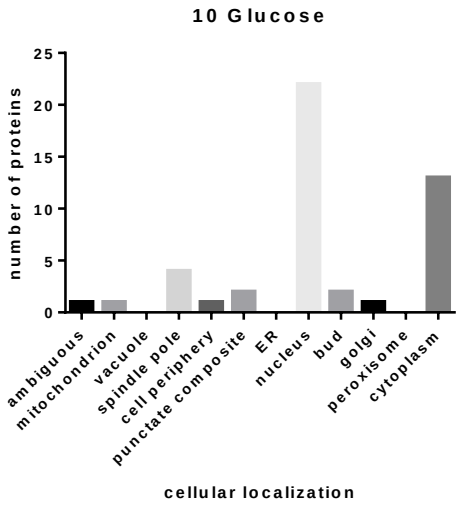
10 Glucose
number of proteins
0
5
10
15
20
25
ambiguous
mitochondrion
vacuole
spindle pole
cell periphery
punctate composite
ER
nucleus
bud
golgi
peroxisome
cytoplasm
cellular localization

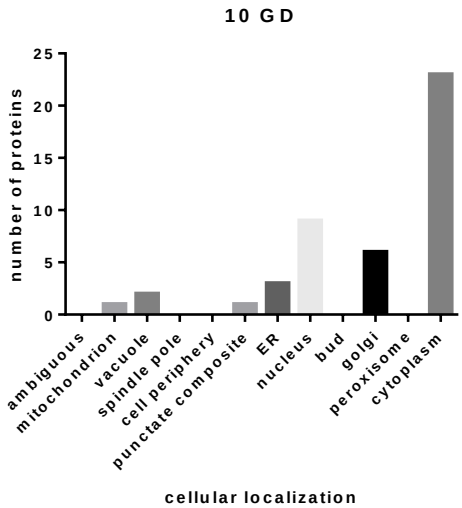
10 GD
number of proteins
0
5
10
15
20
25
ambiguous
mitochondrion
vacuole
spindle pole
cell periphery
punctate composite
ER
nucleus
bud
golgi
peroxisome
cytoplasm
cellular localization

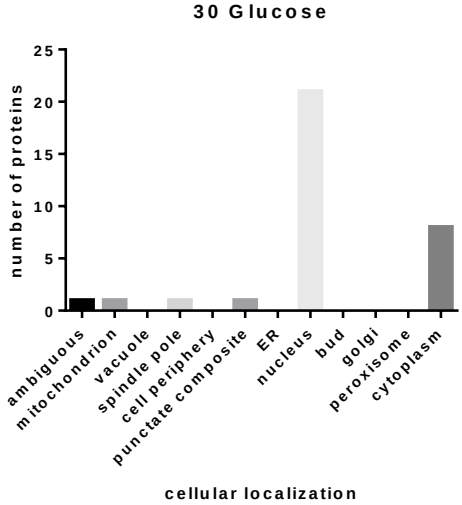
30 Glucose
number of proteins
0
5
10
15
20
25
ambiguous
mitochondrion
vacuole
spindle pole
cell periphery
punctate composite
ER
nucleus
bud
golgi
peroxisome
cytoplasm
cellular localization

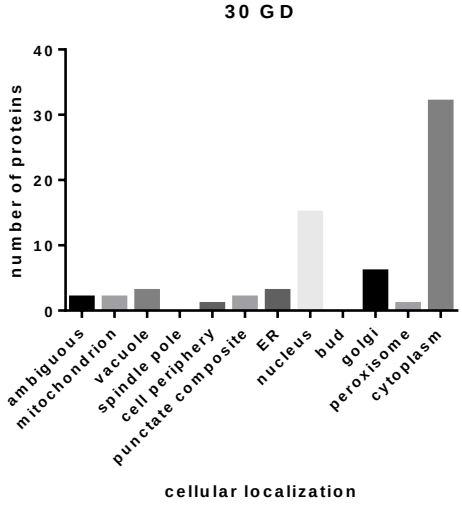
30 GD
number of proteins
0
10
20
30
40
ambiguous
mitochondrion
vacuole
spindle pole
cell periphery
punctate composite
ER
nucleus
bud
golgi
peroxisome
cytoplasm
cellular localization

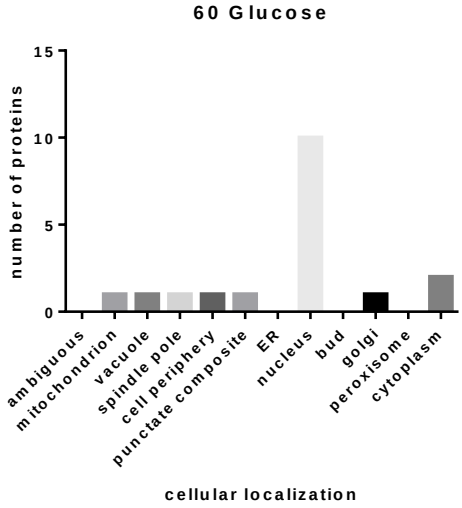
60 Glucose
number of proteins
0
5
10
15
ambiguous
mitochondrion
vacuole
spindle pole
cell periphery
punctate composite
ER
nucleus
bud
golgi
peroxisome
cytoplasm
cellular localization

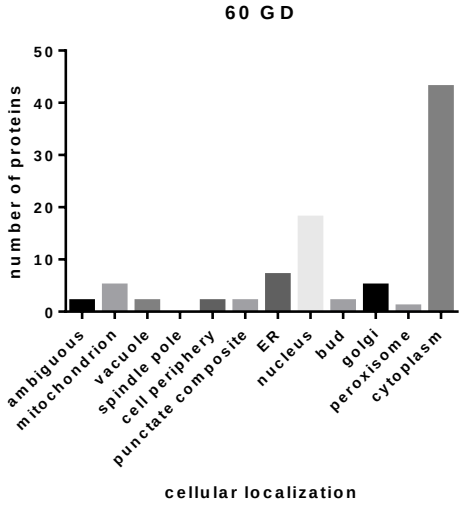
60 GD
number of proteins
0
10
20
30
40
50
ambiguous
mitochondrion
vacuole
spindle pole
cell periphery
punctate composite
ER
nucleus
bud
golgi
peroxisome
cytoplasm
cellular localization

Figure 10: Protein interactors of Esa1-TAP that are lost upon acute glucose deprivation are mostly nuclear while those that are gained are mostly cytoplasmic. Known localizations of the 160 proteins that change in interaction with Esa1-TAP upon each GD condition as determined by high throughput data of GFP tagged proteins produced in (Huh et al. 2003).

localization (Figure 10). As predicted by the GO analysis, the majority of protein interactors lost in each GD condition have either a nuclear, or nuclear related localization. In contrast, the majority of gained protein interactors upon GD have cytoplasmic localizations. This implies that NuA4 may have a role external to the nucleus upon stress and may reflect what is happening in the cell that was not observable by microscopy. Alternatively, it is possible that the previous cytoplasmic proteins become nuclear upon GD, which would not be determined in this screen. It is also possible that the protein levels of the interacting proteins may change in response to GD stress, resulting in an apparent increase in interaction between the protein and NuA4.

3.2.4: Characterization of the Esa1 acetylome upon glucose deprivation.

I next sought to characterize the acetylated proteins that interact with NuA4, and what changes might be detected upon transfer to glucose deprived media. In total 93 different acetylation sites were detected on 45 different proteins (Table 2). *In vivo* light acetylations were detected on 29, 24, 24, and 23 different peptides in the YPD, 10, 30, and 60 minutes of GD conditions respectively, and *in vitro* heavy acetylations were detected on 32, 24, 22, and 16 peptides in the YPD, 10, 30, and 60 minutes of GD . Of the observed acetylation sites only 24 had been previously detected with newly identified sites being found on a variety of proteins including NuA4 complex members Eaf1, Eaf3, Epl1, Esa1, and Swc4. Of the total acetylations identified only 17 were detected in every condition of the experiment potentially indicating that the majority of acetylations may play a regulatory role on the identified proteins in response to a stress such as acute GD. The identification of these new sites indicate many new potential targets of NuA4 regulation.

Table 2: Acetyl lysine residues identified in the Esa1-TAP GD acetylome

protein	lysine	YPD		10			30			60			previously identified
		in vivo	in vitro	in vivo	in vitro	interaction	in vivo	in vitro	interaction	in vivo	in vitro	interaction	
Arb1	K22					↔	x		↔			↔	
Cbf5	K2	x				-			-			↔	
Cct2	K230	x				-			↑			↑	
Cct4	K290					-	x		↑			-	
Eaf1	K848	x	x	x	x	↔	x	x	↔	x	x	↔	1
	K617		x								x		
	K968		x		x			x			x		
Eaf3	K128	x				-			-			-	
Epl1	K345	x	x		x	↔		x	↔		x	↔	1,2
	K353		x		x			x			x		1,2
	K496		x		x			x			x		2
	K512				x			x			x		1,2
	K427		x		x			x			x		1,2,3
	K429		x		x			x			x		
	K432		x		x			x					
	K569	x	x	x	x		x	x		x	x		
	K39	x		x	x		x			x			
	K821		x								x		
	K470		x		x			x			x		
	K395		x					x			x		
	K16				x								
	K648		x										
	K67			x									
Esa1	K13	x	x	x		↔	x		↔	x		↔	1,3
	K6		x				x			x			1,3
	K97	x	x	x	x		x			x			2
	K82		x		x			x					2
	k96	x											
Fas2	K1727					↔	x		↔			↔	
	K1736							x					1
Fun12	K125					-			↓	x		↑	
	K123									x			
Gga2	K18			x		↑	x		-	x		-	
Gus1	K174					↑	x		↑			↑	
Hhf1	K13					-			-	x		-	1,3
	K17									x			1,3

protein	lysine	YPD		10			30			60			previously identified
Hmo1	K157	x							-			-	
Hsp104	K852					↔	x		↔			↔	
	K860						x						
	K861							x					
Ifh1	K83	x				-			-			-	3
	K221	x											
Ino80	K441	x				-			-			-	
Kem1	K381	x		x		↔			↔			↔	
Nop58	K80			x		↔			↔			↔	
Ola1	K225					↔			↔	x		↔	
Pdc1	K233			x		↑			↑	x		↑	1
Pfk1	K901					-		x	↑			-	
Pil1	K165					↔		x	↔			↔	1
Pma1	K417	x		x	x	↔	x		↔	x		↔	
	K416			x									
Pse1	K904		x			-			↑			-	
Rnr4	K23					↑			↑	x		↑	1
Rpg1	K905		x			↔			↔			↔	
	K808			x									
	K957			x									
Rrp5	K868				x	↔			↔			↔	
Scp160	K1050			x		↑			↑			↑	
	K1079						x						
Sla2	K10					-		x	↑			-	
Smc4	K1248					-	x		↑			-	
Snu13	K42	x			x	↔			↔			↔	
Sse1	K273	x				↑			↑			↑	1
Ssz1	K410	x				↑			↑			↑	
Sub2	K219	x				↔			↔	x		↔	
Swc4	K36	x				↔			↔			↔	
	K345		x					x					
	K454	x											
Tef2	K447		x			↔			↔			↔	
	K450		x										
	K406			x	x		x			x			1
	K271	x	x	x			x			x			1
	K79	x		x			x			x			
	K55			x									
	K224		x					x					

protein	lysine	YPD		10			30			60			previously identified
Tef4	K221	x				↑			↑			↑	
	K226		x										
Tif2	K163					↔	x		↔			↔	
	K165						x						
	K357	x		x						x			
Tra1	K361		x			↔			↔			↔	
	K366		x										
	K2956									x			
	K512			x									
	K2795				x								
Vas1	K89					↑	x		↑			↑	
Vtc3	K590				x	↑		x	↑		x	↑	
Yef3	K681	x		x		↔			↔			↔	
	K289		x								x		
Yng2	K208	x	x	x	x	↔	x		↔	x		↔	2,3
	K170	x	x	x	X		x	x		x			1,2,3
	K145		x								x		3

Previously identified refers to: (1) (Henriksen et al., 2012) (2) (Mitchell et al., 2013) (3) (Downey et al., 2015). ↑, ↓, ↔ refer to an increase, decrease, or no change in interaction of the protein with Esa1-TAP upon the specific time point of GD. – refers to no interaction between the protein and Esa1-TAP being detected in the condition.

To greater characterize these acetylation sites I first sought to characterize the sequences surrounding the acetylated lysine to determine if there is a consensus sequence for Esa1-TAP acetylation targets, and if the consensus sequence changes between the different conditions due to a change to NuA4 upon GD stress. This was done by looking at the heavy acetylated lysines identified by the KAT assay of the mChIP-KAT-MS to ensure that these are NuA4 dependent acetylated residues. From these acetylations frequency plots were generated using the WebLogo software (Crooks et al., 2004) to map the residues around the acetylated lysines of interest (Figure 11). Sequences included ±10 amino acids from the acetylation site of interest. Based on the sequence logos there is a slight enrichment for smaller residues (alanine, glycine) at the -1 position in the YPD condition which is consistent with what has been previously identified (Downey et al., 2015; Mitchell et al., 2013). While GD does show some enrichment for these small residues at the -1 position, it also has enrichment for serine at this position, potentially indicating a change in preference upon GD.

A

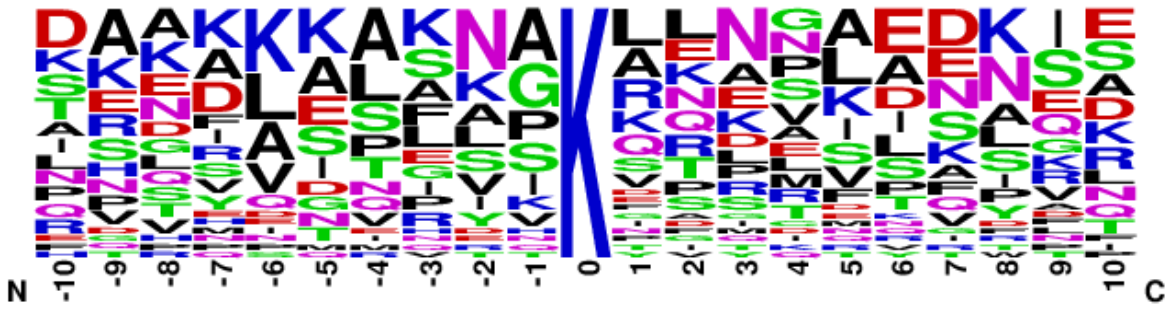
N
-10
-9
-8
-7
-6
-5
-4
-3
-2
-1
0
1
2
3
4
5
6
7
8
9
10
C

B

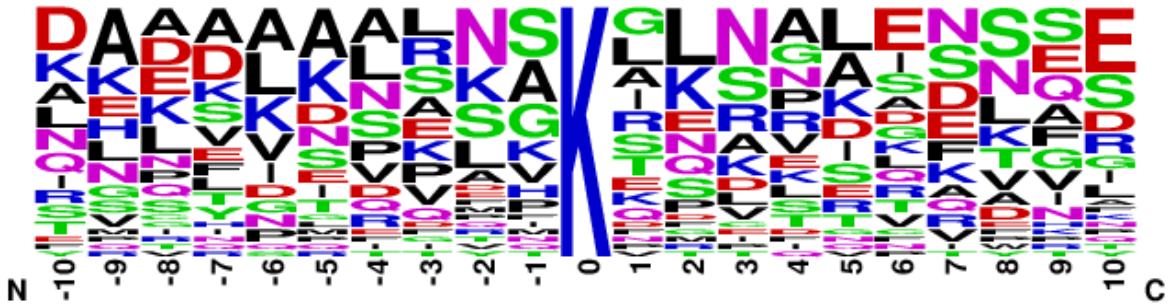
N
-10
-9
-8
-7
-6
-5
-4
-3
-2
-1
0
1
2
3
4
5
6
7
8
9
10
C

Figure 11: Frequency plots of NuA4 specific lysine acetylation targets show a slight enrichment for small residues upon at the -1 position in glucose replete conditions. (A) Frequency of amino acids surrounding acetylation targets under YPD conditions. Frequency of amino acids (y axis) spanning positions -10 to +10 surrounding the acetylated lysine identified in the Esa1-TAP YPD interactome. (B) Frequency of amino acids surrounding acetylation targets under all acute GD conditions. Frequency of amino acids (y axis) spanning positions -10 to +10 surrounding the acetylated lysine identified in the Esa1-TAP YP interactome.

Aim 3: Characterize the interactions of Esa1 with protein interactors Pab1, TINTIN and Fatty Acid Synthetase complex proteins Fas1 and Fas2.

To go further in depth into the Esa1-TAP interactome/acetylome I next sought to validate the results of the mass spectrometry by attempting to greater characterize the interactions between Esa1 and certain proteins of interest.

3.3.1: Characterizing the interaction between NuA4 and Pab1 upon GD.

The Baetz lab has previously shown that Esa1-TAP and Pab1 physically interact under standard growth conditions and that Pab1 is acetylated both *in vivo and in vitro* by NuA4 providing further evidence that it may be regulated by NuA4 in some way (Mitchell et al., 2013). Pab1 (Poly-A binding protein 1) is an essential protein whose function is to bind and protect mRNA prior to translation (Sachs et al., 1987). Under standard growth conditions Pab1 has been shown to have a diffuse cytoplasmic localization, though it is able to shuttle between the cytoplasm and nucleus (Brune et al., 2005; Huh et al., 2003), however under certain stresses such as acute GD pools of Pab1, along with its bound mRNA, have been shown to form cytoplasmic foci termed stress granules (Buchan et al., 2008; Hoyle et al., 2007; Swisher and Parker, 2010). Recently our lab has determined that using deletion mutants of certain NuA4 complex proteins, Pab1 glucose deprived stress granule formation is defective thereby implying a direct effect of NuA4 on Pab1 regulation (unpublished data, M. Rollins). In contrast to the published Esa1-TAP interactome, I only identified Pab1 spectra in the Esa1-TAP co-IP under each GD condition, indicating that there may potentially be an increase in interaction between Esa1 and Pab1 upon GD.

3.3.1.1: The interaction between NuA4 and Pab1 does not change upon GD.

In order to validate the interaction between Esa1 and Pab1 and to determine if the interaction changes upon GD, co-IP experiments were performed. WT and Esa1-TAP strains were cultured to mid-log phase under standard growth conditions, harvested, resuspended in YPD or YP media for acute GD treatments of 10, 30, and 60 minutes and then mChIP of Esa1-TAP was performed. WCE and IP samples were then resolved by SDS-PAGE and western blot analysis was performed (Figure 12). Quantification of the protein levels were done by comparing the signal of the Pab1 band to the housekeeping gene G6PDH in the WCE and to Esa1-TAP in the IP. No significant changes in Pab1 protein levels in the WCE were detected between YPD to any time point of GD. Further, no significant change in the amount of Pab1 co-IPing with Esa1-TAP was detected under any condition, indicating the interaction between the two proteins is not impacted by GD.

3.3.1.2 The interaction between NuA4 and Pab1 is not mediated through mRNA.

I next sought to determine how Esa1 and the greater NuA4 complex interact with Pab1. Both Pab1 (Sachs et al., 1987), and two members of the NuA4 complex, Esa1 and Eaf3, are postulated to be able to bind to RNA (with the latter two potentially binding through their chromodomains (Joshi and Struhl, 2005; Shimojo et al., 2008)). I therefore sought to determine if the interaction between NuA4 and Pab1 is mediated through the binding of the individual proteins to mRNA. To determine if this was the case co-IPs were performed between Esa1-TAP and Pab1 in Esa1-TAP and Esa1-TAP *eaf3Δ* strains, with an RNase treatment prior to IP in order to remove any RNA from the sample. Mid-log phase cells were harvested and then lysed according the mChIP protocol and the lysate was then split in two with one half being treated

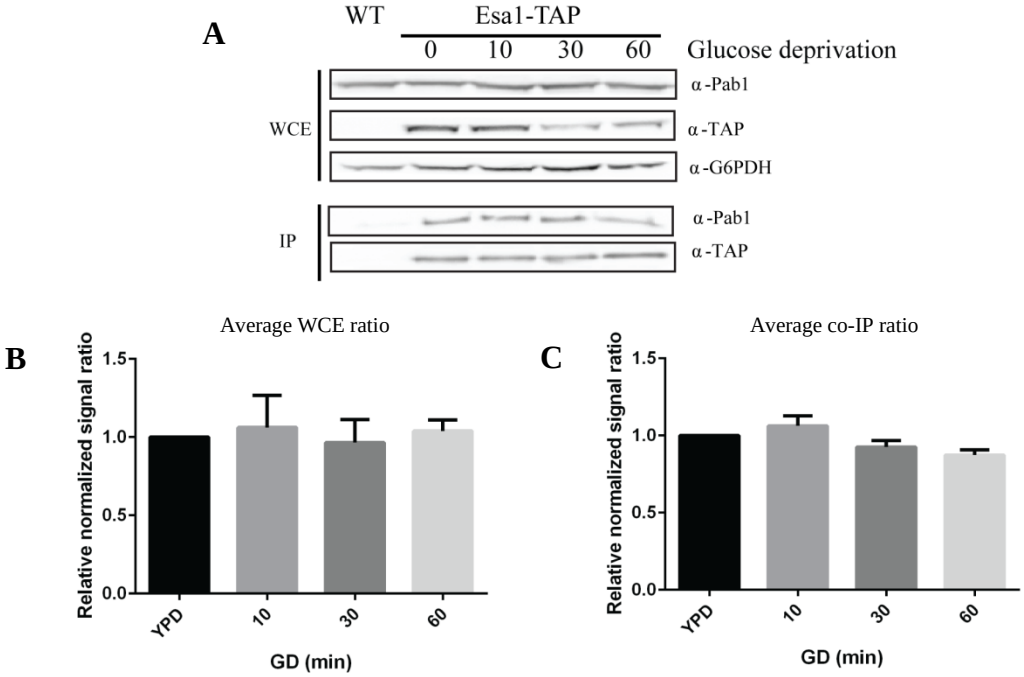
A
WT
Esa1-TAP
0
10
30
60
Glucose deprivation
WCE
α-Pab1
α-TAP
α-G6PDH
IP
α-Pab1
α-TAP
B
Average WCE ratio
Relative normalized signal ratio
1.5
1.0
0.5
0.0
YPD
10
30
60
GD (min)
C
Average co-IP ratio
Relative normalized signal ratio
1.5
1.0
0.5
0.0
YPD
10
30
60
GD (min)

Figure 12: Pab1 protein levels and ability to co-immunoprecipitate with Esa1-TAP do not change in response to GD. Cultured cells of wildtype (WT, YKB1079) and *ESA1-TAP* (YKB3875) were grown to mid-log phase, harvested, resuspended in YP media for the acute GD time points as indicated prior to mChIP of Esa1-TAP. A) Immunoprecipitates were resolved by SDS-PAGE, and quantitative western blot analysis was performed using α-TAP, α-Pab1, and α-G6PDH as a loading control. Images are representative of 3 biological replicates. B) Pab1 protein level does not change upon glucose deprivation. Graph depicts average ratio of GFP signal to G6PDH signal in WCE and normalized to the YPD condition. C) Pab1 co-immunoprecipitation with Esa1-TAP does not change upon glucose deprivation. Graph depicts average GFP IP signal to TAP IP signal normalized to the YPD condition. Error bar indicate standard deviation.

with RNase. After RNase treatment half of the treated and non-treated samples were used to assess RNA content, while the other half of the treated and non-treated samples were used to perform a co-IP. RNA isolated from the extracts before and after RNase treatment was resolved on a 1% agarose gel. After RNase treatment, the majority of RNA was degraded, with the remaining fragments being less than 100 bases, indicating that RNase treatment was effective (Figure 13B). An Esa1-TAP IP was performed on the remaining untreated and RNase treated lysate (Figure 13A). The IP results show that the interaction between Esa1-TAP and Pab1 is not dependent on Eaf3 and is maintained in extracts treated with RNAse. It is however possible that the interaction between NuA4 and Pab1 is dependent on protected mRNA from either Esa1 or Pab1 preventing the RNase from effectively degrading it. One way around this could be by constructing a truncated version of Esa1 that lacks its chromodomain, but still maintains its activity.

3.3.1.3 The interaction between NuA4 and Pab1 is not mediated by the TINTIN subcomplex.

As mutants of the TINTIN subcomplex display defects in Pab1 SG formation (unpublished data M. Rollins), I next sought to determine if the remaining TINTIN subunits Eaf5 and Eaf7 mediate the interaction between Pab1 and NuA4. WT as well as Esa1-TAP, Esa1-TAP *eaf3Δ*, Esa1-TAP *eaf5Δ*, Esa1-TAP *eaf7Δ* cultures were grown to mid-log phase prior to Esa1-TAP mChIP. The WCE and IPed samples were then resolved by SDS-PAGE and western blot analysis was performed against TAP, Pab1 and G6PDH as a loading control housekeeping gene (Figure 14). In each TINTIN deletion mutant Pab1 is able to co-IP with Esa1-TAP indicating that the interaction between NuA4 and Pab1 is not mediated through this branch of the NuA4 complex, but through another mechanism.

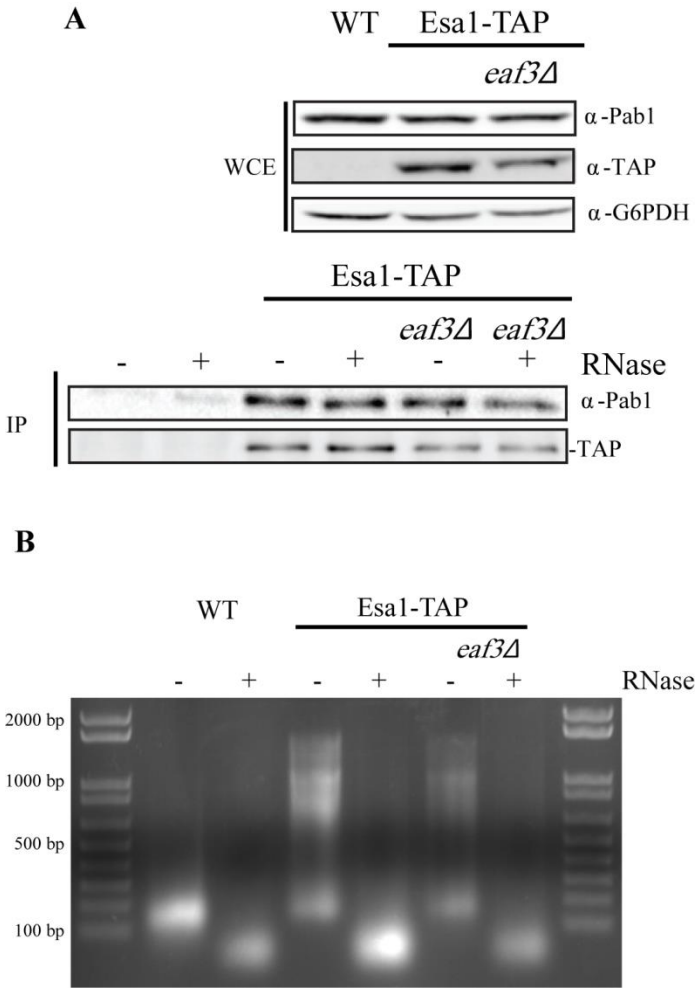
A
WT
Esa1-TAP
eaf3Δ
WCE
α-Pab1
α-TAP
α-G6PDH
Esa1-TAP
eaf3Δ
eaf3Δ
- + - + - +
RNase
IP
α-Pab1
-TAP
B
WT
Esa1-TAP
eaf3Δ
- + - + - +
RNase
2000 bp
1000 bp
500 bp
100 bp

Figure 13: The interaction between Esa1-TAP and Pab1 is not dependent on Eaf3 or full-length mRNA. (A) Cultures of wildtype (WT, YKB1079), *ESA1-TAP* (YKB3941), and *ESA1-TAP eaf3Δ* (YKB765). From this lysate half was treated with RNase A while the other was not treated. Esa1-TAP was IPed from both treated and non-treated samples. The WCE and IPed samples were then resolved by SDS-PAGE and analyzed by western blot against α-TAP, α-Pab1, and α-G6PDH as a loading control. (B) The RNA from the samples prior to and after RNase treatment was isolated, and resolved on a 1% agarose gel and stained with SYBR Safe gel stain. Images are representative of 3 biological replicates.

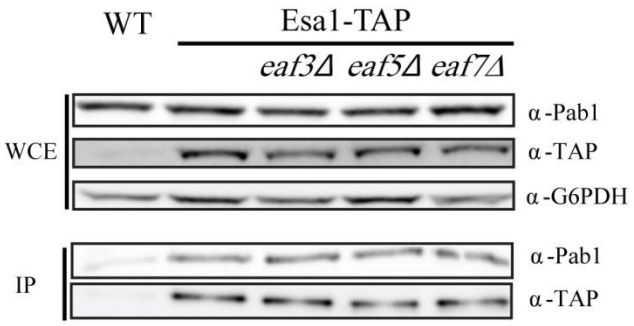
WT
Esa1-TAP
eaf3Δ eaf5Δ eaf7Δ
WCE
α-Pab1
α-TAP
α-G6PDH
IP
α-Pab1
α-TAP

Figure 14: The co-immunoprecipitation between of Esa1-TAP and Pab1 is not mediated through the TINTIN branch of NuA4. Cell cultures of wildtype (WT YKB1079) *ESA1-TAP* (YKB3875),*ESA1-TAP eaf3Δ* (YKB765),*ESA1-TAP eaf5Δ* (YKB854),and ESA1-TAP *eaf7Δ* (YKB 964) were grown to mid-log phase, harvested and mChIP of Esa1-TAP was performed. After lysis WCE and IPs were resolved by SDS-PAGE and analyzed by western blot against α-TAP, α-Pab1 and α-G6PDH as a loading control. Image is representative of three biological replicates.

3.3.2: Characterizing potential changes in interaction between Esa1-TAP and the TINTIN subcomplex of NuA4 upon GD.

The Esa1-TAP acute GD interactome/acetylome also provided potential insight into changes of the NuA4 complex that were undetectable using the silverstain (Fig 6). In the silver stain each of the members of the TINTIN subcomplex were undetected, Eaf5 due to its low molecular weight, Eaf7 due to its highly negative charge, and Eaf3 due to its co-migration with the IgG band. This result is contrasted with the Esa1-TAP interactome where spectra of the protein Eaf3 were only identified under non-stressed conditions while Eaf5 was shown to have more spectra identified under YPD relative to GD conditions. Further, Eaf7 spectra were not detected under any conditions in any trial of the mass spectrometry experiments. I therefore sought to determine if interactions between the TINTIN subcomplex members (Eaf5, Eaf7, and Eaf3) and Esa1-TAP change upon GD.

3.3.2.1: The interaction between Esa1-TAP and all members of the TINTIN subcomplex is unchanged upon glucose deprivation.

The generated interactome detected a decreased co-purification between Esa1-TAP and two TINTIN subunits upon GD (Figure 9). To directly assess these changes in interaction detected by mass spectrometry co-IPs were performed between Esa1-TAP and Eaf5-GFP, Eaf7-GFP and Eaf3-HA. Cells from logarithmically growing cultures were collected, and mChIP of Esa1-TAP was performed. For Eaf5-GFP and Eaf-3 GFP experiments WCE and IPed samples were resolved by SDS-PAGE using the TGX Stain-Free™ FastCast™ Acrylamide Kit for later protein quantification by western blot (Taylor et al., 2013, 2014) (Fig 15 A &B). As I could not detect Eaf7-GFP in WCEs of the mChIP, a TCA lysis was performed in addition to the mChIP to

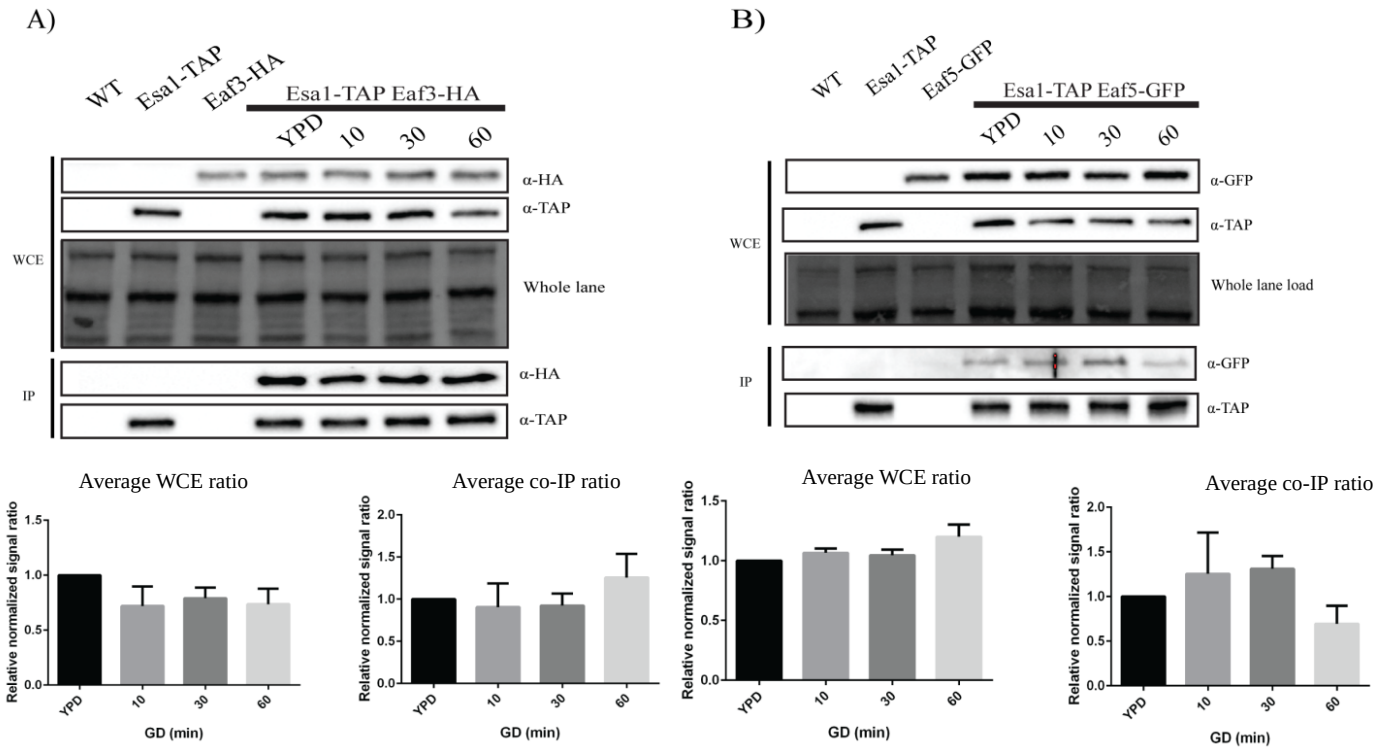
A)
WT
Esa1-TAP
Eaf3-HA
Esa1-TAP Eaf3-HA
YPD
10
30
60
α-HA
α-TAP
WCE
Whole lane
IP
α-HA
α-TAP
B)
WT
Esa1-TAP
Eaf5-GFP
Esa1-TAP Eaf5-GFP
YPD
10
30
60
α-GFP
α-TAP
WCE
Whole lane load
IP
α-GFP
α-TAP
Average WCE ratio
Relative normalized signal ratio
GD (min)
Average co-IP ratio
Relative normalized signal ratio
GD (min)
Average WCE ratio
Relative normalized signal ratio
GD (min)
Average co-IP ratio
Relative normalized signal ratio
GD (min)

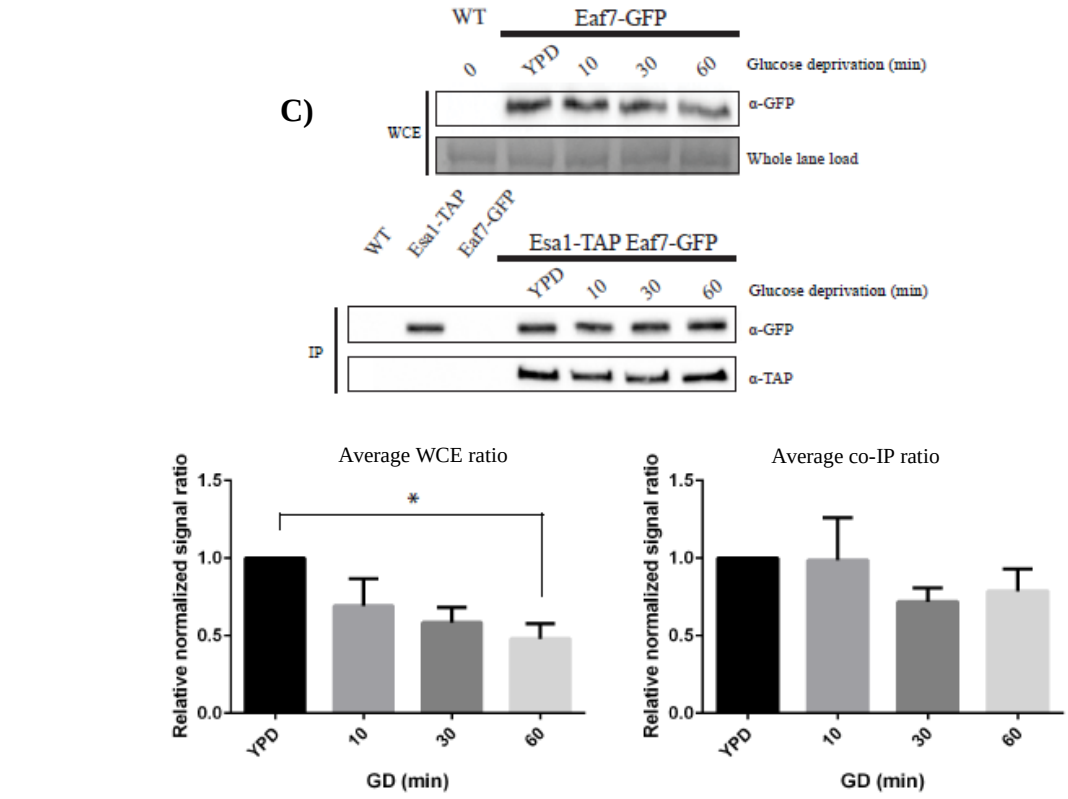
C)
WT
Eaf7-GFP
0
YPD
10
30
60
Glucose deprivation (min)
α-GFP
WCE
Whole lane load
WT
Esa1-TAP
Eaf7-GFP
Esa1-TAP Eaf7-GFP
YPD
10
30
60
Glucose deprivation (min)
IP
α-GFP
α-TAP
Average WCE ratio
*
Relative normalized signal ratio
GD (min)
Average co-IP ratio
Relative normalized signal ratio
GD (min)

Figure 15: The interaction between Esa1-TAP and the members of the TINTIN subcomplex is unchanged upon glucose deprivation. A) Cultured cells of wildtype (WT YKB1079) *ESA1-TAP* (YKB3875), *EAF5-GFP* (YKB2004), *ESA1-TAP EAF5-GFP* (YKB4156) were grown to mid log phase, harvested, resuspended in YP media for GDs of 10, 30, and 60 minutes. After mChIP lysis the IPed sample, as well as WCE extract were resolved by SDS-PAGE using the Stain-Free™ FastCast™ acrylamide system and western blot analysis was performed against α-TAP, α-GFP. Average WCE ratio is the ratio of GFP signal to whole lane signal normalized to the YPD condition. Average co-IP ratio is the ratio of GFP IP signal to TAP IP signal normalized to the YPD condition. B) Cultured cells of wildtype (WT YKB1079) *ESA1-TAP* (YKB3875), *EAF3-HA* (YKB4234), *ESA1-TAP EAF3-HA* (YKB4235) were grown, lysed, and analyzed in the same manner as (A). (C) Cultured cells of wildtype (WT YKB1079) *ESA1-TAP* (YKB3875), *EAF7-GFP* (YKB2006), *ESA1-TAP EAF7-GFP* (YKB4157) were grown and analyzed in the same manner as (A) but the cells were then either lysed by the TCA protocol (for WCE samples) or the mChIP protocol (for IPed samples). ANOVA was performed to identify significant differences in the means ($p<0.05$). Images are representative of 3 biological replicates.

characterize the interaction between Esa1-TAP and Eaf7-GFP. The samples were then resolved and quantified in the same manner as for Eaf5-GFP and Eaf3-HA (Figure 15 C). All three TINTIN components, Eaf5-GFP, Eaf7-GFP, and Eaf3-HA, were found to co-IP with Esa1-TAP under both YPD and all time points of acute GD, indicating no changes of these components in the NuA4 complex in response to GD. In addition protein levels of both Eaf5-GFP and Eaf3-HA remain unchanged upon acute GD indicating their protein levels are not impacted by acute GD. This is not the case however for Eaf7-GFP as by 60 minutes there a significant decrease in the total amount of Eaf7-GFP protein. These results then indicate that the integrity of the TINTIN components in the NuA4 complex is maintained upon acute GD, and that the partial loss of Eaf7-GFP protein during these time points has no effect on the greater complex.

3.3.3: Characterizing the interaction between Esa1 and the proteins of the FAS complex

Members of the Fatty Acid Synthatase complex, Fas1 and Fas2, were selected for further characterization as acetylation sites were detected on Fas2 under glucose deprivation and Fas1 showed an increased interaction with Esa1-TAP upon GD (Table 2 and Figure 9). These proteins are critical to the metabolic process due to their role in fatty acid biosynthesis (Schweizer et al., 1986) where the FAS complex forms fatty acids from malonyl-CoA. This process is a downstream step of glycolysis and pyruvate oxidation which make acetyl-CoA from glucose, which can then be converted to malonyl-CoA through the enzyme Acc1 (Lynen, 1959). Further, prolonged glucose deprivation results in both Fas1 and Fas2 forming punctate cytoplasmic foci indicating a potential regulatory mechanism acting upon the FAS complex upon GD (Narayanaswamy et al., 2009; Suresh et al., 2015).

3.3.3.1: Fas2 protein levels are observed to decrease in mChIP lysis upon acute glucose deprivation.

To validate the results of the mass spectrometry experiments, I sought to confirm the interaction between Fas2 and Esa1 and determine the impact of acute GD on Fas2 protein levels. WT, Esa1-TAP, Fas2-GFP, and Esa1-TAP Fas2-GFP were cultured to mid-log phase prior to GD treatment, harvesting, lysis and IP. The WCE and IPed samples were resolved by SDS-PAGE and analysed by western blot (Figure 16). Reproducing the mass spectrometry results, the interaction between Fas2-GFP and Esa1-TAP does not significantly change from YPD through to any time point of acute GD. However upon acute GD, specifically 30 and 60 minutes, significant loss of Fas2-GFP protein levels is observed in the WCE. This implies that there may be a decrease in total Fas2-GFP protein in response to the stress. Alternatively, it is possible that upon GD Fas2 localization or PTMs change, resulting in a decreased solubility by this extraction method.

3.3.3.2: The members of the FAS complex do not change protein levels in response to acute glucose deprivation.

To attempt to discern whether the decrease in Fas2-GFP upon GD (Figure 16) is a true reflection of protein levels or changes in solubility, I performed a TCA lysis (Kao and Osley, 2003) to look at changing levels of both Fas1 and Fas2 within the cell. The lysis was performed using both Fas1 and Fas2 in both WT and *eaf1Δ* background to not only look at the protein amount under standard conditions, but to also discern if NuA4 (due to the deletion of EAF1 producing PicNuA4) has any potential impact on the protein levels of this enzyme. Cell cultures of WT, Fas1-GFP, Fas1-GFP *eaf1Δ*, Fas2-GFP, and Fas2-GFP *eaf1Δ* were grown to mid-log phase, prior to acute GD treatment. The cells were then lysed according to the TCA protocol

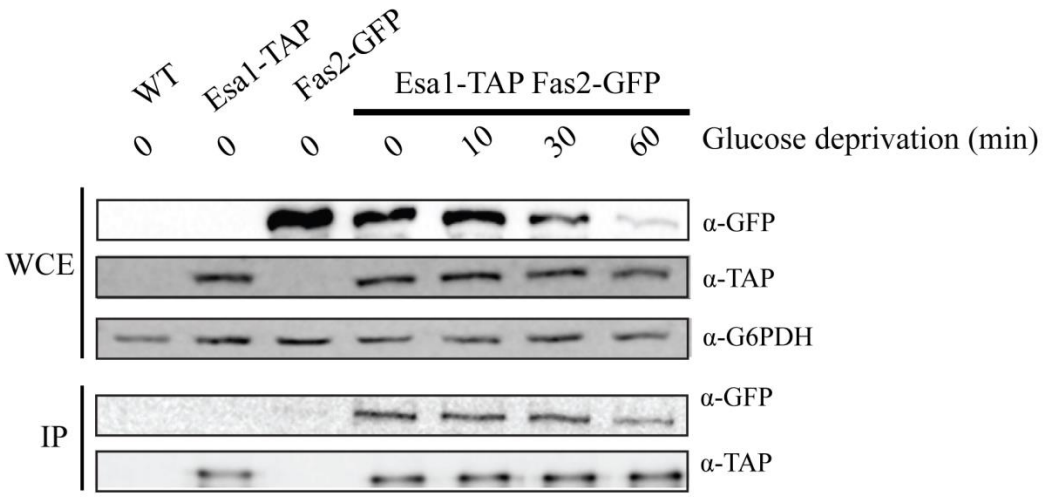

Average WCE ratio

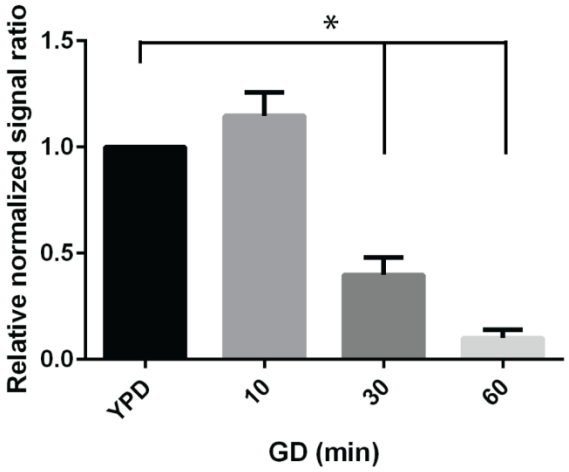

Average co-IP ratio

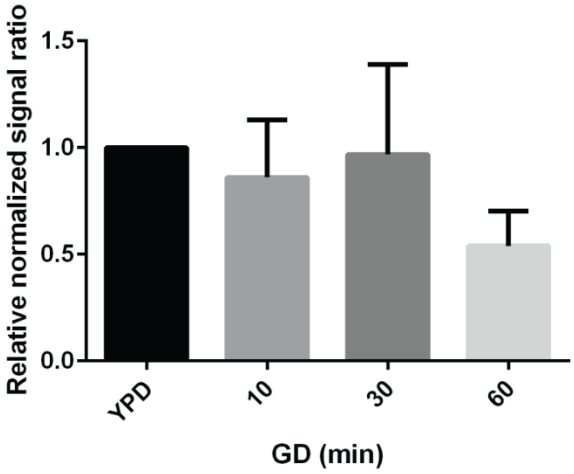

Figure 16: No significant change in interaction between Esa1-TAP and Fas2-GFP is observed upon acute GD. A) Cultured cells of WT, Esa1-TAP, Fas2-GFP and Esa1-TAP Fas2-GFP (YKB 1079, YKB 3875, YKB 4071, and YKB 4128 respectively) were grown to mid-log phase, harvested, resuspended in YP media for 10, 30, and 60 minutes of acute GD, harvested and mCHIP of Esa1-TAP was performed. After lysis the IPed sample, as well as WCE extract were resolved by SDS-PAGE and western blot analysis was performed against α-TAP, α-GFP and α-G6PDH. Image is representative of 3 biological replicates. B) Average WCE ratio is the ratio of GFP signal to G6PDH signal normalized to the YPD condition. C) Average co-IP ratio is the ratio of GFP signal to TAP IP signal normalized to the YPD condition. Statistical significance was determined through the use of ANOVA ($p<0.05$).

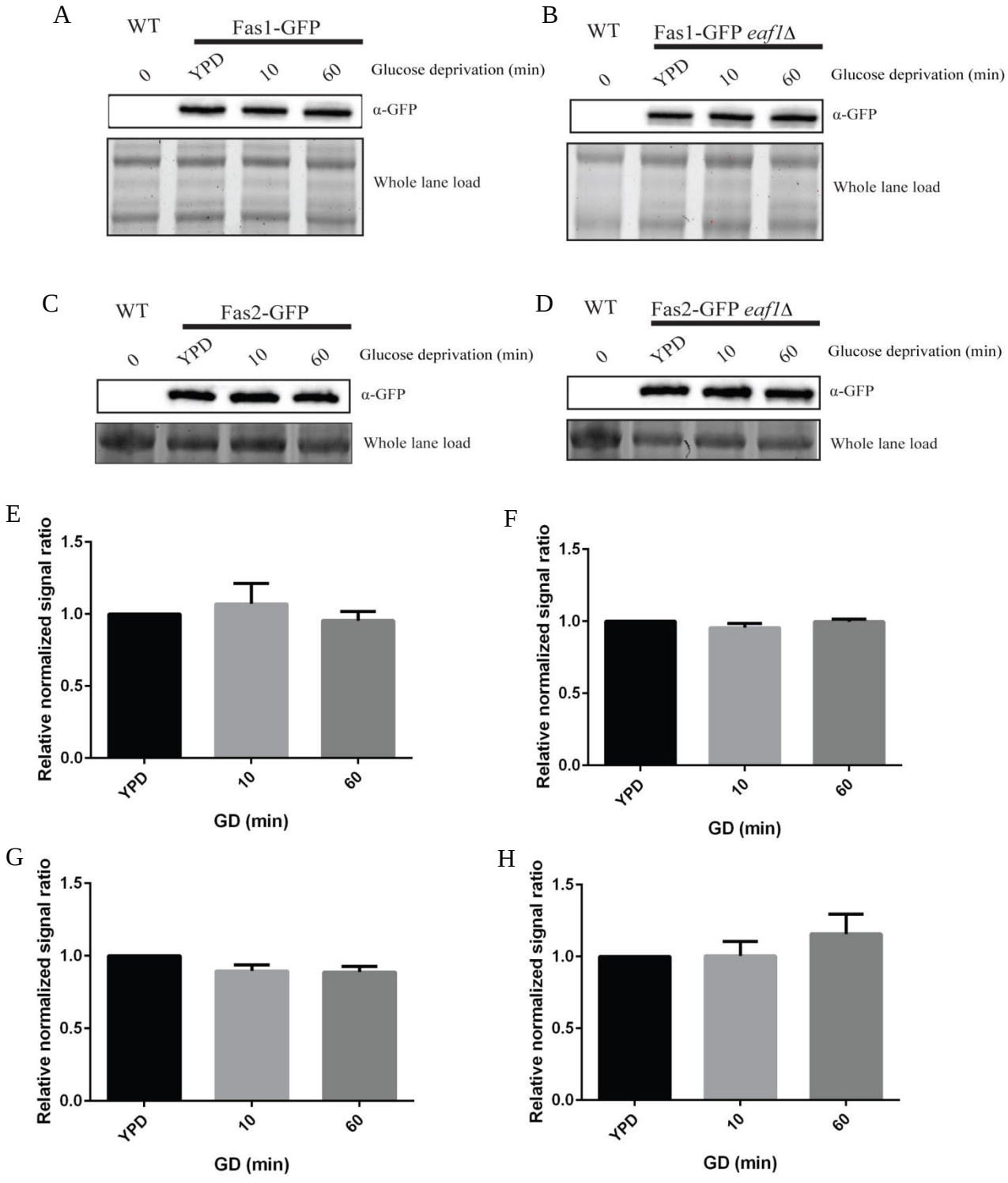
A
WT
Fas1-GFP
0
YPD
10
60
Glucose deprivation (min)
α-GFP
Whole lane load
B
WT
Fas1-GFP eaf1Δ
0
YPD
10
60
Glucose deprivation (min)
α-GFP
Whole lane load
C
WT
Fas2-GFP
0
YPD
10
60
Glucose deprivation (min)
α-GFP
Whole lane load
D
WT
Fas2-GFP eaf1Δ
0
YPD
10
60
Glucose deprivation (min)
α-GFP
Whole lane load
E
Relative normalized signal ratio
1.5
1.0
0.5
0.0
YPD
10
60
GD (min)
F
Relative normalized signal ratio
1.5
1.0
0.5
0.0
YPD
10
60
GD (min)
G
Relative normalized signal ratio
1.5
1.0
0.5
0.0
YPD
10
60
GD (min)
H
Relative normalized signal ratio
1.5
1.0
0.5
0.0
YPD
10
60
GD (min)

Figure 17: Both Fas1 and Fas2 do not significantly change protein levels upon acute GD in both WT and e*af1*Δ backgrounds. (A-D) Cultured cells of wildtype (WT YKB1079) *FAS1-GFP* (YKB3983), *FAS1-GFP* e*af1*Δ (YKB4051), *FAS2-GFP* (YKB4071), and *FAS2-GFP* e*af1*Δ (YKB4293) were grown to mid log phase, harvested resuspended in glucose deprived media for the acute glucose deprivation of 10 and 60 minutes. The cells were lysed by the TCA protocol and WCE resolved by SDS-PAGE using the Stain-Free™ FastCast™ acrylamide system and western blot analysis was performed against α-GFP. Images are representative of 3 independent experimental replicates. (E-H) Average WCE signal is the ratio between GFP signal to the whole lane signal normalized to the YPD condition for A-D respectively.

(section 2.3.2) and the WCE was resolved using the TGX Stain-Free™ FastCast™ Acrylamide Kit to allow for quantitative western blot analysis (Figure 17). No changes in cellular protein levels for either Fas1-GFP or Fas2-GFP was observed in either WT or in an *eaf1Δ* background. This implies that the reduction in Fas2 protein levels upon GD seen when using mChIP lysis protocol is not a reflection of decreasing total amount of protein, but potentially a decrease in solubility, potentially due to change in localization, interactions or PTMs upon GD.

3.3.3.3: Deletion of Eaf1 results in an increase of Fas1–GFP signal in both standard and acute GD conditions.

As the previous results indicate that Fas2, and potentially Fas1 may change localization in response to GD stress, resulting in their change in solubility, I sought to determine if GD and/or NuA4 impacts FAS protein localization. Live fluorescent microscopy was performed on logarithmically growing cells expressing endogenously tagged Fas1-GFP, Fas1-GFP *eaf1Δ*, Fas2-GFP, and Fas2-GFP *eaf1Δ* (Figure 17). The cells were cultured in YPD until mid-log phase, imaged and were then harvested and resuspended in YP for GD imaging. Samples were visualized for glucose replete along with GD time points of 10 and 60 minutes. Fas1 and Fas2 appear to have diffuse cytoplasmic localizations upon YPD growth conditions in both WT and *eaf1Δ* backgrounds, which corresponds to their known localization under standard growth (Breker et al., 2014; Chong et al., 2015; Huh et al., 2003). This diffuse localization is maintained throughout the acute GD time course in both WT and *eaf1Δ* backgrounds. However it was observed that in *eaf1Δ* strains there is greater signal of Fas1-GFP relative to the WT in all experimental conditions, even when taking into account the greater cell size of the *eaf1Δ* strains. This result therefore implies that NuA4 may regulate Fas1 protein levels. The Fas1-GFP signal however remains unchanged across the time course indicating that GD has no impact on Fas1

levels. This is however not the case for Fas2 as in *eaf1Δ* there is a slight, but significant increase in Fas2-GFP signal observed for the protein upon 60 minutes of GD. This result is not observed in either WT strain however. This might imply greater sensitivity of the fluorescent microscopy and that the FAS complex proteins may be increasing in protein amount towards the end of the acute GD treatment. These results contrast the western blots, where the mChIP lysis shows a decrease in soluble Fas2, but the TCA lysis does not, indicating another mechanism, such as a change in protein localization, is preventing the Fas proteins from being soluble by mChIP lysis upon GD conditions.

A

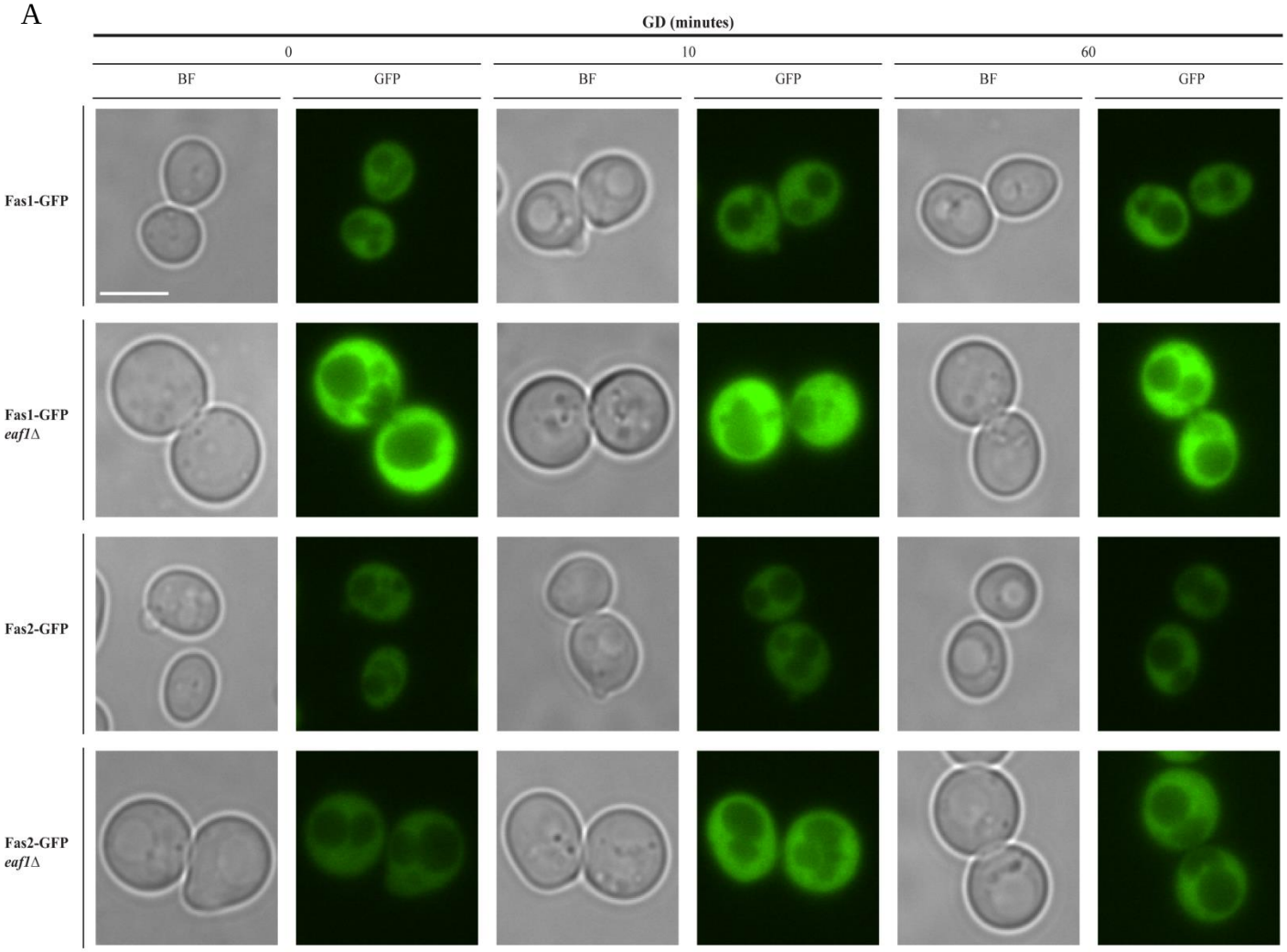
GD (minutes)
0
10
60
BF
GFP
BF
GFP
BF
GFP
Fas1-GFP
Fas1-GFP
eaf1Δ
Fas2-GFP
Fas2-GFP
eaf1Δ

B

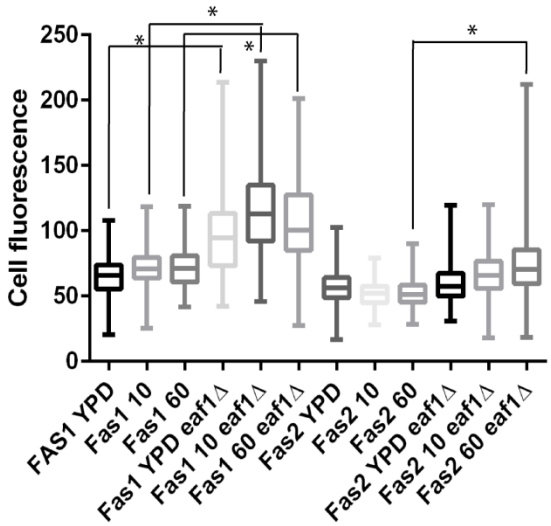
Cell fluorescence
250
200
150
100
50
0
*
*
*
*
FAS1 YPD
Fas1 10
Fas1 60
Fas1 YPD eaf1Δ
Fas1 10 eaf1Δ
Fas1 60 eaf1Δ
Fas2 YPD
Fas2 10
Fas2 60
Fas2 YPD eaf1Δ
Fas2 10 eaf1Δ
Fas2 60 eaf1Δ

Figure 18: Eaf1 has differential effects on Fas1-GFP andFas2-GFP signals. (A) Cell cultures of Fas1-GFP, Fas1-GFP *eaf1Δ*, Fas2-GFP, Fas2-GFP *eaf1Δ* (YKB 3983, YKB 4051, YKB 4071, and YKB 4293 respectively) were grown in YPD media, harvested and then resuspended in SC media for imaging. After imaging cells were then resuspended in warmed (30º C) YP media and incubated for 10 or 60 minutes. These cells were then harvested and resuspended in SC -glucose media and imaged. Cells were imaged on a confocal microscope. For each biological replicate greater than 80 cells were imaged per condition. Mean cell GFP fluorescence was then measured. Images are representative of three biological replicates. (B) Mean cell fluorescence of the cells when compared to background fluorescence. Statistical significance was determined through the use of ANOVA ($p<0.05$). Three independent experimental replicates were performed and greater than 80 cells were imaged and quantified per condition. Size bar 5µM.

4. DISCUSSION:

With an ever growing list of proteins that are acetylated (Choudhary et al., 2009; Downey et al., 2015; Henriksen et al., 2012; Lin et al., 2009; Weinert et al., 2011; Zhang et al., 2009) the next challenges are to connect specific lysine acetyltransferases to their substrates, determine how acetylation impacts protein function, and understand how changes in acetylation upon various stresses remodel cellular pathways. To begin to address these challenges, I here attempt to determine how acute glucose deprivation impacts both the NuA4 complex and its interactome. My results imply that GD has minimal impact on the complex itself, but dramatically remodels its interactome.

4.1 The NuA4 complex remains active upon acute glucose deprivation.

Many lines of evidence suggest that NuA4 complex activity and its homologs are regulated by stress in both yeast and human (Dar et al., 2013; Gupta et al., 2013; Jha et al., 2010; Peng et al., 2012; Reitsma et al., 2011), including changes in complex composition and activity towards histones, (Friis et al., 2009; Lin et al., 2008; Sandmeier, 2002). Therefore it was suprising to observe that acute GD stress has little to no impact on the NuA4 complex. Esa1, the catalytic component of NuA4, shows no significant change in protein levels at 10, 30 or 60 minutes GD (Figure 5). Nor were any changes detectable in protein levels such as gain or loss of the observable members of the complex by silver stain (Figure 6). Additionally, Co-IP and western blot analysis of three members of the complex that were not directly visible by silver stain analysis (specifically the TINTIN components Eaf5, Eaf7, and Eaf3) co-purified to the same degree with Esa1-TAP upon YPD and acute GD indicating constant interaction (Figure 14).While it is possible that co-IP may not replicate *in vivo* changes to the NuA4, together these results indicate that complex integrity of NuA4 remains intact upon acute GD. It is possible that

upon longer time points of acute GD, such as when cells are entering stationary phase, or transiently at time points not measured in these experiments, the complex becomes remodelled, either gaining or losing complex members. It is also possible that changes may be seen to the NuA4 complex during recovery from acute GD, where glucose is reintroduced to the growth media, however none of these conditions were studied here.

As the complex is shown to be maintained throughout the acute GD treatment this might imply that there are different regulatory mechanisms in place to regulate NuA4 during stress such as a change in complex activity, or a change in localization. However at least against its best characterized acetylation target Histone H4, complex activity is maintained *in vivo* throughout all the time points of GD, though changes in the amount of acetylation do appear in the time course (Figure 7). As well, I did not observe any changes in Esa1-GFP localization in response to acute GD (Figure 8). These results imply that change in localization of NuA4 is a stress dependent response as a change in localization for different members of the NuA4 complex have been detected under nitrogen starvation (Yi et al., 2012). Though it also is possible that the sensitivity of our microscope is unable to detect minor changes in Esa1-GFP localization as seen with nitrogen starvation, it is possible that GD does not result in the same effect on Esa1-GFP and that it remains nuclear throughout the experiments conducted here. Given that there are numerous protein interactors of NuA4 that have a cytoplasmic localization (Mitchell et al., 2013) it is possible that some NuA4 does localize outside of the nucleus allowing for their interaction. However it is also possible that the reverse is true and that pools of the proteins localize to the nucleus, to interact with NuA4 there. Future subcellular fractionation or super resolution/sensitivity microscopy will need to be performed in the future to resolve these unanswered questions about NuA4 cellular localization.

4.2 The interactome and acetylome of Esa1 is remodelled in response to acute glucose deprivation.

The Esa1-TAP interactome generated here identified 227 interacting proteins in total. The 72% overlap between my study and the previously published Esa1-TAP interactome under glucose conditions (Mitchell et al., 2013) suggests this is a robust and sensitive approach. Remarkably despite reproducibility under standard growth a majority (160/227) of interacting proteins with Esa1-TAP display either a two fold increase or decrease in interaction based on normalized spectral count (Figure 9). Not unexpectedly, hierarchical clustering of the changing interactome determined the Esa1-TAP interactome under YPD condition is the least similar to all the GD stress conditions. Intriguingly the YPD growth condition shows closest similarity to 60 minutes of GD treatment, potentially indicating that the cells are adapting to the stress, and that NuA4 may be reverting back to its normal interactions. This result is complemented by other data generated by the Baetz lab where we have previously shown that GD-induced stress granules resolve by the 60 minute GD (M Rollins personal communications and Figure 8). The interactome implies that one method by which NuA4 is regulating different mechanisms within the cell is through change in protein interaction. This could be due changes in affinity of the proteins for the complex, or potentially due to changes in subcellular localization of the interacting proteins (both potentially through post-translational modification). It is also possible that the changes in the interactome are a reflection of GD directly regulating either the cellular protein levels of the interacting proteins.

Given that the majority of Esa1 is nuclear under both standard (Breker et al., 2014; Chong et al., 2015; Huh et al., 2003) and acute GD conditions (Figure 8), it was suprising to find that the interacting proteins who are gained upon GD, are not nuclear proteins (Figure 10).

Indeed, most of the protein interactors that are lost upon GD stress were nuclear proteins. These results lend support to the notion that either there is a small amount of NuA4 localizing external to the nucleus that may increase upon GD that I am unable to detect, or that interacting proteins relocalize to the nucleus upon GD. Though protein localization in yeast have yet to assessed on a global scale for acute glucose deprivation high throughput studies using rapamycin treatment and starvation did not result in a change in localization of any of the interaction proteins from their localization to the nucleus (Breker et al., 2014; Chong et al., 2015).

From the changing protein interactors there are enrichments for certain GO terms and pathways. Some of the most prominent biological pathways detected to be lost and gained upon GD are those related to transcriptional and translational regulation, as well as post-transcriptional regulation (Table 1). This would imply that NuA4 is playing a direct or indirect role in the regulation of protein production upon stress, potentially in order to conserve resources and limit production to the essentials during the time of stress. Many of the proteins found in the transcription and translation related terms were also found in the Esa1-TAP acetylome. This further implicates NuA4 in a regulatory role for these pathways as has been previously established (Kaluarachchi Duffy et al., 2012; Uprety et al., 2015).

Given the stress conditions and the known role of NuA4 in glucose metabolism (Lin et al., 2009; Lu et al., 2011), it was not unexpected that interactors gained upon GD were enriched for proteins involved in glycolysis/gluconeogenesis and cellular carbohydrate catabolic process including proteins which catalyze reactions in both glycolysis and gluconeogenesis. Though NuA4 already has an establish role in regulate Pck1 (Lin et al., 2009) my study suggests NuA4's mode of action is broader and potentially required to adapt to the loss of the main carbon source for energy. Additionally genes implicated in the general stress response were enriched in both

interactions lost and interactions gained upon GD in the Esa1-TAP interactome. This is not unexpected given the cellular stress of acute starvation. In addition proteins related to the stress of DNA damage and DNA repair were identified to be enriched in protein interactors lost upon GD. While NuA4 has known roles in the response to DNA damage (Bird et al., 2002; Lin et al., 2008), this response was not expected upon GD as the two stresses impact the cell differently. It is possible that GD itself is causing DNA damage as in cell lines it has been shown to produce reactive oxygen species which can lead to double stranded breaks of DNA (Owada et al., 2013). These GO terms overall show NuA4 to have a varying role to the cell in response to stress.

Analysis of the Esa1-TAP GD acetylome provided greater scope to NuA4 and its potential roles within the cell. The amount of newly detected acetylated proteins, potentially by NuA4, was unexpected. Previous studies had identified 24 acetylated proteins in the NuA4 acetylome with a total of 71 acetylation sites (Mitchell et al., 2013). In this study 45 different proteins with a total of 93 acetylation sites. These results show a potentially expanding regulatory role of NuA4 upon stress due to the newly identified targets as well as show that the full scope of acetylation is yet to be understood and requires more in depth study to further elucidate all of its roles within the cell.

To characterize NuA4 specific acetylation sites the *in vitro* (heavy) acetylated sites sequence analysis was done on the residues surrounding the acetylated lysine. A slight preference for smaller residues (alanine and glycine) at the -1 site was detected in the YPD condition, in agreement with previous results (Downey et al., 2015; Mitchell et al., 2013). However while this preference was still detected upon GD conditions, there is also an increased prevalence for a serine residue upon GD, potentially indicating a change for NuA4 preference under stress. Though serine is not as small as either of alanine or glycine it is not a large amino

acid potentially showing an overall preference for smaller residues with larger ones potentially interfering with the ability of the residue to be acetylated by NuA4. As well as since there is a change in preference upon GD it is possible that there is a modification to NuA4 resulting in a change in substrate recognition. These results however may not represent the NuA4 consensus sequence effectively, as these results are a product of an *in vitro* experiment, as opposed to *in vivo.*

4.3 The interaction between NuA4 and Pab1 is not impacted by glucose deprivation

Pab1 has been previously established by the Baetz lab to be an interactor and acetylation target of Esa1 under standard growth conditions (Mitchell et al., 2013). Further work determined that stress granule formation upon acute GD is reduced in NuA4 deletion backgrounds (unpublished data M. Rollins). However the interaction between Esa1 and Pab1 had not yet been characterized upon GD stress. I have shown here through co-IP that the interaction between Esa1 and Pab1 is maintained from standard growth across all time points of acute GD (Figure 12), yet Esa1-TAP does not colocalize to Pab1 GD SGs (Figure 8). As discussed above, the lack of colocalization may be attributable to insufficient sensitivity of our current microscope. It is also possible that the interaction between NuA4 and Pab1 occurs within the nucleus, as while Pab1 is largely cytoplasmic (whether under standard or stressed growth (Breker et al., 2014; Chong et al., 2015; Huh et al., 2003)) it has also been shown to shuttle between the cytoplasm and nucleus (Brune et al., 2005). In order to attempt to show a direct interaction between NuA4 and Pab1, and where it occurs within the cell will likely require additional experiments. One possibility is to preform FRET, which would show proximity between Pab1 and Esa1, and would allow for determination of where within the cell the interaction is taking place.

In addition I further identify that the interaction between NuA4 and Pab1 is not mediated through the TINTIN subcomplex, implying that the interaction is formed through other parts of the complex (Figure 14). I also show that the interaction between NuA4 and Pab1 is likely to be a protein-protein interaction, and not mediated through mRNA acting as a scaffold, as enzymatic degradation of the mRNA does not impact the interaction between the two proteins (Figure 13). It is however still possible that mRNA was protected from RNase treatment by either protein allowing the interaction between the two proteins to be maintained even after treatment.

4.4 The interaction between Esa1 and the members of the TINTIN subcomplex do not change upon glucose deprivation

The members of the TINTIN subcomplex were also studied in their relation to how they interact with Esa1 as both Eaf5, and Eaf3 showed either a decrease or a complete loss in interaction upon acute GD as determined by the mass spectrometry experiments, and both have been identified to be acetylated under standard growth conditions (Mitchell et al., 2013) potentially indicating a form of auto-regulation of the complex by Esa1. However quantitative western blot analysis suggests TINTIN member co-purifiaction with Esa1-TAP is maintained upon GD (Figure 15). It is possible that the interaction does change and is not a complete loss of interaction, but just a partial loss that was not detected by co-IP despite my attempts of being semi-quantitative. It is also possible that the peptides for these proteins could be masked in the mass spectrometry results due to limits in detectability of numerous peptides at a single timepoint during an experiment. As the interactome changes different proteins are detected by the mass spectrometer, resulting in peptides not being detected as numerous peptides are detected at once.

While no change in interaction between Esa1-TAP and Eaf7-GFP was detected upon acute GD, a significant decrease in protein quantity of Eaf7 in the WCE as determined by western blot was detected upon the latter stages of GD. It is possible that while the NuA4 complex remains intact, free Eaf7 is being degraded and/or not being produced as rapidly in GD. Eaf7 found in the NuA4 complex may be protected from increased degradation or turn-over of free Eaf7 upon GD as this is a known method of protection for other proteins in yeast (Jeong et al., 2009). While I did not test whether GD impacts the stability of cellular levels of the TINTIN complex, the changes in Eaf7 might represent a novel way off differentially regulating complexes.

4.5 Deletion of NuA4 complex protein Eaf1 results in an increase in FAS protein expression

The final interactors of Esa1 that were studied were the members of the FAS protein complex, Fas1 and Fas2. A co-IP was performed between Esa1-TAP and Fas2-GFP showing consistent interaction from standard growth to acute GD conditions. However analysis of the WCE showed a decrease in Fas2 protein levels at both 30 and 60 minutes of GD. These results would imply a loss of protein, however when analyzed using a TCA lysis protocol, protein levels of both Fas1 and Fas2 were shown to remain constant across the acute GD treatment. These contrasting results might imply GD regulation of the FAS proteins in some manner, potentially a change in localization resulting in decreased solubility by mChIP lysis. However my microscopy analysis determined that neither Fas1 nor Fas2 change localization as they remain diffusely cytoplasmic throughout both standard growth and acute GD. A slight increase in Fas2 protein levels by 60 minutes of GD in an *eaf1Δ* mutant was however detected. This result would imply that Fas2 protein levels are regulated by the NuA4 complex, and potentially directly by it, as Fas2 was shown to be acetylated in these mass spectrometry results, and both Fas1 and Fas2

have bene shown to be acetylated previously (Henriksen et al., 2012). As well Fas1 appears to have increased protein expression in an *eaf1Δ* mutant, regardless of glucose availability, implying that NuA4 may have a regulatory effect on this protein. This effect could be studied by directly comparing the Fas1 protein levels under a WT and *eaf1Δ* mutant by western blot. As well a co-IP could be performed between Esa1 and Fas1 in an attempt to show direct interaction, further implying Fas1 regulation by NuA4. A possible explanation for the change in protein expression of the FAS proteins in an *eaf1Δ* mutant could be the related to the precursor subunit of the FAS complex function, acetyl-CoA. Acetyl-CoA has been shown to form malonyl-CoA which is used by the FAS complex to form fatty acids (Lynen, 1959), but is also a required precursor to the acetylation activity of KATs (Galdieri et al., 2014). It is possible that *eaf1Δ* is causing a change in PicNuA4 resulting in it using more acetyl-CoA which could lead to increased expression of the FAS proteins to allow them to use more malonyl-CoA and by extension acetyl-COA.

5. CONCLUSION

This thesis further defines the role of the NuA4 KAT complex within the cell and its role in the cellular response to glucose deprivation stress. I determined the direct effects of acute GD on Esa1 and the NuA4 complex as a whole are minimal, with no significant changes in protein quantity, complex composition, complex activity, and protein localization at any time points of GD. In contrast, I detected a change in Esa1 protein interactors upon acute GD and identified new targets of Esa1-TAP acetylation. This work suggest a model where NuA4 is regulating numerous proteins with a variety of functions related to how the cell might respond to GD stress including proteins related to protein production, apoptosis, and glucose metabolism.

6. REFERENCES

A. Schutz-Geschwender, Y. Zhang, T. Holt, D. Mcdermitt, D.M.O. (2004). Quantitative, Two-Color Western Blot Detection with Infrared Fluorescence.

Allard, S., Utley, R.T., Savard, J., Clarke, A., Grant, P., Brandl, C.J., Pillus, L., Workman, J.L., and Côté, J. (1999). NuA4, an essential transcription adaptor/histone H4 acetyltransferase complex containing Esa1p and the ATM-related cofactor Tra1p. EMBO J. *18*, 5108–5119.

Auger, A., Galarneau, L., Altaf, M., Nourani, A., Doyon, Y., Utley, R.T., Cronier, D., Allard, S., and Côté, J. (2008). Eaf1 is the platform for NuA4 molecular assembly that evolutionarily links chromatin acetylation to ATP-dependent exchange of histone H2A variants. Mol. Cell. Biol. *28*, 2257–2270.

Baetz, K.K., Krogan, N.J., Emili, A., Greenblatt, J., and Hieter, P. (2004). The ctf13-30/CTF13 genomic haploinsufficiency modifier screen identifies the yeast chromatin remodeling complex RSC, which is required for the establishment of sister chromatid cohesion. Mol. Cell. Biol. *24*, 1232–1244.

Bhat, W., Ahmad, S., and Côté, J. (2015). TINTIN, at the interface of chromatin, transcription elongation, and mRNA processing. RNA Biol. *12*, 486–489.

Bird, A.W., Yu, D.Y., Pray-Grant, M.G., Qiu, Q., Harmon, K.E., Megee, P.C., Grant, P.A., Smith, M.M., and Christman, M.F. (2002). Acetylation of histone H4 by Esa1 is required for DNA double-strand break repair. Nature *419*, 411–415.

Boudreault, A.A., Cronier, D., Selleck, W., Lacoste, N., Utley, R.T., Allard, S., Savard, J., Lane, W.S., Tan, S., and Côté, J. (2003). Yeast enhancer of polycomb defines global Esa1-dependent acetylation of chromatin. Genes Dev. *17*, 1415–1428.

Breker, M., Gymrek, M., Moldavski, O., and Schuldiner, M. (2014). LoQAtE--Localization and Quantitation ATlas of the yeast proteomE. A new tool for multiparametric dissection of single-protein behavior in response to biological perturbations in yeast. Nucleic Acids Res. *42*, D726–D730.

Brown, C.E., Howe, L., Sousa, K., Alley, S.C., Carrozza, M.J., Tan, S., and Workman, J.L. (2001). Recruitment of HAT complexes by direct activator interactions with the ATM-related Tra1 subunit. Science *292*, 2333–2337.

BRUNE, C., MUNCHEL, S.E., FISCHER, N., PODTELEJNIKOV, A. V., and WEIS, K. (2005). Yeast poly(A)-binding protein Pab1 shuttles between the nucleus and the cytoplasm and functions in mRNA export. RNA *11*, 517–531.

Buchan, J.R., Muhlrad, D., and Parker, R. (2008). P bodies promote stress granule assembly in Saccharomyces cerevisiae. J. Cell Biol. *183*, 441–455.

Carmona-Gutierrez, D., Eisenberg, T., Büttner, S., Meisinger, C., Kroemer, G., and Madeo, F. (2010). Apoptosis in yeast: triggers, pathways, subroutines. Cell Death Differ. *17*, 763–773.

Carrozza, M.J., Li, B., Florens, L., Suganuma, T., Swanson, S.K., Lee, K.K., Shia, W.-J., Anderson, S., Yates, J., Washburn, M.P., et al. (2005). Histone H3 methylation by Set2 directs deacetylation of coding regions by Rpd3S to suppress spurious intragenic transcription. Cell *123*, 581–592.

Cheng, X., and Côté, J. (2014). A new companion of elongating RNA Polymerase II: TINTIN, an independent sub-module of NuA4/TIP60 for nucleosome transactions. Transcription.

Cheng, X., Auger, A., Altaf, M., Drouin, S., Paquet, E., Utley, R.T., Robert, F., and Côté, J. (2015). Eaf1 Links the NuA4 Histone Acetyltransferase Complex to Htz1 Incorporation and Regulation of Purine Biosynthesis. Eukaryot. Cell *14*, 535–544.

Cherry, J.M., Hong, E.L., Amundsen, C., Balakrishnan, R., Binkley, G., Chan, E.T., Christie, K.R., Costanzo, M.C., Dwight, S.S., Engel, S.R., et al. (2012). Saccharomyces Genome Database: the genomics resource of budding yeast. Nucleic Acids Res. *40*, D700–D705.

Chittuluru, J.R., Chaban, Y., Monnet-Saksouk, J., Carrozza, M.J., Sapountzi, V., Selleck, W., Huang, J., Utley, R.T., Cramet, M., Allard, S., et al. (2011). Structure and nucleosome interaction of the yeast NuA4 and Piccolo-NuA4 histone acetyltransferase complexes. Nat. Struct. Mol. Biol. *18*, 1196–1203.

Chong, Y.T., Koh, J.L.Y., Friesen, H., Kaluarachchi Duffy, S., Cox, M.J., Moses, A., Moffat, J., Boone, C., and Andrews, B.J. (2015a). Yeast Proteome Dynamics from Single Cell Imaging and Automated Analysis. Cell *161*, 1413–1424.

Chong, Y.T., Koh, J.L.Y., Friesen, H., Duffy, K., Cox, M.J., Moses, A., Moffat, J., Boone, C., and Andrews, B.J. (2015b). Yeast Proteome Dynamics from Single Cell Imaging and Automated Analysis. Cell *161*, 1413–1424.

Choudhary, C., Kumar, C., Gnad, F., Nielsen, M.L., Rehman, M., Walther, T.C., Olsen, J. V, and Mann, M. (2009). Lysine acetylation targets protein complexes and co-regulates major cellular functions. Science *325*, 834–840.

Choy, J.S., Tobe, B.T., Huh, J.H., and Kron, S.J. (2001). Yng2p-dependent NuA4 histone H4 acetylation activity is required for mitotic and meiotic progression. J. Biol. Chem. *276*, 43653–43662.

Clarke, A.S., Lowell, J.E., Jacobson, S.J., and Pillus, L. (1999). Esa1p is an essential histone acetyltransferase required for cell cycle progression. Mol. Cell. Biol. *19*, 2515–2526.

Crooks, G.E., Hon, G., Chandonia, J.-M., and Brenner, S.E. (2004). WebLogo: a sequence logo generator. Genome Res. *14*, 1188–1190.

Dar, A., Shibata, E., and Dutta, A. (2013). Deubiquitination of Tip60 by USP7 determines the

activity of the p53-dependent apoptotic pathway. Mol. Cell. Biol. *33*, 3309–3320.

Downey, M., and Baetz, K. (2015). Building a KATalogue of acetyllysine targeting and function. Brief. Funct. Genomics elv045 – .

Downey, M., Johnson, J.R., Davey, N.E., Newton, B.W., Johnson, T.L., Galaang, S., Seller, C.A., Krogan, N., and Toczyski, D.P. (2015). Acetylome profiling reveals overlap in the regulation of diverse processes by sirtuins, gcn5, and esa1. Mol. Cell. Proteomics *14*, 162–176.

Doyon, Y., and Côté, J. (2004). The highly conserved and multifunctional NuA4 HAT complex. Curr. Opin. Genet. Dev. *14*, 147–154.

Doyon, Y., Selleck, W., Lane, W.S., Tan, S., and Cote, J. (2004). Structural and Functional Conservation of the NuA4 Histone Acetyltransferase Complex from Yeast to Humans. Mol. Cell. Biol. *24*, 1884–1896.

Friis, R.M.N., Wu, B.P., Reinke, S.N., Hockman, D.J., Sykes, B.D., and Schultz, M.C. (2009). A glycolytic burst drives glucose induction of global histone acetylation by picNuA4 and SAGA. Nucleic Acids Res. *37*, 3969–3980.

Galdieri, L., Zhang, T., Rogerson, D., Lleshi, R., and Vancura, A. (2014). Protein Acetylation and Acetyl Coenzyme A Metabolism in Budding Yeast. Eukaryot. Cell *13*, 1472–1483.

García-Salcedo, R., Lubitz, T., Beltran, G., Elbing, K., Tian, Y., Frey, S., Wolkenhauer, O., Krantz, M., Klipp, E., and Hohmann, S. (2014). Glucose de-repression by yeast AMP-activated protein kinase SNF1 is controlled via at least two independent steps. FEBS J. *281*, 1901–1917.

Gavin, A.-C., Bösche, M., Krause, R., Grandi, P., Marzioch, M., Bauer, A., Schultz, J., Rick, J.M., Michon, A.-M., Cruciat, C.-M., et al. (2002). Functional organization of the yeast proteome by systematic analysis of protein complexes. Nature *415*, 141–147.

Gaytán, B.D., Loguinov, A. V, De La Rosa, V.Y., Lerot, J.-M., and Vulpe, C.D. (2013). Functional genomics indicates yeast requires Golgi/ER transport, chromatin remodeling, and DNA repair for low dose DMSO tolerance. Front. Genet. *4*, 154.

Ghillebert, R., Swinnen, E., Wen, J., Vandesteene, L., Ramon, M., Norga, K., Rolland, F., and Winderickx, J. (2011). The AMPK/SNF1/SnRK1 fuel gauge and energy regulator: Structure, function and regulation. FEBS J. *278*, 3978–3990.

Guillemette, B., and Gaudreau, L. (2006). Reuniting the contrasting functions of H2A.Z. Biochem. Cell Biol. *84*, 528–535.

Gupta, A., Jha, S., Engel, D.A., Ornelles, D.A., and Dutta, A. (2013). Tip60 degradation by adenovirus relieves transcriptional repression of viral transcriptional activator EIA. Oncogene *32*, 5017–5025.

Halkidou, K., Gnanapragasam, V.J., Mehta, P.B., Logan, I.R., Brady, M.E., Cook, S., Leung,

H.Y., Neal, D.E., and Robson, C.N. (2003). Expression of Tip60, an androgen receptor coactivator, and its role in prostate cancer development. Oncogene *22*, 2466–2477.

Henriksen, P., Wagner, S.A., Weinert, B.T., Sharma, S., Bacinskaja, G., Rehman, M., Juffer, A.H., Walther, T.C., Lisby, M., and Choudhary, C. (2012). Proteome-wide analysis of lysine acetylation suggests its broad regulatory scope in Saccharomyces cerevisiae. Mol. Cell. Proteomics *11*, 1510–1522.

Ho, Y., Gruhler, A., Heilbut, A., Bader, G.D., Moore, L., Adams, S.-L., Millar, A., Taylor, P., Bennett, K., Boutilier, K., et al. (2002). Systematic identification of protein complexes in Saccharomyces cerevisiae by mass spectrometry. Nature *415*, 180–183.

Hoyle, N.P., Castelli, L.M., Campbell, S.G., Holmes, L.E.A., and Ashe, M.P. (2007). Stress-dependent relocalization of translationally primed mRNPs to cytoplasmic granules that are kinetically and spatially distinct from P-bodies. J. Cell Biol. *179*, 65–74.

Huang, D.W., Sherman, B.T., and Lempicki, R.A. (2009a). Systematic and integrative analysis of large gene lists using DAVID bioinformatics resources. Nat. Protoc. *4*, 44–57.

Huang, D.W., Sherman, B.T., and Lempicki, R.A. (2009b). Bioinformatics enrichment tools: paths toward the comprehensive functional analysis of large gene lists. Nucleic Acids Res. *37*, 1–13.

Huh, W.-K., Falvo, J. V, Gerke, L.C., Carroll, A.S., Howson, R.W., Weissman, J.S., and O'Shea, E.K. (2003). Global analysis of protein localization in budding yeast. Nature *425*, 686–691.

Jeong, M.-Y., Kang, C.-M., Kim, J.-H., Heo, D.-H., Chang, M., Baek, I.-J., Ro, H.-S., Choi, I.-D., Kim, T.-H., Yun, C.-W., et al. (2009). A novel function of Aft1 in regulating ferrioxamine B uptake: Aft1 modulates Arn3 ubiquitination in Saccharomyces cerevisiae. Biochem. J. *422*, 181–191.

Jha, S., Vande Pol, S., Banerjee, N.S., Dutta, A.B., Chow, L.T., and Dutta, A. (2010). Destabilization of TIP60 by human papillomavirus E6 results in attenuation of TIP60-dependent transcriptional regulation and apoptotic pathway. Mol. Cell *38*, 700–711.

Johnston, M. (1999). Feasting, fasting and fermenting: glucose sensing in yeast and other cells. Trends Genet. *15*, 29–33.

Joshi, A.A., and Struhl, K. (2005). Eaf3 chromodomain interaction with methylated H3-K36 links histone deacetylation to Pol II elongation. Mol. Cell *20*, 971–978.

Kaluarachchi Duffy, S., Friesen, H., Baryshnikova, A., Lambert, J.-P., Chong, Y.T., Figeys, D., and Andrews, B. (2012). Exploring the Yeast Acetylome Using Functional Genomics. Cell *149*, 936–948.

Kao, C.-F., and Osley, M.A. (2003). In vivo assays to study histone ubiquitylation. Methods *31*, 59–66.

Keogh, M.-C., Mennella, T.A., Sawa, C., Berthelet, S., Krogan, N.J., Wolek, A., Podolny, V., Carpenter, L.R., Greenblatt, J.F., Baetz, K., et al. (2006). The Saccharomyces cerevisiae histone H2A variant Htz1 is acetylated by NuA4. Genes Dev. *20*, 660–665.

Krogan, N.J., Baetz, K., Keogh, M.-C., Datta, N., Sawa, C., Kwok, T.C.Y., Thompson, N.J., Davey, M.G., Pootoolal, J., Hughes, T.R., et al. (2004). Regulation of chromosome stability by the histone H2A variant Htz1, the Swr1 chromatin remodeling complex, and the histone acetyltransferase NuA4. Proc. Natl. Acad. Sci. U. S. A. *101*, 13513–13518.

Krogan, N.J., Cagney, G., Yu, H., Zhong, G., Guo, X., Ignatchenko, A., Li, J., Pu, S., Datta, N., Tikuisis, A.P., et al. (2006). Global landscape of protein complexes in the yeast Saccharomyces cerevisiae. Nature *440*, 637–643.

Lambert, J.-P., Mitchell, L., Rudner, A., Baetz, K., and Figeys, D. (2009). A novel proteomics approach for the discovery of chromatin-associated protein networks. Mol. Cell. Proteomics *8*, 870–882.

Lambert, J.-P., Tucholska, M., Go, C., Knight, J.D.R., and Gingras, A.-C. (2015). Proximity biotinylation and affinity purification are complementary approaches for the interactome mapping of chromatin-associated protein complexes. J. Proteomics *118*, 81–94.

Lin, Y., Qi, Y., Lu, J., Pan, X., Yuan, D.S., Zhao, Y., Bader, J.S., and Boeke, J.D. (2008). A comprehensive synthetic genetic interaction network governing yeast histone acetylation and deacetylation. Genes Dev. *22*, 2062–2074.

Lin, Y., Lu, J., Zhang, J., Walter, W., Dang, W., Wan, J., Tao, S.-C., Qian, J., Zhao, Y., Boeke, J.D., et al. (2009). Protein Acetylation Microarray Reveals that NuA4 Controls Key Metabolic Target Regulating Gluconeogenesis. Cell *136*, 1073–1084.

Lindstrom, K.C., Vary, J.C., Parthun, M.R., Delrow, J., and Tsukiyama, T. (2006). Isw1 Functions in Parallel with the NuA4 and Swr1 Complexes in Stress-Induced Gene Repression. Mol. Cell. Biol. *26*, 6117–6129.

Longtine, M.S., McKenzie, A., Demarini, D.J., Shah, N.G., Wach, A., Brachat, A., Philippsen, P., and Pringle, J.R. (1998). Additional modules for versatile and economical PCR-based gene deletion and modification in Saccharomyces cerevisiae. Yeast *14*, 953–961.

Lu, J.-Y., Lin, Y.-Y., Sheu, J.-C., Wu, J.-T., Lee, F.-J., Chen, Y., Lin, M.-I., Chiang, F.-T., Tai, T.-Y., Berger, S.L., et al. (2011). Acetylation of yeast AMPK controls intrinsic aging independently of caloric restriction. Cell *146*, 969–979.

Lynen, F. (1959). Participation of acyl--CoA in carbon chain biosynthesis. J. Cell. Comp. Physiol. *54*, 33–49.

Mitchell, L., Lambert, J.-P., Gerdes, M., Al-Madhoun, A.S., Skerjanc, I.S., Figeys, D., and Baetz, K. (2008). Functional dissection of the NuA4 histone acetyltransferase reveals its role as a

genetic hub and that Eaf1 is essential for complex integrity. Mol. Cell. Biol. *28*, 2244–2256.

Mitchell, L., Lau, A., Lambert, J.-P., Zhou, H., Fong, Y., Couture, J.-F., Figeys, D., and Baetz, K. (2011). Regulation of septin dynamics by the Saccharomyces cerevisiae lysine acetyltransferase NuA4. PLoS One *6*, e25336.

Mitchell, L., Huard, S., Cotrut, M., Pourhanifeh-Lemeri, R., Steunou, A.-L., Hamza, A., Lambert, J.-P., Zhou, H., Ning, Z., Basu, A., et al. (2013). mChIP-KAT-MS, a method to map protein interactions and acetylation sites for lysine acetyltransferases. Proc. Natl. Acad. Sci. U. S. A. *110*, E1641–E1650.

Narayanaswamy, R., Levy, M., Tsechansky, M., Stovall, G.M., O'Connell, J.D., Mirrielees, J., Ellington, A.D., and Marcotte, E.M. (2009). Widespread reorganization of metabolic enzymes into reversible assemblies upon nutrient starvation. Proc. Natl. Acad. Sci. *106*, 10147–10152.

Owada, S., Shimoda, Y., Tsuchihara, K., and Esumi, H. (2013). Critical role of H2O2 generated by NOX4 during cellular response under glucose deprivation. PLoS One *8*, e56628.

Peng, L., Ling, H., Yuan, Z., Fang, B., Bloom, G., Fukasawa, K., Koomen, J., Chen, J., Lane, W.S., and Seto, E. (2012). SIRT1 negatively regulates the activities, functions, and protein levels of hMOF and TIP60. Mol. Cell. Biol. *32*, 2823–2836.

Reid, J.L., Moqtaderi, Z., and Struhl, K. (2004). Eaf3 regulates the global pattern of histone acetylation in Saccharomyces cerevisiae. Mol. Cell. Biol. *24*, 757–764.

Reitsma, J.M., Savaryn, J.P., Faust, K., Sato, H., Halligan, B.D., and Terhune, S.S. (2011). Antiviral inhibition targeting the HCMV kinase pUL97 requires pUL27-dependent degradation of Tip60 acetyltransferase and cell-cycle arrest. Cell Host Microbe *9*, 103–114.

Rossetto, D., Cramet, M., Wang, A.Y., Steunou, A.-L., Lacoste, N., Schulze, J.M., Côté, V., Monnet-Saksouk, J., Piquet, S., Nourani, A., et al. (2014). Eaf5/7/3 form a functionally independent NuA4 submodule linked to RNA polymerase II-coupled nucleosome recycling. EMBO J. *33*, 1397–1415.

Sachs, A.B., Davis, R.W., and Kornberg, R.D. (1987). A single domain of yeast poly(A)-binding protein is necessary and sufficient for RNA binding and cell viability. Mol. Cell. Biol. *7*, 3268–3276.

Sakuraba, K., Yasuda, T., Sakata, M., Kitamura, Y., Shirahata, A., Goto, T., Mizukami, H., Saito, M., Ishibashi, K., Kigawa, G., et al. (2009). Down-regulation of Tip60 gene as a potential marker for the malignancy of colorectal cancer. Anticancer Res. *29*, 3953–3955.

Sakuraba, K., Yokomizo, K., Shirahata, A., Goto, T., Saito, M., Ishibashi, K., Kigawa, G., Nemoto, H., and Hibi, K. (2011). TIP60 as a potential marker for the malignancy of gastric cancer. Anticancer Res. *31*, 77–79.

Sandmeier, J.J. (2002). RPD3 is required for the inactivation of yeast ribosomal DNA genes in

stationary phase. EMBO J. *21*, 4959–4968.

Santangelo, G.M. (2006). Glucose signaling in Saccharomyces cerevisiae. Microbiol. Mol. Biol. Rev. *70*, 253–282.

Sapountzi, V., and Côté, J. (2011). MYST-family histone acetyltransferases: beyond chromatin. Cell. Mol. Life Sci. *68*, 1147–1156.

Sapountzi, V., Logan, I.R., and Robson, C.N. (2006). Cellular functions of TIP60. Int. J. Biochem. Cell Biol. *38*, 1496–1509.

Schweizer, M., Roberts, L.M., Höltke, H.J., Takabayashi, K., Höllerer, E., Hoffmann, B., Müller, G., Köttig, H., and Schweizer, E. (1986). The pentafunctional FAS1 gene of yeast: its nucleotide sequence and order of the catalytic domains. Mol. Gen. Genet. *203*, 479–486.

Shimojo, H., Sano, N., Moriwaki, Y., Okuda, M., Horikoshi, M., and Nishimura, Y. (2008). Novel structural and functional mode of a knot essential for RNA binding activity of the Esa1 presumed chromodomain. J. Mol. Biol. *378*, 987–1001.

Soussi, T., Legros, Y., Lubin, R., Ory, K., and Schlichtholz, B. (1994). Multifactorial analysis ofp53 alteration in human cancer: A review. Int. J. Cancer *57*, 1–9.

Su, J., Wang, F., Cai, Y., and Jin, J. (2016). The Functional Analysis of Histone Acetyltransferase MOF in Tumorigenesis. Int. J. Mol. Sci. *17*, 99.

Sun, Y., Jiang, X., and Price, B.D. (2010). Tip60: Connecting chromatin to DNA damage signaling. http://dx.doi.org/10.4161/cc.9.5.10931.

Suresh, H.G., da Silveira dos Santos, A.X., Kukulski, W., Tyedmers, J., Riezman, H., Bukau, B., and Mogk, A. (2015). Prolonged starvation drives reversible sequestration of lipid biosynthetic enzymes and organelle reorganization in Saccharomyces cerevisiae. Mol. Biol. Cell *26*, 1601–1615.

Swisher, K.D., and Parker, R. (2010). Localization to, and effects of Pbp1, Pbp4, Lsm12, Dhh1, and Pab1 on stress granules in Saccharomyces cerevisiae. PLoS One *5*, e10006.

Tang, Y., Luo, J., Zhang, W., and Gu, W. (2006). Tip60-dependent acetylation of p53 modulates the decision between cell-cycle arrest and apoptosis. Mol. Cell *24*, 827–839.

Taylor, S.C., Berkelman, T., Yadav, G., and Hammond, M. (2013). A defined methodology for reliable quantification of Western blot data. Mol. Biotechnol. *55*, 217–226.

Taylor, S.C., Posch, A., Taylor, S.C., and Posch, A. (2014). The Design of a Quantitative Western Blot Experiment. Biomed Res. Int. *2014*, 1–8.

Towle, H.C. (2005). Glucose as a regulator of eukaryotic gene transcription. Trends Endocrinol. Metab. *16*, 489–494.

Treitel, M.A., Kuchin, S., and Carlson, M. (1998). Snf1 protein kinase regulates phosphorylation of the Mig1 repressor in Saccharomyces cerevisiae. Mol. Cell. Biol. *18*, 6273–6280.

Ullmann, A. (1996). Catabolite repression: a story without end. Res. Microbiol. *147*, 455–458.

Uprety, B., Sen, R., and Bhaumik, S.R. (2015). Eaf1p Is Required for Recruitment of NuA4 in Targeting TFIID to the Promoters of the Ribosomal Protein Genes for Transcriptional Initiation In Vivo. Mol. Cell. Biol. *35*, 2947–2964.

Weinert, B.T., Wagner, S.A., Horn, H., Henriksen, P., Liu, W.R., Olsen, J. V, Jensen, L.J., and Choudhary, C. (2011). Proteome-wide mapping of the Drosophila acetylome demonstrates a high degree of conservation of lysine acetylation. Sci. Signal. *4*, ra48.

Xu, S., and Elefant, F. (2015). Tip off the HAT– Epigenetic control of learning and memory by Drosophila Tip60. http://dx.doi.org/10.1080/19336934.2015.1080887.

Xu, Y., and Price, B.D. (2011). Chromatin dynamics and the repair of DNA double strand breaks. http://dx.doi.org/10.4161/cc.10.2.14543.

Yi, C., Ma, M., Ran, L., Zheng, J., Tong, J., Zhu, J., Ma, C., Sun, Y., Zhang, S., Feng, W., et al. (2012). Function and molecular mechanism of acetylation in autophagy regulation. Science *336*, 474–477.

Zhang, H., Richardson, D.O., Roberts, D.N., Utley, R., Erdjument-Bromage, H., Tempst, P., Côté, J., and Cairns, B.R. (2004). The Yaf9 component of the SWR1 and NuA4 complexes is required for proper gene expression, histone H4 acetylation, and Htz1 replacement near telomeres. Mol. Cell. Biol. *24*, 9424–9436.

Zhang, J., Sprung, R., Pei, J., Tan, X., Kim, S., Zhu, H., Liu, C.-F., Grishin, N. V, and Zhao, Y. (2009). Lysine acetylation is a highly abundant and evolutionarily conserved modification in Escherichia coli. Mol. Cell. Proteomics *8*, 215–225.

Zhao, H., Jin, S., and Gewirtz, A.M. (2012). The histone acetyltransferase TIP60 interacts with c-Myb and inactivates its transcriptional activity in human leukemia. J. Biol. Chem. *287*, 925–934.

Zhou, W., Liotta, L.A., and Petricoin, E.F. (2012). The spectra count label-free quantitation in cancer proteomics. Cancer Genomics Proteomics *9*, 135–142.

7. Appendix

7.1 Table S1: Proteins and unique spectra of the Esa1-TAP glucose deprivation interactome

protein ID	YPD			10			30			60			interaction
TRA1	223	294	260	49	192	155	46	218	198	50	188	123	↔
EAF1	115	135	124	35	107	68	31	115	100	37	96	56	↔
EPL1	96	131	85	28	84	63	25	92	70	26	98	46	↔
YEF3	83	99	67	72	93	71	88	86	78	70	106	64	↔
TEF2	58	61	39	53	68	49	58	52	54	55	79	37	↔
ESA1	49	65	57	30	52	42	24	49	50	25	54	37	↔
HSC82	46	45	19	47	60	43	66	49	55	53	68	32	↑
SSB2	45			42	41		51			45	44		↑
SWC4	41	54	34	12	33	15	12	36	29	8	38	19	↔
SSA2	40	47	16	28	42	12	36	28	19	28	46	9	↔
ARP4	37	42	41	15	33	19	13	32	31	11	32	16	↔
SSA1	36	39		29	35		34	28			41		↓
PMA1	31	41	26	25	38	19	30	27	28	29	36	15	↔
TIF2	30	41	13	31	40	31	31	37	31	28	40	26	↔
YNG2	30	35	27	9	24	14	6	26	18	7	24	10	↔
GCN1	27	37	5	18	38	7	28	35	19	24	46	7	↔
KAP123	26	34	10	25	31	25	31	30	26	25	36	12	↔
RPL4A	26	26	8	23	15	3	21	16	11	20		2	*
OLA1	22	24	12	16	32	14	19	20	19	18	26	11	↔
ACC1	21	38	5	16	48	9	27	31	17	34	48	5	↑
DED1	21	20	5	19	18	5	19	18	9	17	25	4	↔
CDC19	20	24	10	21	17	10	23	16	27	22	39	6	↔
SUB2	18	23	10	11	33	9	15	21	13	13	26	5	↔
RPS13	18	19	7	12	11	5	16	10	4	13	13	5	*
RPS3	18	17	8	17	9	8	16	8	12	17	14	4	*
RPG1	17	27	5	10	18	3	11	15	14	12	20	3	↔
RPS1B	17	23	7	14	14	3	14	5	3	11	15	3	*
ACT1	15	21	17	7	18	14	10	17	13	10	15	6	↔
RPS1A	15	20		12	13		15	4		8	15		*
NOP58	15	17	10	15	15	3	11	14	4	12	15	4	↔
RPL12A	15	16	6	19	16	6	14	12	9	15	17	4	*
RPL7A	15	14	10			3	15		7	13	14	3	*
RPS17A	15	13	5	12	8	2	9	10	4	14	10		*
URA2	14	26	4	23	29	3	28	21	12	21	46		↑
NEW1	14	21	5	10	28	5	12	17	13	14	24		↔

YAF9	14	15	9		12			9	4		9	2	↓
RPS5	14	15	5	11	15	4	12	8	7	14	11	3	*
PDC1	14	15	3	14	22	5	21	11	12	15	26	2	↑
SAR1	14	14	6	11	13	9	10	10	12	12	15	6	↔
RPL8A	14		3	7	8	5		4	6			3	*
RPL13A	14			6	3	2	9	4	5	10	5	2	*
VPS1	13	15	4	8	17	2	9	13	8	5	12		↔
RPS16B	13	14	5	13	7		13	4	10	13	8		*
TEF4	13	12	6	16	15	15	16	16	14	17	21	4	↑
GUS1	12	21	2	22	26	6	24	19	14	23	26	5	↑
TDH3	12	20			19			12			22		↓
EFT2	12	16		11	9	6	11	8	4	11	15		↔
RPS4B	12	15	7	10	10	4	13	5	7	10	11	2	*
NOP56	12	13	8	8	14		9	9	4	4	12	2	↔
RPL16B	12	13	7	10	7	3	12	6	5	10	11		*
SCP160	12	12	3	14	23	10	22	15	12	13	28	6	↑
RPS14B	12	12	3	9	5		10	6	3	9	9	2	*
RPS11B	12	11	6	6	6	4	6	3	6	8	13		*
RPL3	12	11		7	5		11	4		4	8		*
RPS6A	12	9	8	11	9		10	7	3	10	13	2	*
RRP5	11	17		7	15		9	7	2	9	13	3	↔
SEC26	11	16	4	6	11	5	9	12	8	6	15	3	↔
RPS0A	11	15	10	10	11	15	15	10	16	10	17	6	*
CDC48	11	14	2	17	23	9	23	15	14	16	23	3	↑
RPS24B	11	13	3	7	9	2	9	7	2	8	8		*
SEC21	11	11		8	19		9	14	8	7	18	2	↑
RPS12	11	9	3	10	11	3	9	10	4	13	14	3	*
RPS2	11	6		7	2		6			8	9		*
RPL14A	11						8						*
SUP45	10	14	7	8	13	8	10	12	11	9	14	3	↔
DHH1	10	13	5	6	10	2	8	10	5	7	14	2	↔
RPL27B	10	11	5	8	7	3	8	6	4	5	8	2	*
SAC6	10	11	4	6	12	8	8	9	9	7	14	7	↔
RPL1A	10	9		3	5		3			6			*
ARB1	10	8	6	6	4	6	9	6	5	10	11	3	↔
RPL6B	10	7	2	10		2	11	5		11	13		*
RPS8A	10	7	2	5	5	2	8	3	3	5	7		*
RPL2B	10	7	2	4	5		7	3	2	3	7		*
RPS9B	9	14					8			8	5		*

RPP0	9	11	12	12	14	10	12	10	14	10	13	4	↔
EAF6	9	10	7		5			8	2		5	2	↓
RPS18A	9	10	4	8	6	2	9	6	5	10	12		*
HHF1	9	9	6	9	10	4	8	7	7	9	11		↔
RPS7A	9	9	2	7	8		6	4		6	9		*
HSP104	9	9		7	12	2	7	9	3	11	17		↑
RPS22A	9	6	2	8	7	4	8	3	4	8	7		*
DPS1	9			8			7			6			
RPL31A	9			2			3			3	2		*
EAF5	8	15	11		8	2		6	5		4	2	↓
RPL19B	8	11	3	6	5	3	9	5	3	7	6		*
NIP1	8	10	3	7	11	2	5	5	4	10	12		↔
RPS19B	8	9	3	7	6	3	6	2	4	7	8		*
NPL3	8	7		4	3		4			4	5		↑
PIL1	8	6	2	4	5		4	4	3	8	6		↔
RVB1	8	6		5	7		5	7	5	2	7		↔
RPS26B	8	5		4			3			3	5		*
CHC1	7	17	2	6	14	2	12	8	5	12	19		↔
VMA2	7	14	3	5	13	3	7	7	5	11	17		↔
VMA5	7	12	2	5	13	7	11	14	10	11	18	4	↑
RPL17A	7	11		7			7	4	4	5	6		*
GCN20	7	10		3	8		5	5	2	5	10		↔
FAA4	7	10		2	8		4	5	4	4	5		↔
CLU1	7	9	6	6	6		3	9	4	6	12	3	↔
ASC1	7	9	4	3	2	3	4		3	5	3		↔
GCD11	7	9		8	6	3	6	5	4	9	9		↔
RPL5	7	8	2	3	5		5	2	4	4	5	4	*
RPL15A	7	7	6	4	5	3	7	3	3	6	5		*
IDH2	7	6		5	6		4	5		5	7		↔
RPL28	7	6		3	3		4	4		6	4		*
RPP2A	7	5	4	4	7		3	3	3		4		↑
RPL20A	7	5	2		6	2	7	4	4	6	9		*
SSZ1	7	5		12	3	4	15	6	3	9	15		↑
VMA13	7	5		5	9		6	7	5	8	10	3	↑
KEM1	7	4			5	3	6	2		4	7		↔
PAB1	7			5	3		15	3	2	9	11		↑
DBP5	6	17	4	6	8		3	9	3	6	10		↔
ADE5	6	11	2	9	14	4	13	10	7	10	15	2	↑
GSP1	6	8	5	7	6	11	8	8	11	8	13	7	↑

PRT1	6	8	5		9	3	6	7	3	7	6		↔
MIR1	6	8	4	5	7	3	6	8	5	7	9	3	↔
SRP1	6	8	4	3	7		2	8	5	3	10	2	↔
YRA1	6	8		6	4		5	2		7	4		↔
NOG1	6	6	5		6			3	4	2	6		↓
PET9	6	6	3	6	8	2	9	10	7	11	6		↑
SSC1	6	6		4	6		6			8	8		↓
CRM1	6	5	2	3	6		3	9	2		7		↓
SPT16	6	5	2								2		↓
SNU13	6	5		3	4		3	2		3	5		↔
KAP95	6	5			5		3	4		4	8	2	↑
RPL10	6	4	2	5	5		4	4		4	7		*
NOP1	6	4		3	3		3	3		2	4		↔
RPS25A	6	4		2	2		3			4			*
SUI3	6			7			5	2		3			↑
LSP1	6						3			5			
RPL16A	5	8	5				4			5	4		*
RPL30	5	7			5		5	3		6	7		*
KAR2	5	7			4			4			8		↓
NSR1	5	6	5	6	6		6	4	2	6	6		↔
YKT6	5	6		3	6		5	4	3		6		↓
RPS20	5	6		3	3		4	3		5	4		*
ATP1	5	6		3	2		4	2		5	5		↔
AHA1	5	6			2		4	4	2	3	6	2	↓
EAF3	5	5	6										↓
FAS2	5	5		3	6		4		4	2	6		↔
RPS7B	5	5		3	5		4	2		4	6		*
RPL35B	5	4	2	6	4		4	4		4	7		*
GPM1	5	4		5	3		9	2		9	3		↑
RPL9A	5	4			4		5				5		*
FUN12	5	4			3		5		2	5	6		↓
RPL36A	5	3		5	4	2	4	2	2	6	5		*
VAS1	5	2		6	5		9	2	2	8	7		↑
THS1	5			7			9			10	3		↑
ENO2	4	12		9	6		12	5	9	9	11		↑
RPL11B	4	7		4	3		9	3	3	5	6		*
CCT2	4	6	2	2	6		6	4		6	6		↔
SUI2	4	6		6	5		5	3		6	9		↑
FBA1	4	6		5	4		7	3	4	5	8		↑

TUB2	4	6		4	6	5	6	5	5	5	8		↑
RPS31	4	6		4			4	2			5		*
RPL23A	4	5	3	3	5	2	4	2	2	4	5		*
SSE1	4	5		14	9	4	17	6	10	20	17		↑
SRV2	4	5		3	5		5	4		4	5		↔
ARF1	4	4	4	9	9	5	5	8	7	7	12	3	↑
TIF34	4	4	2	3	6	2	5	7	3	3	9		↑
RNR4	4	4		7	7	3	9	5	5	8	13		↑
PHO84	4	4		3	5			4			2		↓
CCT3	4	4		3	3		3	2	2	3	2		↔
CDC33	4	4		2	4		5	2		2	5		↔
FKS1	4	4		2	3		5	3		2	3		↔
RPN2	4	4		2			2		2	3	5		↓
SEC7	4	4			3			4		2	3	3	↓
UTP10	4	4			2				2	3	2		↓
MDN1	4	3		4	7		2	6			7		↓
DBP2	4	3			3						2		↓
PBP1	4	2	2	4			3	4		3	3		↓
DNM1	4	2			2						2		↓
KRS1	4			3			7			4			
RPL33A	4			3			3	3		3			*
NUD1	3	12	7		4			5	6		4		↓
HSP60	3	9	3	2	10		6	6	8	6	15	3	↑
SPC29	3	7	5		2	2		5	6		5		↓
RPL26A	3	7		5	4		6			4	4		*
RPL38	3	7		3	5		4			3	4		*
YHB1	3	6		9	3		8	2		4	10		↑
RPS10B	3	6					2			2	3		*
RPL18B	3	5	3	5	4	4	5	4	4	9	6		*
RPL25	3	5		7	5	4	3	3		5	5		*
POR1	3	5		4	7	4	6	3	6	5	8		↑
SRO9	3	5		3	4		4		2	2	5		↔
ATP2	3	5		3	4		4	5		6	4		↑
RVS161	3	5			3		2		3	3	7		↓
NPA3	3	5			2						3		↓
KRE33	3	5									3		↓
CMD1	3	5						4			2		↓
HTB2	3	4	3	6	4		5			5	3		↓
TUB1	3	4	3	2	6	2		4	6		4		↓

RNA1	3	4		3	6		6	4	4	4	7		↑
RPP2B	3	4		2	2		3			3	2		↓
CBF5	3	4			5			2		3	5		↓
RPS15	3	4			2		4			3	3		*
IFH1	3	4											↓
INO80	3	4											↓
RPA190	3	4											↓
GVP36	3	3		3	2		3			4	4		↓
HMO1	3	3			2								↓
RPS21B	3	3					2				4		*
PRP43	3	3									3		↓
HTA2	3	2	3	3	2		3	3		2			↓
TIF35	3	2	3		2	3	3		3	3	3		↔
RPL32	3	2		4	2	2	3	2		4	3		*
RTN1	3	2		2	4		4		2	3	3		↑
NOG2	3	2			3		2	3			3		↓
RVS167	3	2			3			2					↓
RLP7	3	2			2								↓
TRX2	3	2					3		3	4	4		↓
GAR1	3				3								
RPL24A	3								3				*
RPL43A	3										4		*
DBP3	3												
RPL22A	3												*
YPR097W	3												
SPC110	2	14	5					5	5		6		↓
COP1	2	10	3	2	6	3	3	6		3	8		↔
ECM29	2	8			2			4			4		↓
TCP1	2	7	3	3	4		3	8		5	7		↔
YDR341C	2	7		5	8	2	8	5	3	6	11	3	↑
PGK1	2	7		3			10	2	5	6	5		↓
EMW1	2	7			3		3	2		3	4		↓
FPR1	2	6		3	2		3	3		5	4		↑
CDC31	2	5	8			3		5	6			3	↓
CCT8	2	5		2	4		2	4	3	3	4		↔
FAS1	2	4		3	7		4	2	2	4	9		↑
GPD2	2	4		3	5		4	4	2		7		↓
LYS20	2	4			3					2	3		↓
YPK1	2	4									3		↓

VTC4	2	3		4	3		4	5		2	4		↑
RPT6	2	3		2	3		3				4		↓
RPP1A	2	3			2		2	2		2			↓
RPL39	2	3					2			2	2		*
RPS23B	2	3							2				*
SUP35	2	2	2		3		2				4		↓
HXK2	2	2		6	5		8			9	5		↓
RPL21A	2	2		3	3	2	5			3	5		*
NOP7	2	2		2			2			2	3		↓
TCB3	2	2			4			4		2	8		↓
PUB1	2	2			3				2	2	2		↓
CCT4	2	2			2		3	3			7		↓
HXT3	2	2			2		2						↓
PAT1	2	2			2						2		↓
SEC27	2	2			2			3			2		↓
MTR4	2	2								2	4		↓
RRP12	2	2									5		↓
ARC1	2			6			3			4	5		↑
DED81	2			3			3			3	3		↑
RPL34B	2			2			3	2		3			*
SPT5	2				3					2	2		↑
PFK1	2				2		2		3		4		↑
RHR2	2				2						4		
FPR4	2									3	2		↑
NAT1	2										2		
CDC14	2												
DRS1	2												
EAF7	2												
NMD5	2												
HSP82		43					55			47	60		↑
SSB1		38	19			25		31	40			14	↓
RPL8B		19					11			13	9		*
CNM67		12	5		6	2		5	8		6	3	↔
RPL14B		11		4	7	4		6	5	6	10	3	*
RPL13B		11											*
RPN1		7		2	6		5	3		3	8		↑
LYS12		7			4		3	4			4		↑
GPD1		6			11		9	6	4	5	11	2	↑
BMH1		5		3	2		2	2		2	3		↑

MYO2		5			6			2		2	4		↑
YPL225W		5			3		3	3		2	7		↑
RPL33B		5			2						5		*
ARF2		4			7	4	3	6		6			↑
SRP54		4			2			2			4		
RBG1		4											
RPL31B		4											*
PSE1		3	3		5		2	3	3		4		↓
RET2		3		5	5		5	4		3	6		↑
GUA1		3			5		2	2		3	4		↑
NUG1		3			4		3	4	2		5		↑
RPT1		3			4		3	4			5		↑
HEK2		3			4			3			3		
OAC1		3			3			2		2	2		↑
SAM1		3			2				2		4		
RIX7		3			2								
RPO21		3			2								
BUB2		3											
MAK21		3											
NOC2		3											
PFY1		3											
RPL42B		3											*
RPT4		3											
UBP3		3											
SPC42		2	4						2				↓
CYS4		2		5	9		6	4		6	8		↑
TRP5		2		5	7		6	7	4	2	12	2	↑
VMA1		2		3	2	2	5				5		↑
SXM1		2		2	4		4	3	2	4	6		↑
MCK1		2		2	4		3	3		3	4		↑
RPA49		2		2	2								↑
HGH1		2			4	2							↑
SLA2		2			3		3	4			6		↑
SEC31		2			2		2	2		2	4		↑
LSM12		2			2		2						
CCT7		2			2						4		
RMT2		2			2						3		
YNL010W		2			2			4			3		
SPT6		2			2						2		

TSA1		2					3			2			
RNR1		2					2				3		
DCS1		2					2				2		
RPS27B		2					2						*
PFK2		2									4		
SPF1		2									4		
CEX1		2									2		
PHB2		2									2		
BEM2		2											
CDC39		2						2					
DIM1		2											
FPR3		2											
MSN5		2											
NOP15		2											
OSH2		2											
RBG2		2											
RFC5		2											
RPC40		2											
SCH9		2											
SEC28		2											
URB1		2											
YJL113W		2											
YJR027W			6	14			15		5		18		↑
TDH2			4	11		6	17		10	13		3	↑
RPS9A			4	4	5	2			5				*
NCP1			3						3				
BBP1			2						2				
RPL7B				9	11			11					*
VTC3				5	2		8	2	5	6	3		↑
GGA2				3	6			5			5		↑
SEC4				3	2		3				3		↑
ZUO1				3			3			3			
LAT1				3			3						
TIF5				3			2				2		
MYO3				3									
NAP1				2	4						4		↑
FAA1				2	3		5		2	2	3		↑
HOG1				2	3		3			2	4		↑
GET3				2	2		3			2	3		↑

RNR2				2		2	4		3	3			↑
LEU1				2			3			3	5		↑
GRS1				2			3			3			
DEF1				2			2			2			
IMD4				2			2			2			
YHR020W				2						3			
HHT1				2						2			
SCS2				2							2		
CMK2				2									
DYN1				2									
RRP14				2									
YEA6				2									
YML045W					14								
URA7					5		2			3	6		↑
RPL17B					5								*
RPL6A					5								*
RPS26A					5			3					*
UBA1					4					3	3		↑
GEA2					4								
GLK1					3		3			4			
CCT6					3		2		2		4		↑
GFA1					3						4		
RVB2					3			3			3		
CCT5					3			2			2		
BBC1					3								
SLC1					3								
UTP21					3								
SEC24					2		7			5	4		↑
PSA1					2		2				5		
CSE1					2			2	2				↑
RPT2					2				2				
ARX1					2					2	3		↑
VIP1					2			2			4		
PDR5					2						2		
RPN3					2						2		
RRP3					2			2			2		
TOM40					2						2		
YKR018C					2						2		
ERG3					2								

LSC1					2								
MDM20					2								
MLC1					2								
SPP41					2								
TUF1					2								
WTM1					2								
KAP104						2		2					
CAM1							7				5		
RPT3							3				4		
SMC4							3	2					↑
DPM1							2			3	2		↑
VTC2							2			2			
PAA1							2	2			5		↑
MTD1							2				2		
SSH1							2	2			2		↑
APA1							2						
APT1							2						
HTS1							2						
KES1							2						
SEC61							2						
TPS2							2						
YDR098C-B										10			
HXK1										4		2	↑
HXT6										4			
MRPL25										3			
SEC18										3			
ALY2										2			
KAP122								2		2			
STO1										2			
UBX4										2			
RPL4B											22		*
ALD6											6		
EFM1											3		
HAS1											3		
IST2											3		
PHO81											3		
BCH1											2		
DBP6											2		

ERG1											2		
ERG11											2		
GCD1											2		
HIS5											2		
HRR25											2		
MEX67											2		
NAN1											2		
NUM1											2		
PEP4											2		
PNO1											2		
RFC3											2		
RPN6											2		
SAC1											2		
SIS1											2		
SRP21											2		
SUI1											2		
TCB1											2		
TOM70											2		
UTP20											2		
UTP22											2		
YOR021C											2		
YAR010C												3	
RIM15												2	
YNL247W												2	
IFM1								2					
PDS1								2					
RPB2								3					
RPT5								2					
SKG6								2					
SSA3								15					
VMA8								3					
YHM2								3					
YPT1								3					

Interacting proteins are characterized by whether or not their interaction is changed with Esa1-TAP upon GD either having an increased interaction (↓), decreased (↑) as depicted in figure 9, or as unchanged in interaction with Esa1-TAP upon GD (↔). Ribosomal proteins were not included in further analysis and are noted by a *. All proteins without an interaction symbol are those that did not meet the criteria for interaction with Esa1-TAP.

7.2 Table S2: Strain list

YKB	Auxotrophies	Reference
440	*MATa trp1-1 ura3-1 leu2-3,112 his3-11,15 ade2-1 can1-100* ESA1-TAP::TRP1	(Lambert et al., 2009)
765	*MATa trp1-1 ura3-1 leu2-3,112 his3-11,15 ade2-1 can1-100* ESA1-TAP::TRP1 *Eaf3Δ*KAN	(Mitchell et al., 2008)
854	*MATa trp1-1 ura3-1 leu2-3,112 his3-11,15 ade2-1 can1-100* ESA1-TAP::TRP1 *Eaf5Δ*KAN	(Mitchell et al., 2008)
964	*MATa trp1-1 ura3-1 leu2-3,112 his3-11,15 ade2-1 can1-100* ESA1-TAP::TRP1 *Eaf7Δ*KAN	(Mitchell et al., 2008)
1079	*MATa his3Δ1 leu2Δ0 met15Δ0 ura3Δ0*	Open Biosystems
2004	*MATa his3Δ1 leu2Δ0 met15Δ0 ura3Δ0* EAF5-GFP::HIS	(Huh et al., 2003)
2006	*MATa his3Δ1 leu2Δ0 met15Δ0 ura3Δ0* EAF7-GFP::HIS	(Huh et al., 2003)
3875	*MATa his3Δ1 leu2Δ0 met15Δ0 ura3Δ0* ESA1-TAP::HIS	This study
3941	*MATa his3Δ1 leu2Δ0 met15Δ0 ura3Δ0* ESA1-TAP::HIS GDS1-HA::KAN	This study
3983	*MATa his3Δ1 leu2Δ0 met15Δ0 ura3Δ0* FAS1-GFP::HIS	(Huh et al., 2003)
4051	*MATa his3Δ1 leu2Δ0 met15Δ0 ura3Δ0* FAS1-GFP::HIS *eaf1Δ*::KAN	This study
4069	*MATa his3Δ1 leu2Δ0 met15Δ0 ura3Δ0* ESA1-GFP::HIS PAB1-mCh::KAN	This study
4071	*MATa his3Δ1 leu2Δ0 met15Δ0 ura3Δ0* FAS2-GFP::HIS	(Huh et al., 2003)
4128	*MATa his3Δ1 leu2Δ0 met15Δ0 ura3Δ0* ESA1-TAP::URA FAS2-GFP::HIS	This study
4156	*MATa his3Δ1 leu2Δ0 met15Δ0 ura3Δ0* ESA1-TAP::URA EAF5-GFP::HIS	This study
4157	*MATa his3Δ1 leu2Δ0 met15Δ0 ura3Δ0* ESA1-TAP::URA EAF7-GFP::HIS	This study
4234	*MATa his3Δ1 leu2Δ0 met15Δ0 ura3Δ0* EAF3-HA::HIS	This study
4235	*MATa his3Δ1 leu2Δ0 met15Δ0 ura3Δ0* ESA1-TAP::URA EAF3-HA::HIS	This study
4236	*MATa his3Δ1 leu2Δ0 met15Δ0 ura3Δ0 esa1*D ESA1-L245P::URA	This study
4293	*MATa his3Δ1 leu2Δ0 met15Δ0 ura3Δ0* FAS2-GFP::HIS *eaf1*Δ::KAN	This study